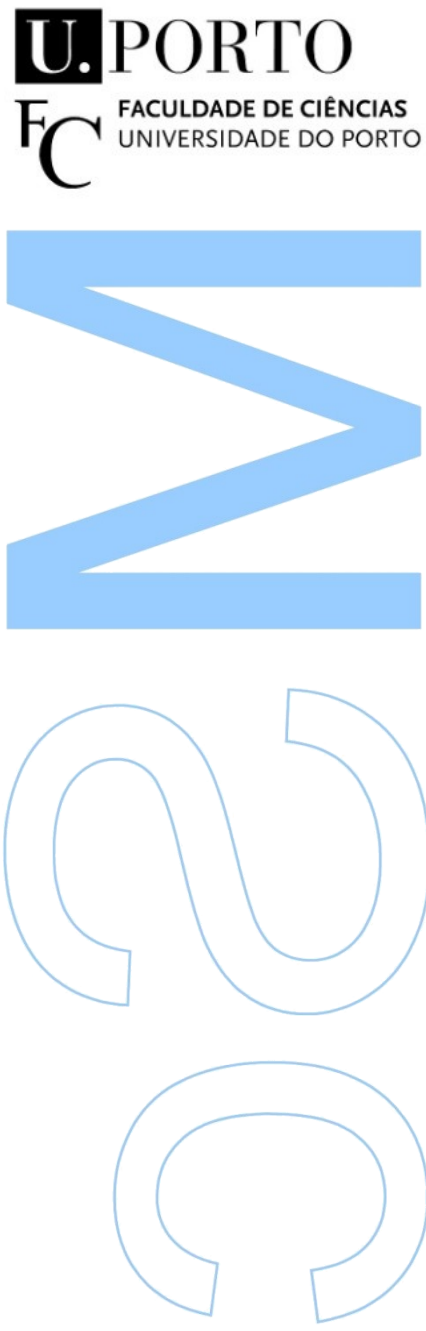
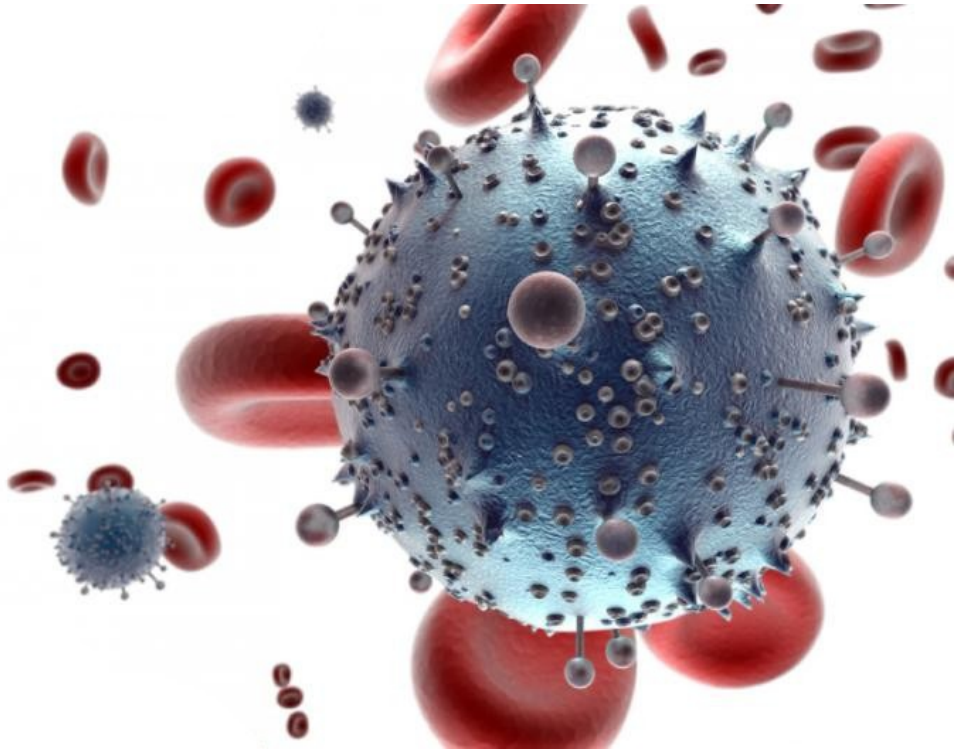


Travels into Several Remote Models of HIV-1 Immune Response. In Four Parts.





Travels into Several Remote Models of HIV-1 Immune Response. In Four Parts.

Ricardo Pereira de Magalhães Cruz

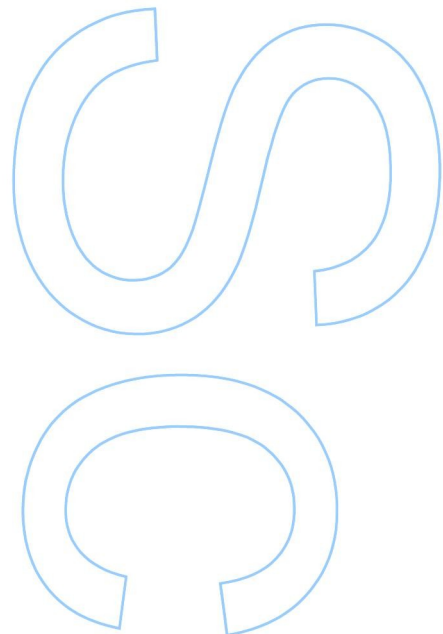
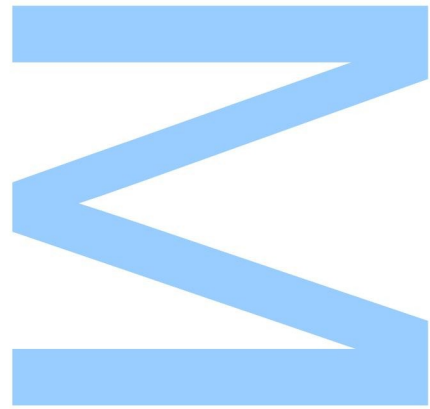
Mestrado em Engenharia Matemática

Departamento de Matemática

2015

Orientador

Prof. Doutor João Nuno Tavares, FCUP

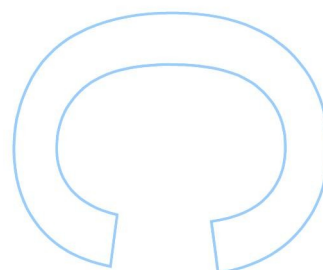
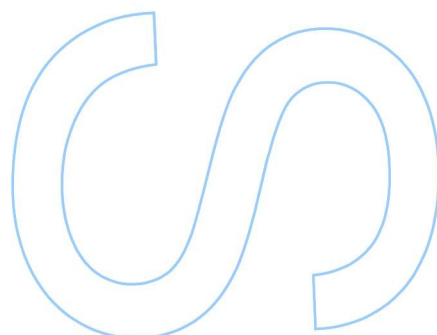
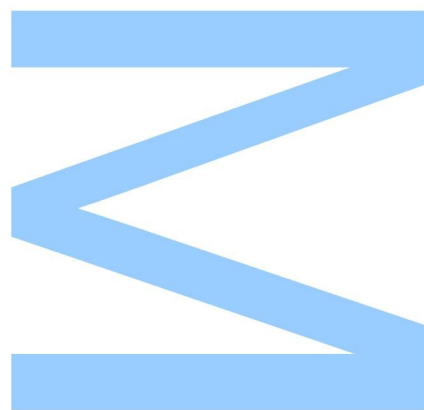




Todas as correções determinadas pelo júri, e só essas, foram efetuadas.

O Presidente do Júri,

Porto, / /



Resumo

Introdução: Desde a sua descoberta e categorização em 1989, o HIV-1 tem se revelado uma doença de patogenese ilusiva. A maioria das descobertas sobre o HIV continuam a ser resultado de experiências *in-vivo* que são dispendiosas e potencialmente mortais, porque a experimentação *in-silico* (em computador) ainda deixa muito a desejar. Muito trabalho tem sido desenvolvido ao nível de epidemiologia comunitária; menos trabalho tem sido realizado no estudo do vírus em si.

Trabalho: Esta tese é uma aventura em paradigmas tais como autómatos celulares, equações diferenciais, modelos baseados em agentes e simulações estocásticas, na esperança de esboçar, em traços gerais, o que as ciências matemáticas têm para oferecer aos médicos que tratam esta doença. Uma perspectiva dos vários veículos de modelação é apresentada para se averiguar qual terá maior potencial.

Resultados: Vários modelos são explorados e é feita uma tentativa de elucidar como poderá a patogénese ser estudada de forma holística. Dos vários modelos e métodos estudados, foram obtidas as seguintes conclusões: os modelos de autómatos celulares deveriam ser sujeitos a previsões de forma a poderem ser validados por outros métodos; as simulações estocásticas podem ajudar a responder a questões que as equações diferenciais não conseguem; que a modelação baseada em agentes não é a panacea prometida por alguns autores, mas uma ferramenta complementar que pode produzir simulações mais rápidas que as simulações estocásticas em alguns casos, e que, noutros casos específicos, podem responder a questões que as últimas não conseguem.

Contribuições: Todos os resultados foram reproduzidos por nós, a não ser quando dito o contrário. Estamos a considerar a publicação dos seguintes trabalhos em particular:

- O modelo de autómatos celulares mais citado é dissecado e o seu poder explicativo é cuidadosamente analisado.
- Um modelo baseado em agentes proeminente é re-trabalhado em termos duma simulação estocástica, e renderizado sob a forma duma rede de reacções cinéticas; esclarecendo alguns dos compromissos entre ferramentas de modelação.

Palavras-chave: biologia teórica; epidemiologia; modelação do HIV; biologia sistémica; autómatos celulares; equações diferenciais ordinárias; modelação baseada em agentes; simulação estocástica; método de Gillespie.

Abstract

Background: Since its discovery and categorization in 1989, HIV-1 has been shown to be a disease of elusive pathogenesis. Most HIV discoveries still happen by *in-vivo* experimentation which is expensive and potentially deadly, because *in-silico* experimentation still leave much to be desired. Much work has been done at the community epidemiological level; less work has been studying the virus itself.

Work: This thesis is an adventure through such paradigms as cellular automata, differential equations, agent-based models, and stochastic simulations in hopes of sketching in broad strokes what mathematical sciences have to offer physicians trying to fight this malady. This is to be a perspective on which modeling avenue might be worthwhile exploring.

Results: Several models are explored. An attempt is made at illuminating how pathogenesis can be studied holistically. From the several models and methods studied the following conclusions were arrived at: cellular automata models may benefit from making predictions that could potentially be validated by other methods; stochastic simulations may help answering questions that differential equations models cannot; and how agent-based modeling is seldom the panacea some authors promise, but a complementary tool that can produce faster simulations than stochastic simulations in some cases, and in other specific cases, can effectively answer questions that the latter cannot.

Contributions: All results were reproduced by us, unless stated otherwise. We are considering publication of the following work in particular:

- The most cited cellular automaton model is dissected and its explanatory power is carefully analyzed.
- One prominent agent-based model is re-worked in terms of a stochastic simulation, and rendered as a kinetic reaction network; shedding light into some modeling trade-offs.

Keywords: theoretical biology; epidemiology; HIV modeling; systems biology; cellular automata; ordinary different equations; agent-based modeling; stochastic simulation; Gillespie method.

Acknowledgments

I would like to thank my supervisor, Prof João Nuno Tavares, for suggesting the theme of the thesis and on how to go about tackling the vast literature which is HIV-1 modeling; together with the rest of the “HIV team” who work in related topics of epidemiology and have accompanied the work: Prof Carla Pinto, and Prof Sónia Gouveia — as well as colleagues Ana Rita Carvalho and Diana Rocha.

Thanks to “beta testers” — Andreas Hillmann and Renato Fernandes — for testing my implementations and the friendly feedback. Shi, Tridane, and Kuang for clarifying questions with regard to their CA model [STK08]. Nuno Fachada, author of Simullm [Fac05], for sharing his experience and bringing me down to earth by dissuading us from the original Sisyphean task of reimplementing SIMMUNE [MM99].

Last but not least, a hat tip to the two persons who have been the most inspiring of my life: Michael Meeks and Rodrigo Marcos. A loving thank you to my mother, PSauro, Joaninha, Sofia.

Contents

Immune System Glossary	xi
Acronyms	xiii
1 Introduction	1
2 Background Knowledge	5
2.1 Grand Summary	6
2.2 Antigen Presenting Cells	9
2.3 HIV Close Encounter and Tropism	10
2.4 Lymphocytes	11
2.4.1 B Cell and Antibodies	11
2.4.2 Helper T Cell (T_H)	13
2.4.3 Killer T Cell (T_C)	14
2.4.4 Natural Killer	14
2.5 Thymus & Bone Marrow (distributed generator)	14
2.6 Specificity	15
2.7 Maturation (distributed learning)	15
2.8 Cytokines (distributed communication)	16
2.9 Lymph Nodes	16
2.10 HIV	17
2.10.1 HIV Treatment	19
2.10.2 HIV Dynamics in Time	20
2.10.3 HIV Dynamics in Space	20
2.10.4 HIV Dynamics in Mutation Space	22
3 Cellular Automata Models	23
3.1 A First Approach	25
3.1.1 Sensitivity Analysis	28
3.2 Wave Propagation	30
3.3 Viral Incubation	33
3.4 Neighborhood Configuration	34
3.4.1 Variable Neighborhood	36
3.5 Treatment	37

4	Differential Equations Models	41
4.1	Aggregate Models	41
4.2	Disaggregate Models	44
4.2.1	Humoral Response	44
4.2.2	Cell-Mediated Response	48
4.2.3	Spatial Dynamics	48
4.2.4	Shape Dynamics	49
5	Agent-Based Models	53
5.1	General Purpose Artificial Immune Systems	54
5.2	Formalism	55
5.3	Event-driven versus time-driven simulation	57
5.4	From ODE to ABM	58
5.5	HIV Modeling	58
5.6	Affinities	59
5.7	Lin-Shuai Model	61
5.7.1	Sensitivity analysis	65
6	Stochastic Simulations Models	69
6.1	Formalism	70
6.1.1	Examples	72
6.1.2	Assumptions	73
6.2	Deterministic Approximation	73
6.3	Chemical Master Equation	74
6.4	SSA Simulation (Gillespie Algorithm)	75
6.4.1	Direct Method	75
6.4.2	τ -leaping Method	75
6.4.3	Chemical Langevin Equation (CLE)	77
6.5	Delay Reactions	77
6.5.1	Delay as Duration	79
6.5.2	Purely Delay Approach	80
6.6	From Agents to Markov Chains	82
6.6.1	Well-Stirred Space	82
6.6.2	Shape Space	86
6.6.3	Reactions Network	88
6.6.4	Results	90
6.7	Spatial Gillespie	91
7	Conclusion	95
7.1	Methodology Remarks	96
7.2	Stochasticity	96
7.3	Physical Space	97
7.4	Shape Space	98
7.5	Medical Usefulness	98
7.6	Technical Acknowledgments	98

Bibliography	101
Appendix	111
A Santos CA implementation (in NetLogo)	111
B Culshaw ODE and SSA delay implementation (in R)	113

List of Figures

2.1	Schematic representation of the process of activation of the elements of the adaptive immune system	9
2.2	B cell state diagram	12
2.3	Anatomy of the lymph node	17
2.4	A sketch of HIV immune response flowchart	18
2.5	Three-stages representation of AIDS	20
2.6	Spatial compartments of differing HIV dynamics	21
3.1	Example of an 1D cellular automaton (CA) of $L = 8$ (of periodic boundary conditions) with 2 possible states: black is <code>true</code> and white is <code>false</code> , following the local rule <code>or</code> on its 2 neighbors	24
3.2	Our schematic diagram based on Santos and Coutinho's model	26
3.3	Our results based on Santos and Coutinho's model	27
3.4	Unbounded boundary conditions reproduction of the model	27
3.5	Several snapshots of the model (using 8-neighbors / Moore neighborhood)	27
3.6	Our sensitivity analysis to various parameters, and respective results in terms of the primary peak, and AIDS phase	29
3.7	Stripped down Santos and Coutinho's model	31
3.8	The behavior of most waves	31
3.9	Under certain conditions, as in $t = 5$ in Figure 3.8, what is called as an "oscillator" in CA literature is formed	31
3.10	Comparing growth functions between regular and oscillator waves	33
3.11	Schematic of part of the model suggested by Shi, Tridane, and Kuang [STK08] featuring viral incubation delay	33
3.12	Our alternative model	33
3.13	Contrasting neighborhood configurations	35
3.14	The different wave patterns, for the aforementioned 2D rules	35
3.15	Our sensitivity analysis to various periods and respective result in terms of the primary peak, and AIDS phase	35
3.16	[STK08]'s model	38
3.17	[STK08]'s model	38
3.18	[STK08]'s model	38
3.19	Adding treatment as in González et al. [Gon+13]	39
3.20	Our approximation to [Gon+13]	39
3.21	Adding treatment to the model as suggested by Shi, Tridane, and Kuang [STK08]	39

3.22 Counter-intuitively, disease resistance actually makes diffusion more aggressive by making oscillator patterns more likely	39
3.23 However, under a more aggressive treatment, oscillator patterns become again less likely	39
4.1 Our numerical simulations of the “fundamental model of HIV” as solid line	44
4.2 Spatial dynamics HIV ordinary differential equation (ODE) model.	49
4.3 Virus mutation model by Nowak.	50
4.4 Virus mutation model by Zhdanov	51
5.1 Example of a potential B cell state diagram	56
5.2 Layers in an agent-based model (ABM) model	59
5.3 Representation of the commonest affinity interaction rules between two cells	59
5.4 Probability of interaction as a function of the Hamming distance between two strings .	60
5.5 Representation of [LS10]’s model	61
5.6 The model stores this information for each molecule	62
5.7 UML static class diagram of Lin Shuai’s model	63
5.8 Our reproduction of the model as a timeseries of the density of agents x (T_H cell), z (T_C cell), and v (HIV)	66
5.9 Number of HIV strains	66
5.10 Our Lin and Shuai’s model sensitivity analysis	66
6.1 Michaelis-Menten enzyme kinetics model	72
6.2 Our deterministic and stochastic reproduction of the fundamental HIV model	72
6.3 Sketch of the model being benchmarked	78
6.4 Our comparison between the DM and the τ -leaping method	78
6.5 Respective performance of both methods with respect to the initial values	78
6.6 SSA reproduction of time-delay HIV model	79
6.7 Graphical comparison of the semantic of both types of delays	80
6.8 Homogeneous representation of the model wherein each molecule type is spread across vectors of length L^2 and in which interactions happen by matching indexes . .	83
6.9 Histograms of the various candidates from which to sample interaction counts based on the ABM model by Lin and Shuai [LS10]	85
6.10 Histograms of the various candidates from which to sample how many new cells may be created based on the population constrains of the model	86
6.11 Histograms of the various candidates from which to sample the incubation period of the model	88
6.12 Demonstration of time complexity trade-off between ABM (agents) and SSA (parameters)	90
7.1 The expressive power of each modeling tool in a set diagram	96
7.2 Illustrating modeling assumptions implicit in kinetic studies	97
A.1 Our Santos and Coutinho’s model implementation in NetLogo	112

List of Algorithms

1	Typical CA algorithm	24
2	Adding an internal clock (delay) to a traditional CA	24
3	Synchronous update scheme	57
4	Asynchronous time update scheme	57
5	Hamming distance computed in C	60
6	Our pseudo-code reformulation of Lin and Shuai's model	63
7	Gillespie's Direct Method	76
8	Gillespie's τ -leaping approximation	76
9	Delay as duration algorithm	81
10	Purely delay algorithm	81
11	Gillespie's First Reaction Method	92
12	Next Reaction Method	92
13	Next SubVolume Method	92

List of Tables

2.1	Major classes of immune cells	7
2.2	Major classes of lymphocytes	8
2.3	Antigen responsible for AIDS	9
3.1	Santos and Coutinho's parametrization of the model	26
3.2	Infected A2 radius R considered for different neighborhood rules	35
5.1	Hamming distances between two strings of 3 bits	60
5.2	Lin and Shuai's parametrization of the model	64
6.1	Example of types of reactions, and respective propensity functions	71
6.2	Illustration of algorithm times	78
7.1	Qualitatively comparison of the several modeling methods	96

Immune System Glossary

adaptive system

immune “database” that learns from previous infections. (pp. ix, 5)

affinity

See: specificity. (pp. ix, 15, 59)

antibody

B Cell Receptor (BCR) part of the B cell that gets released into the blood stream and binds to foreign antigens. *Related:* B cell. (pp. ix, 19)

antigen

any molecule that is targeted by the immune system. (pp. ix)

antigen presenting cell

cells that display foreign antigens in major histocompatibility complex (MHC) on their surfaces, for presentation to T cells. (pp. ix, 7, 9)

apoptosis

cellular self-destruction mechanism; used to dispose of damaged or unneeded cells. *Related:* lysis (pp. ix)

B cell

attacks non-self molecules by the production of antibody molecules into the blood stream, part of the humoral response. *See:* section 2.4.1. (pp. ix, 5, 6, 8, 11–17, 19, 22)

CD4

protein used by HIV to bind to the cell; found predomently in the T_H cell, dendritic cell and macrophage. (pp. ix)

cytokine

protein produced by cells that can be seen as means of immune communication. *See:* section 2.8. (pp. ix, 6, 9, 10, 12–14, 16–18, 58)

dendritic cell

“sentinel” cell which takes up positions beneath the barriers of epithelial cells, acting as APC. (pp. ix, 5–7, 9–14, 16, 17, 21, 22, 48)

enzyme

catalyst that converts molecules (substrates) into other molecules (products); for instance, the reverse transcriptase. (pp. ix, 18)

HIV

human retrovirus which causes AIDS, a molecule containing RNA and several enzymes. *See:* section 2.10. (pp. ix, 3, 9, 14, 23, 24, 28, 30, 36, 41, 42, 47–49, 58, 61, 62, 65, 82, 86, 88, 95, 97)

innate system

white blood cells that identify and neutralize the inborn “database”. (pp. ix, 5)

lymph node

an oval-shaped organ widely distributed throughout the body, from which antibodies are produced by B cells. *See:* section 2.9. (pp. ix, 7, 9–13, 16, 17, 20–22, 26, 28, 30, 44, 45)

lymphocyte

family of cells that can be found primarily in the lymph node. *See:* section 2.4. (pp. ix, 7, 9)

lysis

cell death by bursting, often by a virus or other means by which the integrity of the cellular membrane is compromised. *Related:* apoptosis. (pp. ix)

macrophage

“sentinel” cells that lack mobility; the immune system garbage collectors, also acting as APC. (pp. ix, 5–7, 9–11, 13, 14)

major histocompatibility complex

proteins presented in the cell when activated by an antigen. *Related:* section 2.2. (pp. ix, 6, 9)

natural killer

destroys cells that fail to produce class I MHC molecules, since those might be e.g. hiding a virus. *See:* section 2.4.4. (pp. ix, 5, 8, 14)

neutrophils

first line of defense, these cells destroy everything in sight. (pp. ix, 5, 7, 48)

opsonized

an antigen is said to be opsonized when it features an opsonin molecule, which is a mark that the antigen is to be phagocytosed. (pp. ix, 9)

pathogen

infectious agent; any microorganism, such as a virus, bacterium, prion, fungus or protozoan, that causes disease in its host. (pp. ix, 5, 13)

phagocytosed

a process by which a cell engulfs a solid particle, breaking it down; performed by antigen presenting cells (APCs). (pp. ix)

point mutation

type of mutation that causes the replacement of a single base of nucleotide, such as DNA or RNA. Also known as single-base-pair mutation. (pp. ix, 59)

provirus

a virus genome that is integrated into the DNA of a host cell. (pp. ix)

red blood cell

blood cells that carry oxygen. (pp. ix, 6)

retrovirus

family of enveloped viruses that replicate in a host cell through the process of reverse transcription; this enzyme converts its RNA into DNA making its DNA a provirus. (pp. ix)

reverse transcriptase

enzyme that converts a RNA template into complementary DNA; transported and used by the HIV molecule. (pp. ix, 18)

specificity

molecular specificity refers to the complementary needed for two molecules to bind. *See:* section 5.6. (pp. ix, 15)

T_C cell

activates apoptosis of infected cells.

Also known as: killer T cell; cytotoxic T cell; CTL; CD8⁺ T cell. *See:* section 2.4.3. (pp. ix, 5, 6, 8, 13–15, 18, 19, 48, 49, 61, 62, 64–66, 82, 83, 87, 88)

T_H cell

acts as a decision maker, by stimulating B cells and T_C cells.

Also known as: helper T cell; CD4⁺ T cell. *See:* section 2.4.2. (pp. ix, 5, 7–20, 38, 41, 42, 48, 49, 56, 61, 62, 64–66, 72, 82, 83, 87, 88)

white blood cell

blood cells responsible for defense. (pp. ix, 5, 6, 13, 15, 18, 28)

Acronyms

ABM	agent-based model (pp. ix, 2, 3, 23, 50, 53–55, 57–59, 61, 62, 69, 82, 83, 85–87, 89–91, 93–95)	complex)
APC	antigen presenting cell (pp. ix, 6–10, 18, <i>Glossary</i> : antigen presenting cell)	ODE ordinary differential equation (pp. ix, 2, 3, 41–45, 47–49, 54, 58, 59, 69, 71, 73, 74, 77, 82, 93–97)
BCR	B Cell Receptor (pp. ix, 12, 13)	PDE partial differential equation (pp. ix, 2, 48, 53, 93, 94)
CA	cellular automaton (pp. ix, 2, 3, 23–26, 28, 30, 31, 34, 38, 40, 41, 48, 51, 93–97)	SDE stochastic differential equation (pp. ix, 93)
CTMC	Continuous Time Markov Chain (pp. ix, 3, 82, 85, 86, 90)	SSA stochastic simulation algorithm (pp. ix, 2, 3, 54, 69, 75, 82, 89, 90, 93–95)
DDE	delay differential equation (pp. ix, 79–82)	T_C cell killer T cell. <i>See in glossary</i> : T _C cell (pp. ix)
HIV	human immunodeficiency virus (pp. ix, 9)	T_H cell helper T cell. <i>See in glossary</i> : T _H cell (pp. ix)
MHC	major histocompatibility complex (pp. ix, 6, 7, 9, <i>Glossary</i> : major histocompatibility	TCR T Cell Receptor (pp. ix)

Chapter 1

Introduction

Every discourse, even a poetic or oracular sentence, carries with it a system of rules for producing analogous things and thus an outline of methodology.

Jacques Derrida

With over 35 million infected people at present [Uni13], the HIV-1 retrovirus is today the main focus within infectious diseases. HIV-1 may very well be the most well funded, and intensely studied viral pathogen in the history of science, and yet one of the most mysterious. Despite the huge scientific effort, many aspects of HIV infection dynamics and disease pathogenesis within a host remain elusive. One of the least uncharted details of the virus is its propagation within the human host, which takes place by both cell to cell transmission and plasma diffusion. Spatial dynamics might prove to be a successful venue in helping researchers better understand the virus and the efficiency of drug treatments. Another important aspect of the virus is its rapid rate of mutation. Furthermore, because AIDS is a disease of great variance, we are interested in exploring these models for their stochasticity.

Models serve either to **describe** a phenomenon (from the past), or to **predict** events (into the future). They can also be used to **hypothesize** and test theories with regard to internal congruence. Depending on exactly what one wants to describe or predict, several approaches have been undertaken for the study of HIV dynamics. HIV may very well be the disease with the widest scope of modeling apparatus. Because of privacy concerns and the research costs involved, data is hard to obtain, and no data has been used in the elaboration of this thesis. It is still a good idea to keep in mind what data is available because models should be designed so they can be eventually empirically validated. Most blood measurement tests provide us with the number of free virions (RNA copies), and also (though not always) CD4⁺ T cell counts, that are orders of magnitude smaller and thus harder to measure.

The title of the thesis is a pun on the full title of Gulliver's Travels [Swi26]. In the book, four lands are explored, while in the course of the thesis four major modeling themes are explored:

- ordinary differential equation (ODE)
 - cellular automaton (CA)
 - agent-based model (ABM)
 - stochastic simulation algorithm (SSA)
- $\left. \begin{array}{l} \text{deterministic} \\ \text{stochastic} \end{array} \right\}$

The thesis is divided into the following chapters:

- Chapter 2 provides background on immunology and, in particular, HIV-1;
- Chapter 3 covers present work on CAs models focusing on local spatial aspects of the disease;
- Chapter 4 covers both the aggregate HIV-1 models in ODEs which can and have been validated, and more disaggregated ODE modeling attempts;
- Chapter 5 presents strikes at all-encompassing ABMs models which try to emulate all aspects of the disease;
- Chapter 6 in which we formalize a framework and re-write one ABM, hopefully demonstrating a smarter way to go about simulating ABMs using the SSA, showing the two methods can be made to simulate the same model;
- Chapter 7 closes, presenting some concluding remarks.

Furthermore, a biological glossary is presented at the head of the thesis.

Brief Overview

Perelson, Kirschner, and De Boer [PKD93] worked out a first model of HIV dynamics using a system of **ODEs**. The model tracked: healthy helper T cells (T), latently infected helper T cells (T^*), productively infected helper T cells (T^{**}), and free virions (V). Usually, productively infected and latently infected are merged to a single infected helper T cell variable (T^*), as simplified in a later article [Per+96]. These three variables suffice to allow for a statistically significant fit of patients' disease history, and we can therefore find some interesting parameters and properties about their disease. A system of ODEs is used to model the disease, whereby variables are used to represent the various agents, in their various states. These models may even carry spatial information [GP13]. Some examples are presented in Chapter 4.

At the other end of the spectrum, **ABMs** are disaggregate models where what is modeled are individuals (or agents) and not populations. This paradigm turns things upside-down; each individual in the model stores its properties, rather than individuals being categorized into variables. It is a more natural paradigm for domain experts because it is logically structured closer to the phenomenon at study. It is a more direct mapping of reality into model. Other advantages are that ABMs allow us to trace the fate of a particular agent; also, ABMs can easily associate continuous quantities to an agent; these quantities have to be discretized for most other mathematical models. Continuous variables are possible using partial differential equations (PDEs), but easily become unmanageable and numerical integration boils down to discretization. Their complexity depends heavily on the implementation but, usually, particle simulators (which can be seen as a type of ABM) have execution times of time complexity $\mathcal{O}(n^2)$, and space complexity of $\mathcal{O}(n)$ [Gro15]. Here, n refers to the number of agents, not of variables as in a system of ODEs or reactions as in the SSA algorithm; so it is conceivable that an

ABMs is faster than a ODE model for very small population that require properties being represented into many variables. (Chapter 5.)

The primogenitor and computationally less demanding versions of ABMs models are **CAs**, whereby space (which may not be physical space) is divided in cells, which are usually squares connected to its 4 neighbors (up,down,left,right, also known as von Neumann neighborhood) or 8 neighbors, if we include the diagonals (Moore neighborhood). (Chapter 3.)

In 1976, Gillespie proved his algorithm of **stochastic simulation** of biochemical reactions gave the same results as conventional kinetic treatments using ABM particle simulators [Gil76; Gil77]. The original algorithm used two random variables: one to control the time until the next event/reaction, and another to choose which reaction would occur — it may be seen as a SSA, a type of Continuous Time Markov Chain (CTMC) simulation. Further optimizations are available, as discussed in the respective chapter. As we will show, there is a trade-off between ABM and SSA methods; the first has a complexity that increases with number of agents, but there are no marginal costs in increasing parameters. Increasing parameters has a substantially negative impact when it comes to running SSA and ODE models, since it implies increasing the number of variables. As we will show, models being represented by kinetic reaction networks can be solved deterministically using ODEs or stochastically using the SSA. (See Chapter 6)

The thesis will be an exploration of both: methodology, and specific HIV models.

Out of many scientific papers, a few theoretical models were selected and are presented. Most of the models have not been validated, and are impossible or expensive to verify using current technology. It should be stressed that, while there are thousands of mathematical papers on HIV, few models manage to reproduce all three stages of the disease. We mostly limited the scope of our review to models that were able to reproduce all these three stages. Also, many computational models are not fully described or provided by their authors and so could not be reproduced.

HIV theorists today have been scarcely cited within the medical literature; the main focus of theoretical biology seems to be in presenting congruent and plausible models, and to elaborate methods to be used to computationally simulate them. In the same spirit of Galileo's famous thought experiment, from the book *On Motion*, by showing any other theory for gravitation would be absurd, if HIV modeling is to be useful, it ought to focus on invalidating absurd propositions while making a few clear predictions to be confirmed by experimentation. Medical experimentation is expensive, ridden by ethical questions, and potentially lethal, so there is a vacuum that could be filled by mathematical models.

By methodology, we mean methodology in the purest sense of the word as the study of methods. We sometimes focus more on the methods than on the models themselves. More important than the models reviewed, the idea is to ultimately explore potential pathways to study HIV.

Background Knowledge

I form the light, and create darkness: I make peace, and create evil: I the LORD do all these *things*.

Isaiah 45:7

The greatgrandfather of the immune system is thought to have been a system of self-replicating particles from the primordial soup that managed to form bodies through self-self binding. The immune system is that which distinguishes between self and non-self molecules, in order to keep bodies whole. It stops foreign molecules at entrance, or expels them afterwards. [Som12]

The human immune system is usually divided into innate and adaptive components. The **innate system** is common to all animals (including plants and fungi), and consists in great part of physical and chemical barriers; the gastric acid of the stomach would be such an example, reducing chances of food contamination by killing worm parasites at entrance. But more than that, the innate system encompasses white blood cells that identify and neutralize the historically most common invaders by recognizing patterns of molecules characteristic of general categories of pathogens. The big “selling points” of the innate system are its fast response (in the order of minutes), and not requiring previous exposure to the pathogen.

On the other hand, the **adaptive system** is a “recent” invention, only available to vertebrates. It identifies molecules (usually specific proteins) found only in a specific strain of the pathogen. It requires exposure and is slower — in the order of weeks for a first exposure, and in the order of days in following exposures. It combines synergies and works in harmony with the innate system.

A small listing of main actors involved in both systems:

innate { macrophages
neutrophils
dendritic cells
natural killers

adaptive { T_H cells
T_C cells
B cells

The immune system is an intertwined, complex system that is not yet fully charted. It is not perfect, and is the target of much research. For our study, we are interested in how HIV overpowers and shuts down the immune system, leaving it vulnerable to opportunistic invaders. Other interesting areas of research include: why the immune system fights transplanted tissues and organs; does not kill out of control cells (cancer); and the misdirection of defenses, such as over-the-top immune response against non-pathogens (allergy) or when the immune system identifies self tissues as non-self and

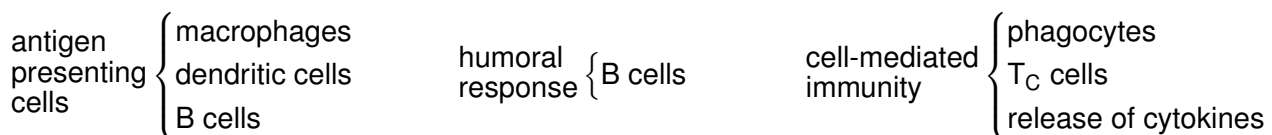
attacks them (autoimmune disease). Interestingly, many attempts have been made at learning how to deal with computer viruses from immune response [OO10].

Despite the intense research funding, HIV-1 is a deeply elusive retrovirus about which there are more questions than answers. Most often than not, the answer to questions as to its *modus operandi* is “we do not know”. There is another species of this virus, HIV-2, which evolved independently from HIV-1, and, while it has been identified outside of Africa, it is mostly confined to West Africa, which is why it is mostly ignored in the literature [Hir+89]. In fact, most literature uses HIV as synonymous to HIV-1, and so will we. Both HIV viruses are mutations from the African SIV virus which only produce AIDS for some of the non-human simians. It also infects humans, but only produces the primary infection stage (fever), and is then eliminated by the immune system. We know both HIV evolved by mutation, and not by genetic recombination like most other species, because they reproduce asexually by infection, as will be detailed later this chapter.

2.1 Grand Summary

This is a general listing of types of cells that constitute our immune defenses. After centrifugation of a blood sample, these are the cells that can be found in the liquified segment layered between the red blood cells (which carry oxygen) and blood plasma (the blood fluid). After centrifugation, they have a white tonality which is why they are known as *white blood cells*, also known as *leukocytes*. They make up less than 1% of total blood volume of an adult [Alb+02, Table 22-1].

The various cells can be divided by their various functions, some of which overlap:



- **Antigen presenting cells (APCs)** are cells that display foreign antigens in class II major histocompatibility complex (MHC) on their surfaces, for presentation to T cells. *See:* section 2.2.
- **Humoral response**, also known as antibody-mediated beta cellularis immunity, refers to the production of antibodies, and the process leading to it. Antibodies are then expelled from the body through several fluids such as mucus and excrement. These fluids are also called humors, hence the “humoral” in “humoral response”, because it was thought that bodily fluids were related to humor states of mind, in ancient medicine.
- **Cell mediated immunity** is the response that does not involve antibodies, but rather phagocytes directly, ingesting foreign molecules, T_C cells destroying infected cells, and by the release of various communication cytokines molecules.

A listing follows of major classes of immune cells, together with the *average* concentration found in a white blood sample, in order to provide a picture of their overall importance. We also specify whether they are usually modeled in HIV dynamics, which will be explored in the following chapters.

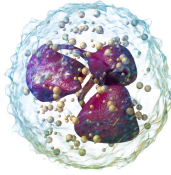
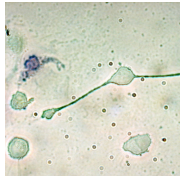
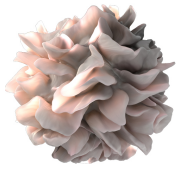
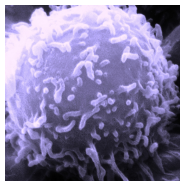
Cell	Summary	Concentration*	Relation to HIV†
	Neutrophils are the white blood first line of defense; these cells destroy everything in sight. Fortunately they are also fast lived and quickly regulated by T _H cells, so they act as a first preempt defensive strike. “Pus” is mostly made of neutrophils.	Blood: 60%	Target of HIV? no Modeled? no
	Macrophage is a “sentinel” cell that lacks mobility. Its main function is cleaning up debris in the blood, phagocytosing debris as a garbage collector. But it may be recruited for infection fighting, phagocytosing antigens directly. It is an antigen presenting cell (APC) (since it displays class II MHC complexes). It is thought it acts as APC, so that experienced T cells can be restimulated while traveling in the blood stream.	Blood: 0.04% before differentiation	Target? yes (they feature CD4 and CCR5) Modeled? sometimes
	Dendritic cell is a “sentinel” cell which take up positions beneath the barriers of epithelial cells. It is starfish-shaped and so can capture opsonized antigens. Once activated, it migrates to the next lymph node where it interacts with T cells and B cells to initiate and shape the adaptive immune response.	Blood: < 0.1%	Target? yes (CD4 and CCR5) Modeled? sometimes
	Lymphocyte is any of a family of cells: T cell, B cell and Natural Killer. These cells are named lymphocytes because they are the main cells found in the lymph node. See: section 2.4.	Blood: 35% (2500 count/μL)	(See below)

Table 2.1: Major classes of immune cells.

Lymphocytes (of the adaptive system) are classified in the following Table 2.2.

*Concentration of blood refers to peripheral blood, which is the circulating pool of blood not sequestered within the lymphatic system, spleen, liver, or bone marrow. The numbers cited are for elucidation purposes; numbers may vary, we used averages from Abbas, Lichtman, and Pillai [ALP15, Table 2-1 and Table 2-2]. Dendritic cells negligible count comes from Jenkins et al. [Jen+98].

†Relation to HIV: *Target of HIV?* details whether the cell is prone to HIV infection; for infection to be possible it must feature the CD4 protein and either the CCR5 or the CXCR4 protein, depending on the virus strain. Usually HIV of the CCR5 strain (M-tropic) are found at the genesis of the disease because it is thought macrophages are the first cells to be infected. *Modeled?* means whether most published models include the cell as an endogenous variable.

Lymphocyte	Concentration	Relation to HIV
<p>T_H cell (helper T cell) acts as a gateway between dendritic cells and B cells, as a decision maker, sniffing the non-selfness of the presented antigen. Note: B cells are only activated after confirmation by a T_H cell for most antigens as is the case for HIV (these antigens are known as T-cell dependent antigens).</p> <p>Also known as: CD4⁺ T cell. See: section 2.4.2.</p>	<p>Blood: 35-60%</p> <p>Lymph: 50-60%</p> <p>Spleen: 50-60%</p>	<p>Target of HIV? yes (CD4 & CCR5/CXCR4)</p> <p>Modeled? always</p>
<p>T_C cell (killer T cell) activates apoptosis of cells when it is able to bind to their class I MHC molecules, which are located within the interior of the cell.</p> <p>Also known as: cytotoxic T cell; CTL; CD8⁺ T cell. See: section 2.4.3.</p>	<p>Blood: 15-40%</p> <p>Lymph: 15-20%</p> <p>Spleen: 10-15%</p>	<p>Target? no</p> <p>Modeled? often (because they kill infected cells)</p>
<p>Treg (regulatory T cells) suppresses other T cells in order to regulate the escalation of the immune response.</p>	<p>Blood: rare</p> <p>Lymph: 10%</p> <p>Spleen: 10%</p>	<p>Target? yes</p> <p>Modeled? no</p>
<p>B cell attacks non-self molecules, detected by the adaptive system, through the production of antibody molecules into the blood stream which binds to them. This is called the humoral response. See: section 2.4.1.</p>	<p>Blood: 5-20%</p> <p>Lymph: 20-25%</p> <p>Spleen: 45-55%</p>	<p>Target? no</p> <p>Modeled? often</p>
<p>Natural killer is the corollary to the T_C cells. It destroys cells that fail to produce class I MHC molecules, indicating “stressed” cells, or ones hiding a virus. It kills indiscriminately, and is therefore categorized as part of the innate system. They are not T cells. See: section 2.4.4</p>	<p>Blood: 5-30%</p> <p>Lymph: rare</p> <p>Spleen: 10%</p>	<p>Target? no</p> <p>Modeled? no</p>
<p>γδ T cells (delta gamma T cell) is a rare and mysterious cell that performs the function of both T_H cell and T_C cell.</p>	<p>rare</p>	<p>Target? yes</p> <p>Modeled? no</p>
<p>Natural killer T cells is a rare cell, not to be confused with the T_C cells or natural killers, but it does perform some of the same functions.</p>	<p>Blood: 0.1%</p>	<p>Target? some</p> <p>Modeled? no</p>

Table 2.2: Major classes of lymphocytes.

Long story short, all cells feature a class I MHC (and are destroyed by NK cells otherwise), but only APC cells feature class II MHC. Class I MHC is probed by T_C cell to identify certain conditions of the cell. Class II MHC function as billboards to the rest of the immune system about captured antigens.

A fuller listing of the agents involved within the immune system can be gathered from the online PDF material by Novotny [Nov14]. Last but not least, the leading star...

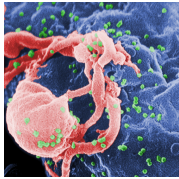
Molecule	Summary	Concentration
 (represented as small green molecules next to the lymphocytes)	HIV refers to the human retrovirus causing AIDS. A retrovirus is a lifeless molecular envelope of RNA, and of several enzymes which convert and merge viral RNA into cellular DNA. They are not considered alive; life is by definition any molecule that is able to self-replicate — retroviruses require injecting replication instructions (DNA) into a host cell. Two HIV virus species exist, both infecting cells displaying CD4 proteins on the surface — primarily, T _H cells. This (and most) work concerns HIV-1 which is the variant of HIV widespread outside of Africa. Two main strains of HIV-1 exist, infecting only cells that have either CCR5 or CXCR4 proteins on their membrane, in addition to CD4. See: section 2.10.	Perceptible when > 40 – 75 copies/mL in the plasma. Mostly found in the lymph node.

Table 2.3: Antigen responsible for AIDS.

2.2 Antigen Presenting Cells

Antigen presenting cell (APC) are cells that display foreign antigens in major histocompatibility complex (MHC) on their surfaces, for presentation to T cells (see Figure 2.1). These cells incorporate an antigen (such as an opsonized pathogen, that is a cell marked for phagocytosis) and codify it for display in proteins on their surface called class II major histocompatibility complex (MHC). They serve to activate and stimulate lymphocytes, triggering immune response, as explained in section 2.4 on page 11. Activation is also known as priming in the literature. While circulating, T cells are restimulated by macrophages. Dendritic cells are also APC cells, where the “close encounter” first takes place.

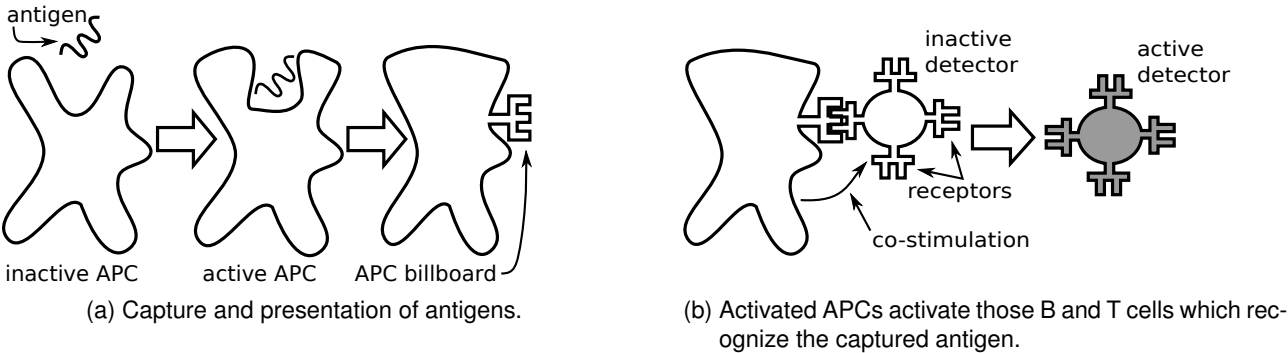


Figure 2.1: Schematic representation of the process of activation of the elements of the adaptive immune system. [FC08, Figure 5.4]

Dendritic cells are classified as APC cells because they are “sentinel” cells that take up positions beneath the barriers of epithelial cells. When the tissue in which they reside becomes a battle site, cytokines produced by the innate system activate dendritic cells and induce them to travel to the closest lymph node, in order to present antigens to the lymphocytes there. The antigens captured

are advertised in the class I MHC molecules they feature on their surface; which are then upregulated after being activated. Their lifetime after activation is small so that following dendritic cells may report more updated information on the infection; also their lifetime is prolonged when they engage with the T_H cell. Dendritic cells are imprinted with the local infection cytokines, which means that, as they come to lymph nodes, other cells know the source of the infection. These dendritic cells are not to be confused with the follicular dendritic cells which make up the lymph node structure.

Dendritic cells found in epidermal skin and mucus are known as *Langerhans cells*. These cells are one of the first contact points of HIV-1 since they can be found in the foreskin of the penis, as well as in vaginal and oral mucosa. The initial infection contact of HIV is still contested, but it appears that dendritic cells are one of the first cells to be infected and transfer the virus to T_H cells [Kaw+05]. Such transfer may occur locally in inflamed mucosa or after dendritic cells have matured and migrated to local lymph nodes.

Note: these cells are not to be confused with “follicular dendritic cells”. Lymph nodes are made up of a mesh of “follicular dendritic cells”, which, despite the name, are completely unrelated to “dendritic cells”. They are derived from a different lineage.

Another type of APC cells are **macrophages**. These cells lack mobility. They have been considered crucial for HIV dynamics because they feature CD4 proteins in their surface, and so are prone to infection. They are deemed important because the primary infection seems largely restricted to relatively homogeneous M-tropic HIV virus. The fact that M-tropic HIV virus is prevalent during primary infection seems to imply infection and an important role for macrophages [NH03]. This is because there are two strains of HIV virus which can be divided into the categories studied next.

2.3 HIV Close Encounter and Tropism

There are two strains of HIV virus, which are known as the two HIV tropisms:

- **M-tropic** virus mostly uses beta-chemokine receptor CCR5 for entry, and can infect both T_H cells and macrophages;
- **T-tropic** virus mostly uses alpha-chemokine receptor CXCR4 for entry, and infects primarily T_H cells, but may also infect macrophages. [CS02]

These are the extremes: M-tropic HIV does better with CCR5 receptors, while T-tropic HIV does better with CXCR4 receptors. This does not mean M-tropic HIV can enter only cells display CCR5 proteins, and not CXCR4. HIV which are equally good with both proteins are said to be dual-tropic. Other subtle variations exist as well; this is a simplification [BMF99]. Beyond having a larger breadth of potential hosts, M-tropic HIV also seem to infect faster than T-tropic [PS07].

Humans who carry the “delta 32” mutation are resistant to M-tropic strains of HIV-1 infection because of a defection in CCR5 expression. These people are largely immune to HIV-1. The “Berlin patient”, the only known patient to apparently have been cured of HIV-1, was cured by received bone marrow transplant from a person having this mutation.

Research publications agree that dendritic cells play a role of important magnitude in HIV-1 infection. However, there is disagreement on the direction of the contribution. Some argue that HIV directly infects T_H cells in the foreskin or in mucus, and act as a barrier for HIV propagation because,

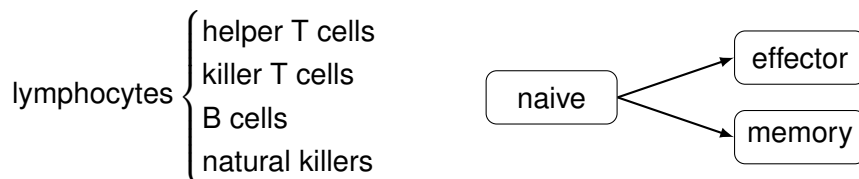
once captured by an APC, the virus quickly degrades. Others however argue these dendritic cells are the ones responsible for taking the virus to T_H cells [WNG08]. And, while dendritic cells can be infected *in vitro*, there is dispute on whether they are actually infected *in vivo*, because no evidence of such has been found in humans, though experiments with monkeys do show infected dendritic cells [Wil+05].

The probability of infection of immature dendritic cells is low, and happens through C-type lectin receptors (CLRs). The most common CLR in both dendritic cell and macrophage is DC-SIGN. The low probability leads to a negative selection of T-tropic HIV, and viruses that persist beyond the 24 hour travel time of the dendritic cell to the lymph node. [Tur+03] As dendritic cells mature, the “quasi-monopoly” of CCR5 over CXCR-4 receptors is challenged, as CCR5 receptors are down-regulated. Infection of dendritic cells is also of lower productivity than that of T_H cells and of macrophages; and it has been suggested that infection of dendritic cells may not be necessary, and these cells act only as vehicles to transport the virus to the lymph node. However, this point is still contended since HIV progressively degrades during the 24h travel time. It is probably safer to assume dendritic cell infection is the vehicle for transport and subsequent breeding of the virus in the lymph node.

Most mathematical models however avoid this question by ignoring any dynamics prior to the first T_H cell infection. Some older models like ones based on ImmSim did assume dendritic participation in fomenting disease (see section 5.1 on page 54 from Chapter 5) [Sie+90].

2.4 Lymphocytes

By definition, **lymphocyte** refers to such cells as T, B and natural killer. The name comes from the fact these are the cells mainly found at the lymph node. There is no other biological basis for the definition; they are actually produced from different organs: T cells from the thymus, while B cells come from the bone marrow, which is why they are called T and B cells, respectively. While they serve very different functions, they go through a similar maturation process after which from the naive state, they become either active effector cells or inactive memory cells.



Some properties are common to all lymphocytes, which are the main defense coordinators and responders, all while operating from one of the several lymph nodes. B and T cells will be described afterwards in more detail. These cells proliferate when exposed to an antigen, forming effector and memory lymphocytes. Effector lymphocytes act to eliminate the antigen; either by releasing antibodies (B cells), cytotoxic granules (killer T cells), or by signaling to other cells (helper T cells). Memory lymphocytes remain in the system and circulate for an extended period ready to respond to the same antigen upon future exposure.

2.4.1 B Cell and Antibodies

B cells make up the humoral response of the system, by producing *antibodies* that bind against the attacker. A molecule that binds to an antibody is called an *antigen*.

The antibody protein is just like the B Cell Receptor (BCR), except that it lacks the protein sequences at the tip of the heavy chain which anchors the BCR to the surface of the cell; so antibodies are the receptors that are released from the cell. They travel through the blood stream and bind to epitopes of antigens, neutralizing them. It is not known exactly how the BCR protein is sequenced. We do know that all BCRs of a mature B cell share the same protein sequence. It is the result of a mix and match strategy, so each B cell has their own receptor specification; there is such a multitude of possible receptors, that collectively, B cells could recognize virtually any organic molecule [Som12, Lecture 3]. B cells mature in the bone marrow. (T cells mature in the thymus.) They are found primarily in lymph nodes, though they also circulate.

B cells are not easily triggered to produce antibodies. The BCR (outside the surface) recognizes the antigen but the activation signal is only sent by $Ig\alpha$ and $Ig\beta$ proteins which are located inside the cell. Since these two parts of the cell are disjoint, the activation signal is only sent when many BCR cluster at the surface of the cell — they are then said to have been *crosslinked*, although they are not actually linked — which can happen when several BCR bind to epitopes on antigens that are clumped together. The B cell also has a receptor protein that recognizes an opsonized antigen, speeding up the process of B cell activation and reducing the number of BCR that must be clustered. An antigen is said to be opsonized when it is disabled by an antibody — meaning the cell knows the antigen has already been recognized as a threat previously. Before being activated, a B cell is said to be naive or virgin. Afterwards they are said to be experienced.

Crosslink is not enough to fully activate the B cell; a further signal is necessary. This co-stimulatory signal may be supplied by an activated T_H cell, when a T_H cell surface protein called CD40L plugs into the CD40 protein at the surface of the B cell. The B cell is then activated, if it was crosslinked. In certain cases the activation signal may be T-cell independent; that can happen with certain antigens that have repeated epitopes which can crosslink a multitude of BCR receptors, and the B cell recognizes molecular patterns characteristic of certain bacteria and parasites. We are concerned only about T-cell dependent activation in our case study.

Once B cells have been activated and have proliferated to build up their numbers, there comes the next stage of B cell life cycle: maturation. Maturation can be divided into three steps, not necessarily sequential: *class switching*, in which the B cell chooses what class of antibody to produce; *somatic hypermutation*, in which the rearranged genes of the BCR undergo mutation and *selection*, which further increases affinity to the antigen.

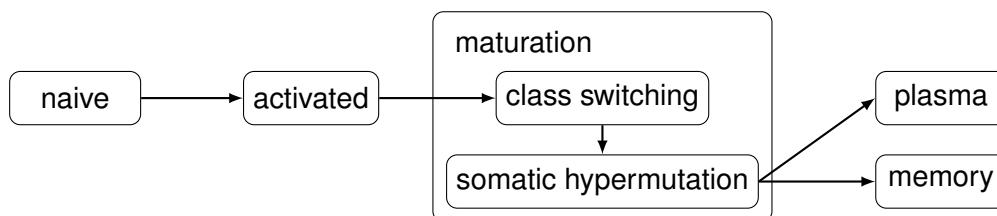


Figure 2.2: B cell state diagram.

During **class switching**, the B cell comes to produce different antibodies. What influences class switching are the cytokines of the environment. The cytokines are usually produced by the T_H cells while activating the B cell; T_H cells in turn know which cytokines to produce based on the source cytokines imprinted in dendritic cells. The region in the antigen that binds to the antibody is always the same. But the antibody region (called the F_C region) differs; this means they are better suited for

different tasks. For example, IgA antibodies are good at collecting pathogens together in clumps that are swept out of the body with mucus or feces — in fact, rejected bacteria account for 30% of normal fecal matter. The default class of antibodies are IgM, which are common to lower vertebrates as well. IgG is particularly suited for viruses, and are the ones produced in response to HIV. [Som12, Lecture 3]

Ordinary mutation rates are pretty low — about one base per 100 million bases per DNA replication cycle. But, during **somatic hypermutation**, B cells may reach mutation rates as high as one mutated base per 1,000 bases per generation. For B cells to continue to proliferate and build up numbers, they must be continually re-stimulated, by binding to its cognate antigen; this results in a selection pressure for higher affinity B cells, since those that respond more easily to the antigen would also proliferate more easily. Current models (using strings and Hamming distance) are incapable of capturing the richness of such phenomenon. Somatic hypermutation is also controlled by T_H cells' cytokines. [Som12, Lecture 3] [Woo06, Chapter 5]

To give an idea of the magnitude of numbers that mathematical models have to wrestle with, here are some from the B cell; Production: one billion per day. BCR count: 100,000 per cell. Antibody production: 2,000 per cell per second. [Som12, Lecture 3].

There are few mathematical models that explain HIV dynamics by recurring to humoral response, at least endogenously. Most focus on T_C cell response in killing infected T_H cells, rather than antibodies killing free viruses. In large part, this is probably because the medical literature is still lacking in the area, because professionals are very much unsure what role humoral response plays in HIV dynamics [MF09].

2.4.2 Helper T Cell (T_H)

Helper T cells (T_H) act as decision makers and informers of B cells, after collecting information from a dendritic cell.

Like the B cell, for a T_H cell to be activated, its receptors must recognize their cognate antigen, as displayed by class II MHC molecules on the surface of activated dendritic cells, thus ensuing crosslink. Furthermore, a co-stimulatory signal is required from the dendritic cell; this signal involves protein B7 located on the surface of the dendritic cell to plug to a protein called CD28 on the surface of the T cell. Resting dendritic cells also feature B7 proteins and low levels of MHC molecules, but only when they become activated do they produce B7 and MHC in quantities enough to stimulate virgin T cells. Three types of antigen presenting cells have been identified: activated dendritic cells, activated macrophages, and activated B cells. Like the other white blood cells, antigen presenting cells are continuously being replenished. It is estimated that B cells (as antigen presenting cells) are 100 to 10,000-fold better at stimulating T_H cells. Notice that dendritic cells continue being the main antigen presenting cells, because they are the first to encounter and signal the infection.

T_H cells differentiate to produce different cytokines, depending on the cytokine produced by the dendritic cell as it arrives the lymph node — which in turn depends on the source of the dendritic cell, as previously seen. There are three major subsets of helper T cells: T_{H1} , T_{H2} , and T_{H17} (usually they are a mixture). Different T_H cells produce different cytokines which instruct B cells about which antibodies to produce after class switching. We are mostly concerned with T_{H1} cells. Virgin T cells mature as T_{H1} cells when presented with the IL-12 cytokine by the dendritic cell. They will in turn

secrete TNF cytokines that help activate macrophages and natural killers. They also produce IFN- γ which influences B cells to class switch to produce IgG3 antibodies. Furthermore, they also produce IL-2, which is a cytokine that commands growth, and thus stimulates proliferation of T_C cells, natural killers, and T_{H1} cells themselves. Interestingly, there are some T_H cells, so-called T_{H0} , that never choose a function and can perform the action of all previous T_H cell types. [Som12, Lecture 5 and 6] [Woo06, Chapter 4]

HIV targets the CD4 protein, which is mainly found in T_H cells — this is also why T_H cells are sometimes called $CD4^+$ T cells. In HIV dynamics, only T_H cell infection is usually considered, given that they make up the majority of $CD4^+$ cells. The CD nomenclature refers to clusters of proteins primarily found at the surface of cells. The number in the CD nomenclature refers not to any specific trait or configuration of the protein, but merely to the chronological order in which they were discovered. Because cells have several proteins in its surface, they are sometimes referred with a “+” suffix indicating the cell expresses the protein, or a “-” suffix indicating that it does not.

2.4.3 Killer T Cell (T_C)

Killer T cell (T_C) destroys cells if it binds to its class I MHC molecules, which are located within the interior of the cell and indicate the presence of an antigen.

When a virus infects a cell and the cell becomes productively infected, those molecules allow the T_C cells to find proteins produced by the antigen within the cell it has infected. Viral epitopes cannot hide from T_C cells [MR01]. When virus-infected cells die by apoptosis, the DNA of unassembled viruses is destroyed along with the target cell’s DNA; everything is then disposed of by macrophages.

Interestingly, killer T cells are also responsible for the destruction of misbehaving cells, such as cancerous cells. They are therefore an important part of our immune system, and are often times included in immune models. It is still a mystery how killer T cells become activated. But it is thought that without the help of a helper T cell, killer T cells do not last long.

2.4.4 Natural Killer

Natural killers complement T_C cells by destroying cells that fail to produce class I MHC molecules; those may be “stressed” cells, or may be hiding a virus.

Two classes of Major Histocompatibility Complex (MHC) exist. **MHC I** may be found in the interior of all nucleated cells, and is inspected by T_C cells. On the other hand, **MHC II** molecules are found in any antigen presenting cell (from the dendritic cells to the B cell) and are external to the cell, advertising the antigen to T_H cells. Hence cells featuring MHC II are called antigen presenting cells. The first MHC to be discovered was class I, and it was discovered in relation to transplant rejections, hence its name [Som12, Lecture 4].

2.5 Thymus & Bone Marrow (distributed generator)

Thymus and the **bone marrow** are primary lymphoid organs producing T cells (thymus) and B cells (the bone marrow; as well as dendritic cells and all other myeloid cells). These primary organs are not usually explicit in the model, and their function is modeled exogenously, through a continuous, constant or variable, production of white blood cells. When the production of cells is

variable, — meaning the production rates of new cells is impacted by the disease — it is said these organs are implicitly modeled.

Each newborn (naive) cell is different from each other, in order to react to different molecules. Through the daily production of white blood cells in the order of the billions, this guarantees our immune system has somewhere a cell that can react to virtually any molecule in the universe. They are “tested” against self-molecules of the body, and, if they react, they are not allowed into the system. This process called of negative selection serves as the pillar of the self-nonself recognition system.

Both helper and killer T cells (T_H cell and T_C cell) are continuously produced and trained in the thymus. Like the bone marrow for B cells, the thymus produces T cells with different specificities that can respond to different organic molecules. There is a process of negative selection so that only T cells that do not respond to self molecules are allowed to exit the thymus. They must be activated before they can perform their respective function [Plo13].

In mathematical modeling, the specificity affinity potential between T and B cells and their cognate antigen is most often calculated as the Hamming distance between two binary strings which is randomly assigned at start to the two cells being compared (described next). Nowak first introduced viral strains in differential equation models, though without a concept of binding affinities (model 4.6 on page 49) [NMA90].

2.6 Specificity

Variance in the shapes of proteins on the cells’ surface is what allow the immune system to recognize non-self invaders, giving rise to different degrees of cellular **specificity**. White blood cells have different degrees of affinity between each other; also known as the shape space as proposed by Perelson and Oster [PO79].

Given the virtual impossibility of realistically simulating molecular binding, a common approach, which started with Sieburg et al. [Sie+90] from the ImmSim simulator, and then Nowak et al. [Now+91], is to take specificity of the receptor or paratope of each cell or virion as a 8-bit string (a byte). At creation, each cell or molecules is attributed a string, which is then tested for affinity. Technical details will be fully explored in section 5.6 on page 59 from Chapter 5.

2.7 Maturation (distributed learning)

This is the process explored earlier whereby T and B cells transit from the naive state into the mature state. All this happens within the primary organs (thymus and bone marrow), and thus are irrelevant to us.

Babies are born with little protection against disease, since their white blood cells have not yet mature. However they are not completely defenseless. It is thought that mother’s milk contains antibodies produced by the mother. The immune system of the mother is compelled to produce antibodies through her contact with the baby, namely kissing. [Som12, Lecture 7]

2.8 Cytokines (distributed communication)

Cytokines are a broad category of small proteins that are used in cell signaling. Cytokines include chemokines, interferons, interleukins, lymphokines, tumour necrosis factors. These are molecules released by cells to communicate. They are released mainly by immune cells, but also by other cell, for instance when damaged.

Chemokines induce movement, directing chemotaxis in nearby responsive cells. Chemotaxis refer to the gradients that guide movement along the environment; chemotaxis gradients may be either positive or negative.

Chemokines are particularly interesting because they bind against cellular CCR5 and CXCR4 co-receptor proteins. This means that the more chemokines exist in the environment, the less of these proteins are available for viral entrance into the cell. They serve effectively as an inhibitor, or a natural non-intended barrier to HIV [Kin+00]. Actual vaccines have been proposed in light of this [KMV11]. This is little studied in mathematical models though.

2.9 Lymph Nodes

For our case study, we are mainly concerned on the function of the secondary lymphoid organs known as **lymph nodes** (Figure 2.3 on the following page). These nodes complement the primary organs (the thymus and the bone marrow seen in section 2.5 on page 14). These are nodes strategically located along the body, in places next to possible antigen invasion vectors. Examples of these nodes are: the spleen (blood infections), the appendix, “Peyer’s patches” in the intestine (to defend against food with parasites), tonsils and others (because of respiratory influx). These is where usually antigen is presented, and T and B cells are activated.

Conventional lymph nodes are made of loose networks of follicular dendritic cells (not to confuse with the previously mentioned sentinel dendritic cells), and are filled up mostly by B cells. In case of disease, lymph nodes tend to swell as B cells proliferate in germinative centers. Follicular dendritic cells, due to their location, also capture opsonized antigens, especially because they have receptors that bind to antibodies, and thus help keeping B cells in the germinative centers alive and producing antibodies. B cells multiply in germinative centers and can double every 6 hours. [Som12, Lecture 7]

500 billion lymphocytes circulate each day through the various lymph nodes. 10,000 lymphocytes exit the blood and enter the average lymph node every second by passing between **high endothelial venules (HEV)**. T_H cells in particular recirculate the blood stream in cycles of 12 to 24 hours, helping other lymph nodes. They tend to accumulate in the **paracortex** (also known as the T cell area), being retained there by adhesion molecules — which makes sense since dendritic cells are also found in the paracortex. Within the cortex is a reticular network (RN) — a system of collagen fibers and extracellular matrix (ECM) — produced and wrapped by fibroblastic reticular cells (FRC); the space between reticular fibers is $[5,20] \mu\text{m}$ (micrometer), accommodating two or three lymphocytes. While migration velocity of lymphocytes is $[12,28] \mu\text{m min}^{-1}$, it will also depend on the density of the fiber. [Kal+01]

Dendritic cells arrive at the subcapsular sinus (SCS) through afferent lymph, carrying information from the peripheral tissues, and then migrate into the paracortex to interact with T cells. Several macrophage subsets are distributed at the medulla and SCS regions, where lymphocytes are relatively sparse. While these structures provide lymphocytes enough room for mobility, their exact role

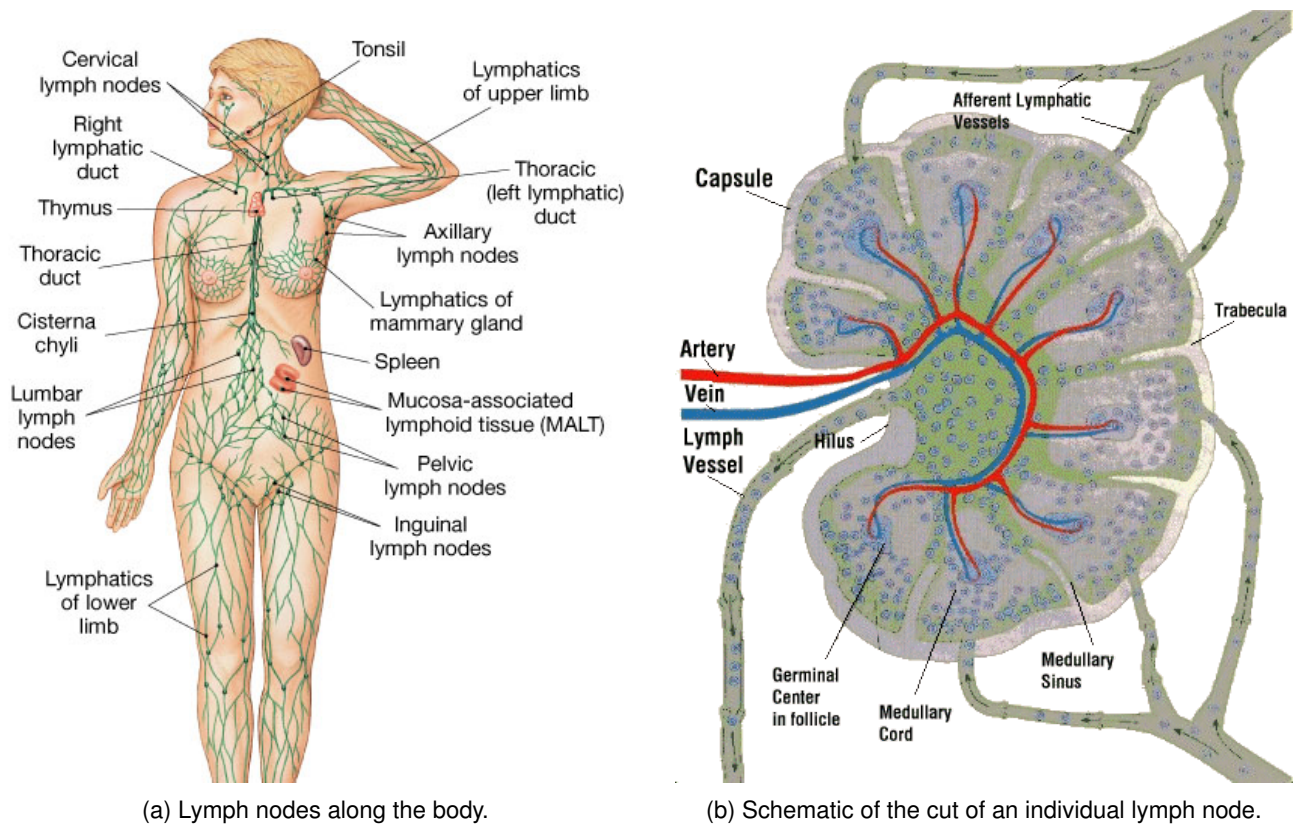


Figure 2.3: Anatomy of the lymph node. © Copyright 2004 Pearson Education, Inc., publishing as Benjamin Cummings

is elusive [Kat+04].

Naive B cells upon entering the lymph node express receptors for the CXCL13 cytokine produced by follicular dendritic cells in the areas where opsonized antigen is being presented. Upon finding its cognate antigen, B cells downregulate the expression of CXCL13 receptors and upregulate the expression of CCR7 receptors. These receptors detects the cytokine that is produced by cells in the border region where activated T_H cells and B cells meet. Likewise, T_H cells which have been activated by dendritic cells also upregulate the expression of CCR7 receptors — afterwards, some T cells lose the CCR7 and upregulate a receptor that guides them into the B cell follicles to help with class switching and somatic hypermutation.

HIV free virions exist primarily in the lymph node. It is estimated that the FDC-associated pool of HIV RNA is about 10^{11} copies in a 70kg HIV-infected individual; FDC pool RNA is greater than plasma RNA in the orders of 10^2 to 10^4 , sometimes a few orders higher. [Haa+96] The effectiveness of differing treatments has also been found to differ for FDC-associated virions. [HSP00]

2.10 HIV

AIDS was first clinically observed in 1981, and was named in 1982. HIV, the virus that causes AIDS, was named in 1986. Genetically, it is clear HIV comes from a mutation of a virus from the simian immunodeficiency virus (SIV) family which often infects humans that illegally eat wild chimpanzees, but is otherwise inoffensive. The immune system is successful in fighting SIV, only resulting in flu-like symptoms for this duration. HIV however is fatal; it puts the immune system working in overdrive, completely obliterating it by continuously activating it [SF03]. According to an United Nations report,

approximately 35.3 million people are reportedly living with HIV worldwide [Uni13]. Like most authors, we are only considering HIV-1 which is widespread in the West, and not HIV-2 which is endemic to West Africa.

An HIV free virion is an enveloped RNA virus of 120 nm (nanometer) of diameter (in average) [Zhu+03], whose outer surface bears the glycoprotein gp120, containing several enzymes besides the RNA [CS02]. Free virions infect target cells by the binding of gp120 to CD4 and a chemokine coreceptor on the target cell surface, as discussed in section 2.3 on page 10.

The virus contains within the envelope the following enzymes which will be elaborated later over section 3.5 on page 37 on HIV treatments:

- reverse transcriptase enzyme
- protease enzyme
- integrase enzyme

It is much smaller than white blood cells, and are produced at massive quantities; in any given blood sample, they are many orders of magnitude more common than white blood cells; they grow from billions per milliliter of blood in a seropositive individual to the hundreds of billion when AIDS is first diagnosed [Pia+93]. In fact, usual HIV tests only measure free virion RNA copies, since T cells counts are not as easily measured. The massive viral quantity proves to be a challenge to more exact, stochastic methods.

HIV dynamics are similar to those of any other T-cell dependent disease. It is properly detected and the immune system is activated as expected. Symptoms are identical to those of the flu, as the immune system broadcasts cytokines to prepare all the players for battle (Figure 2.4).

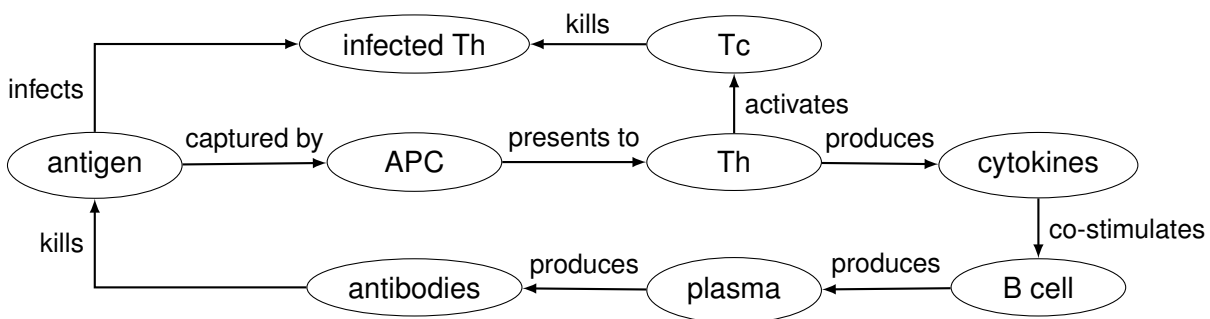


Figure 2.4: A sketch of HIV immune response flowchart.

The disease starts when the virus penetrates the rectal or vaginal mucosa infecting CD4⁺ cells. As the virus infects these cells (most commonly, T_H cells), the reverse transcription enzyme it carries converts the RNA it carries into DNA. Another enzyme it carries (protease) cuts cellular DNA, allowing viral DNA to merge with the cell's. The cell is therefore instructed to produce HIV copies — until the cell bursts when it no longer can comport the thousands of HIV copies produced within itself. It is thought there is a latency period, during which no HIV copy is produced, and during which the infection is not detected by T_C cell. Only later, in response to unknown signals, it is thought the virus starts to be produced. Furthermore, HIV's reverse transcription enzyme is, as any physical process, error-prone, and, because the magnitude of copies is so large, rapidly new “beneficial” mutations are born. Due to the rapid mutation rate, the new strain may not be recognized as well by T_C cells and antibodies, that were trained and negatively selected for the old strain. According to this theory, HIV dominates the immune system mainly because:

1. the virus has a high replication rate — this is why it is never fully cleared;
2. it can hide as a provirus (in the form of DNA), where it goes undetected;
3. it mutates too rapidly, forcing the adaptive system to go through the process of fighting a new virus, all the while attacking a crucial component of the system. [Som12, Lecture 13]

Another popular school of thought — immune network theory — says HIV manages to mutate in such a way as to have its epitopes resemble too closely the V regions of the main population of antibodies. These are the regions antibodies bind to. This means B cells come to produce antibodies that kill the immune system's own T_C cells. Vaccines are in the works based on this theory. Few mathematical work, none studied hereby, has been done in this alternative explanation [Hof+12].

2.10.1 HIV Treatment

Several treatments in the form of drugs exist. In fact, treatments have been so successful that HIV has in some parts of the world become a chronic disease. The first drug (AZT, now called ZDV) was approved in 1987 — the fastest drug ever to be approved, due to the panic of the booming disease — and since then about other 30 drugs have been approved. Due to the high mutation rate of the virus — rather than using one drug at a time — a cocktail of drugs is used so that it is very much less likely the virus mutates resistance against all drugs at once. This technique is called Highly Active Antiretroviral Therapy (HAART) and it combines several antiretrovirals, sometimes in the same pill [Air+10]. Those antiretrovirals include:

- **Nucleotide Reverse Transcriptase Inhibitors (NRTIs, aka “nukes”)** and **Non-Nucleoside Reverse Transcriptase Inhibitors (NNRTIs, aka “non-nukes”)** both inhibit the reverse transcriptase enzyme, which converts viral RNA into DNA — nukes act in the genetic material, while non-nukes act directly on the enzyme. It is a distinction without a difference from the point of view of intercellular modeling. The first drugs (such as AZT) were reverse transcriptase inhibitors. NRTIs can interfere with mitochondrial DNA, while NNRTIs have neuro-psychiatric effects including suicidal ideation.
- **Protease inhibitors (PIs)** inhibit the protease enzyme, which is used to cut cell's DNA [Ho+95].
- **Integrase inhibitors (INSTIs)** inhibit the integrase enzyme, which is used to integrate viral DNA into the cell's DNA. They are recent, but seem the best tolerated.
- **Entry or fusion inhibitors** target $CD4^+$ receptors which HIV uses to infect the cell. Maraviroc targets T_H cells CCR5 receptor, and, in some case, HIV mutates to target the CXCR4 receptor. Enfuvirtide is a peptide drug that acts on HIV's gp41. [Woo06, Chapter 12] [Som12, Lecture 13]

There used to be some discussion as to when treatment should be started: if early, or delayed as much as possible. Most physicians favored starting early, though some still favored delayed treatment in order to avoid negative selection for resistance strains. Several points were made by each side of the debate, but suffice to say we now have an answer to the dilemma on early or late treatment. A massive American study whose results were just released in a press release on May, 27th of this year says unequivocally it is better to start early [NN15]. This contradicts the results of some CA models as will be seen in the next chapter.

2.10.2 HIV Dynamics in Time

HIV infection is characterized by **three phases** (Figure 2.5). **Acute phase.** For the first 2-6 weeks after HIV enters the host, patients experience flu-like symptoms. Then, during the 9th to the 12th week, viral load experiences a sharp decline and the number of T_H cells returns almost to normal levels. **Chronic phase or clinical latency.** The second phase consists in a long asymptomatic period, which may last for 1 to 10 years, or even more. During this phase, viral load is low, but the population of T_H cells keep dropping down to a critical point. It is not known exactly what happens during this stage; we see many sudden “blips” in the data, so some suspect HIV is incubated in T_H cells until it bursts them from inside and is released, or that blips are the result of treatment; while others think the blips in the data need not be explained by bursts, and the data can be reproduced by continuous reproduction under a stochastic simulation. **Profound immuno-suppression.** In the final phase, the impaired immune system no longer can fight infections and opportunistic diseases take over. The patient is considered to have AIDS. This is declared when T_H cells count drops below 200 cells/ μ L and the viral load increase beyond the 125 copies/ μ L.

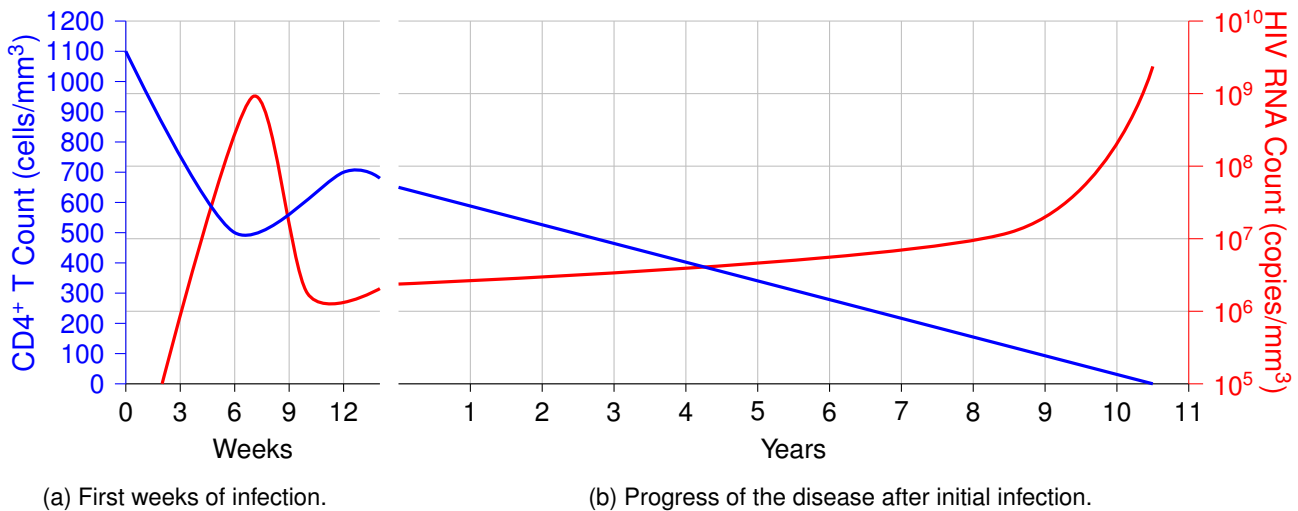


Figure 2.5: Three-stages representation of AIDS. [PGF93, Figure 1]

2.10.3 HIV Dynamics in Space

HIV has different dynamics in different parts of the body (Figure 2.6 on the following page). For instance, the clearance rate of the virus (the rate at which it is destroyed) is higher when in the blood (300 day⁻¹) than when in the lymph node (5.5 day⁻¹). The virus is most plentiful in lymph nodes, the spleen, and other organs rich in CD4⁺ cells. Models should take this into account. [GP13]

Less is known about the exact movements of HIV molecules. We do know it is independent of chemokine gradients, unlike the other immune cells, so they are moved only by fluid flow — a wide range of approaches has been employed to study this problem, as surveyed in the following chapter.

As a first approximation to the movement of the disease it is interesting to divide the model by compartments with different viral dynamics — namely, to compensate differing rates of viral replication and clearance [GP13]. The virus can either spread through free transmission through the body, subjecting itself to humoral mediated neutralization (antibodies), opsonization and phagocytosis; or they can transmit through cell-to-cell contact avoiding exposure to plasma components, but limiting

its scope to the neighborhood of local target cells, spreading like a wave. Cell-to-cell transmission has been shown to be several fold more efficient than close melee transmission. This may explain why HIV can be found in areas densely populated with appropriate target cells, such as in the lymph node. While this first approximation of the disease makes sense, we only have HIV counts on efferent blood stream. Most mathematical models which integrate spatiality end up speculating on HIV movement within the lymph node, not through the organism.

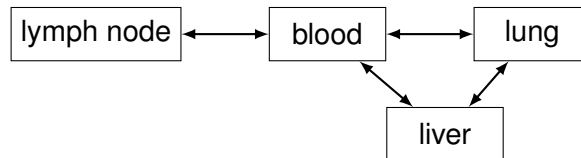


Figure 2.6: Spatial compartments of differing HIV dynamics.

Motility of immune cells is of utmost importance in HIV dynamics. Some studies have been performed on immune cell motility using photon imaging techniques. T cells move in random walks within the lymph node. Miller et al. [Mil+03] finds this is so even when considering the entire 3D space, while Miller et al. [Mil+04b] finds T cells are not attracted to dendritic cells by chemotactic gradients but rather encounter them by chance. Miller et al. [Mil+02], by harvesting lymph nodes from mice and performing two-photon imaging on them, has found that the mean absolute displacement of T and B cells from their origin increases proportionally with the square root of time, indicating that both cell types use a random-walk search strategy within the lymph node. However, when challenged by an antigen, they move in “swarms” in stable clusters [Mil+02]. Cells move by deforming their shapes; the receptors that are stimulated “push” into that direction, provoking an elongation of the cell into that direction, and eventually movement. Furthermore, Miller et al. [Mil+02] has found that T cells (on mice), when stimulated, can either form tight clusters which are relatively stationary, or form clusters which roam more freely, moving in “swarms” looping within regions a few tens of micrometers across. On the mice, stationary cells (velocity $< 2 \mu\text{m min}^{-1}$) increased from 3% to 25% when activated/primed, and the diameter of this clusters were 1.5 times than the unactivated/unprimed ones. These clusters were contributed mostly by priming and dividing cells — clusters of cells that have divided three or more times were found to have 21% of stationarity cells rather than 10% of the others — but the velocity of motile cells seem on average identical, irrespective of the number of divisions. Freely motile cells that encountered one of these clusters would usually get stuck, but sometimes dissociated and moved freely again.

T cells encounter dendritic cells randomly, decelerating only slightly while in contact with dendritic cells, and quickly migrating away after ~ 3 min, while immunized cells seem to suffer no motility dropback. Furthermore, Miller et al. [Mil+04a] finds dynamics very much dependent on the timeline. Before the 2 h, it seems that encounters results in T cells moving in loops, making serial encounters with the same dendritic cell or any neighboring dendritic cells — as a result, motility decreases (mean velocity = $5.4 \mu\text{m min}^{-1}$ and motility coefficient = $9.7 \mu\text{m}^2 \text{min}^{-1}$), and interactions were found to be more prolonged when in the presence of antigen (mean = 11.4 min for the unimmunized mice). In the next stage, [2,14] h, T cells remained associated with dendritic cells for longer (~ 60 min) — interactions were either interrupted by the T cells moving away or the dendritic cells withdrawing their dendrites. Entire clusters of T cells transferred sometimes between dendritic cells. During this period, average T cell velocity was $2.6 \mu\text{m min}^{-1}$, and the motility coefficient was $2.3 \mu\text{m}^2 \text{min}^{-1}$. Interactions within [16,24] h involved interactions of an average 20 min, while T cells looped in “swarms” at veloci-

ties of $4.1 \mu\text{m min}^{-1}$ and motility coefficient of $6.3 \mu\text{m}^2 \text{min}^{-1}$, although some T cells remained stably associated with its dendritic cells. After the 24 h, T cell swarming diminished and many T cells migrated autonomously making infrequent and brief contacts of mean ~ 12 min — overall T cell velocity was of $4.6 \mu\text{m min}^{-1}$, while for individual blasts was of $[8,9] \mu\text{m min}^{-1}$, and many instances of cell division were observed; daughter cells regained motility rapidly. Finally, by 40 h most T cells had undergone one or more rounds of division. Mempel, Henrickson, and Von Andrian [MHV04] argues the dynamics can be divided in just 3 stages, while Mirsky et al. [Mir+11] hypothesizes on how a working mathematical model could result from these dynamics. Motility coefficients are calculated assuming random walks: $M = x^2/4t$.

For our study, the most interesting regions of the lymph node are primary follicles (PF), diffuse cortex (DC), medulla (M), afferent lymphatics (AL), and efferent lymphatics (EL). T cells can be found uniquely in the DC, while B cells are found mostly in the PF. The lymph node is compartmentalized, and the fluid flows are isolated from the bulk flow of the lymph or blood. Movement of cells is directed by chemokine gradients, whose cells' receptors respond to, and structural pathways of the organ.

Oddly enough, only in systems biology, which work closely with laboratories, this level of detail is studied. No published mathematical paper was found where this level of detail is integrated; usually everything is considered to move in random walks. HIV treatment is obviously also influenced by spatiality, though this is less often modeled.

A further complication would be HIV locomotion within the infected cell. Because of the high viscosity of the cytoplasm, it is unlikely diffusion alone suffices for the reach of the nucleus. Different viruses employ different strategies. McDonald et al. [McD+02] uses microscopic analysis to argue HIV uses cytoplasmic dynein (a molecular motor) to move towards the nucleus of the cell in curvilinear paths. Few mathematical models go into this level of detail, though there are some [Zar+10].

2.10.4 HIV Dynamics in Mutation Space

Another kind of space dynamics that has been more intensively studied with regard to the evolution of HIV strains is often referred as the “shape space” of HIV, as originally studied by Perelson and Oster [PO79]. Several of the models hereby considered integrate HIV mutation distribution dynamics, and speculate if the immune system follows this “shape space” distribution. As will be seen, models that integrate mutation dynamics will prove the most successful.

Chapter 3

Cellular Automata Models

Nature operates in the shortest way possible.

Aristotle, *Physics*

In the realm of HIV-1 modeling literature, there are many models which portrait themselves as cellular automata (CAs) models. But some of these use rules whereby agents move and interact when they collide, not neighboring rules. Models in this chapter are restricted to those whose states change as a result of neighbor-based rules. Other models will be covered later in Chapter 5 as agent-based models (ABMs).

CAs originated as one of many simulation techniques created by Stanislaw Ulam and John von Neumann in the 40s, while in the Manhattan Project. They were used mostly as curiosities by mathematicians. They hit mainstream when in the 70s were used by Nobel laureate Thomas Schelling to more vividly show how from a simple rule — white and black people want to have at least 20% neighbors of the same race — could explain wide racial segregation in city dwellings.

Because of the performance of its simulations, and in some cases analytical introspection, CA model is used in a wide range of fields — in fact, the name is completely unrelated to *biological cell*, even though here it shall be used in that sense. These models may be seen as the primogenitors and computationally less demanding versions of ABMs. The grid may represent physical space and will be used in that sense, unless otherwise stated, but it may also represent other concepts of space — such as shape space representing HIV mutations [Her+01]. Since each cell is in one of a finite number of states and is layed out in a grid, they will be rendered visually in different colors.

Definition. A **cellular automaton (CA)** is a model representation of both time and space. Space is discretized in an D -dimensional *lattice* composed of *cells*, each of this cells is in a given *state*:

$$s_i(t) = (\text{state of cell } i \text{ in time } t) \in S.$$

The number of states is finite, $|S| = k$. For example, $S = \{\text{Healthy}, \text{Infected}\}$. The lattice has length L , and an area (number of cells) of L^D . The model designer then provides a function f , used by all cells of the lattice, *homogeneously* modeling time and space. This function models the next state of each cell in the iteration as a function of both its current state and that of its n neighbors. This function is known as the **local rule**:

$$f: S^{n+1} \rightarrow S.$$

This function is then called $\forall i$ as:

$$s_i(t + 1) = f(s_i(t), \text{neighbors-states}_i(t)).$$

Because the local rule is common to all cells, it is also known as a *finite state machine* in computer science literature, or as an *automaton*. The neighbors function would be the two immediate neighbors for 1D, $\text{neighbors-states}_i = \{i - 1, i + 1\}$, or the 8 neighbors for the 2D case. Neighbor rules and their impact in the HIV models will be surveyed later. [HM07]

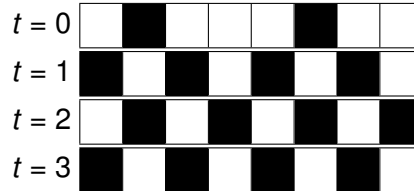


Figure 3.1: Example of an 1D CA of $L = 8$ (of periodic boundary conditions) with 2 possible states: black is `true` and white is `false`, following the local rule `or` on its 2 neighbors. The pattern repeats itself, $s(t = 2) = s(t = 4)$; this is called an oscillator of period 2.

Each update cycle is called a “tick”, as time advances from t to $t + 1$. It is common in discrete mathematics to use i for time, meaning iteration, but we will use $t \in \mathbb{Z}$, since i is also a common variable for indexing. The update process is sketched as pseudo-code in Algorithm 1.

```

Require: CA[] of size L
1:  $t \leftarrow 0$ 
2:  $CAb \leftarrow CA$  # buffer
3: while  $t < t_{\max}$  do
4:   for  $i \leftarrow 1$  to  $L$  do
5:      $n \leftarrow CA[i]$ 
6:      $m \leftarrow f(n, \text{neighbors-states}(CA, i))$ 
7:      $CAb[i] \leftarrow m$ 
8:   end for
9:    $CA \leftarrow CAb$ 
10:   $t \leftarrow t + 1$ 
11: end while

```

Algorithm 1: Typical CA algorithm. These pseudo-codes are our own. We present our code here because we think not every author is implementing delays the same way, as we discuss.

```

Require: CA[] of size L
1:  $t \leftarrow 0$ 
2:  $CAb \leftarrow CA$ 
3:  $T \leftarrow$  vector of ones of size L
4: while  $t < t_{\max}$  do
5:   for  $i \leftarrow 1$  to  $L$  do
6:      $n \leftarrow CA[i]$ 
7:      $m \leftarrow f'(n, \text{neighbors-states}(CA, i), T[i])$ 
8:     if  $n \neq m$  then
9:        $CAb[i] \leftarrow m$ 
10:       $T[i] \leftarrow 1$  # disputable
11:    else
12:       $T[i] \leftarrow T[i] + 1$ 
13:    end if
14:  end for
15:   $CA \leftarrow CAb$  # expensive
16:   $t \leftarrow t + 1$ 
17: end while

```

Algorithm 2: Adding an internal clock (delay) to a traditional CA.

HIV CA models are not typical CAs because they require an internal clock (see Algorithm 2). Their local rules makes use of this internal clock. For instance, one Healthy cell becomes an Infected cell when one Infected cell is its neighbor — it then stays Infected for 4 weeks. This wait rules are represented with the keyword “wait” in our diagrams. Here local rule f' is extended to take an extra integer representing the internal clock.

The local rule f and f' may be either **deterministic or stochastic**. In the latter case, a different return value may be returned for the same input, according to a given probability distribution.

$$f(\mathbf{n}) = \begin{cases} s_1 & \text{with probability } P(\mathbf{n} \rightarrow s_1) \\ \vdots & \\ s_k & \text{with probability } P(\mathbf{n} \rightarrow s_k), \end{cases}$$

where \mathbf{n} are the neighbors states of cell i , $s_1 \dots s_k \in S$, and $P(\mathbf{n} \rightarrow s_j)$ being the **transition probability** (independent of time) that specifies the conditioned probability that cell i evolve to state s_j . This transition probability has of course to satisfy the condition: $\sum_{j=1}^{|S|} P(\mathbf{n} \rightarrow s_j) = 1$.

In the stochastic case, no unique **global rule** may be derived to reproduce the process. The global rule is called to a function that can reproduce the results of the CA at the population level of the various states S , without the penalty involved in simulations from the local rule.

Technical notes. Algorithm 1 and 2 on the previous page are in fact agnostic as to the dimensionality of space. For the 2D case, function $f(n, i, t)$ can then convert i to 2D coordinates by using $(x, y) = (i \bmod L, i \div L)$, where \bmod and \div are the modulo and integer division operators, respectively, where $L = l^2$. The same rationale can be used to use the algorithm for the 3D case, as we will later use.

The algorithm is generic — knowing the particulars of the model being simulated, it might make sense to develop a more fine tuned simulator. Our simulator fine-tuned for the main HIV model [SC01] run in less than 2 seconds, while under this code it takes about 20 seconds. This was done by avoiding the command marked as “*#expensive*” by replacing it with an extra structure that keeps track of the number of Infected neighbors, which are the only neighbors tested by local rules.

Delays can of course also be converted into states, so that $\boxed{A} \xrightarrow{2 \text{ ticks}} \boxed{C}$ can be converted into $\boxed{A} \rightarrow \boxed{B} \rightarrow \boxed{C}$, whenever wait times are deterministic. The “*#disputable*” comment means that it is not clear from the articles below analyzed if every author is starting time at 0 or 1 because few produce any code or pseudo-code. Hence, a 2 ticks transition might either mean that the transition is delayed 2 times, staying frozen 3 times, or that it waits 1 time and stays in the same state 2 times (our interpretation). Comparing graphics producing by our implementations to the graphics of several authors, it seems there are sometimes a discrepancy that could be explained by this miscomprehension.

Given that the time step update is synchronous, parallelizing the cycle at each iteration time t is an option, though the system overhead from the parallelization is not usually worth it, definitively not if several runs of the simulation are already being parallelized. We will want to run several times the simulation, in order to find average behavior and measures of deviation. We have typically used 50 simulation runs, which was in general found to be a good compromise between robust results and the computational power at our disposal.

3.1 A First Approach

Published in the prestigious Physical Review Letters and with over a hundred citations (Google Scholar), Santos and Coutinho [SC01] is by far the most revered and the first model to successfully reproduce all three HIV stages using nothing but space dynamics. An example of this model imple-

mented in NetLogo [Wil99] is provided in Appendix A. Despite concerns as to its realistic application [SL01], with over 150 derived papers, every other spatial model has since been an extension of Santos and Coutinho work. Most extensions to this model add some form of treatment or include other corporal compartments.

In HIV spatial dynamics, this and other derivative models can be seen as representatives of cell-to-cell transmission within a given organ, most prominently the lymph node (please refer back to section 2.10.3 on page 20).

Its set of states S are $\{H, A1, A2, D\}$, where they represent respectively: Healthy, infected stage 1, infected stage 2, and Death cell. At $t = 0$, most states start as H , except for a minority fraction p_{HIV} which kick off already infected as $A1$. Local rule f is here represented by the state diagram in Figure 3.2.

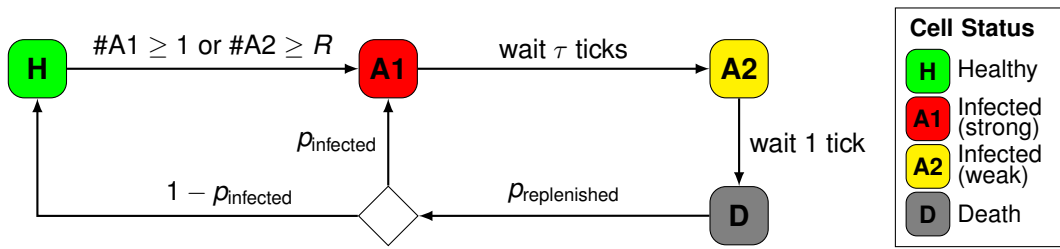


Figure 3.2: Our schematic diagram based on Santos and Coutinho's model. Operator $\#$ represents how many of the 8-neighbors have a given state. The colors of the states will be reused as much as possible.

Our rendering of the local rule as diagrams is inspired by the diagrams used by Shi, Tridane, and Kuang [STK08], and statemachine diagrams from UML, also known as statecharts, as to be discussed in Chapter 5. A state is represented as a rounded square, \square , while conditions are represented by a diamond, \diamond . Conditions are transient states; they do not actually exist. For example, $D \xrightarrow{p_1} \diamond \xrightarrow{p_2} A1$ and $D \xrightarrow{p_1} \diamond \xrightarrow{1-p_2} H$ means that the transition will take place with probability p_1 . If the transition takes place, the end state ($A1$) will be chosen with probability p_2 , or (H) otherwise. For easier comprehension, the opposite probability, $1 - p$, is usually rendered; even though it could be omitted.

Parameter	Description	Value [SC01]
L	length of the CA grid square	700
p_{HIV}	fraction of initial infected $A1$	0.05
R	minimum $\#A2$ of contagious neighbors	4
τ	waiting time for $A1 \rightarrow A2$ transition	4 weeks
$p_{replenished}$	probability of death cells to be replaced	0.99
$p_{infected}$	probability of replenished cells to be infected	10^{-5}

Table 3.1: Santos and Coutinho's parametrization of the model.

Parameters represent biological constants. The model represents the lymph node. It hypothesizes that healthy cells are infected when in contact with 1 strongly infected cell ($A1$) or R weakly infected cells ($A2$). A strongly infected cell becomes weakly infected after τ ticks/weeks. The next tick it becomes death, (D), and is then replenished by the thymus at a probability $p_{replenished}$. This new cell may already come infected with a very low probability of $p_{infected}$. At $t = 0$, p_{HIV} cells begins

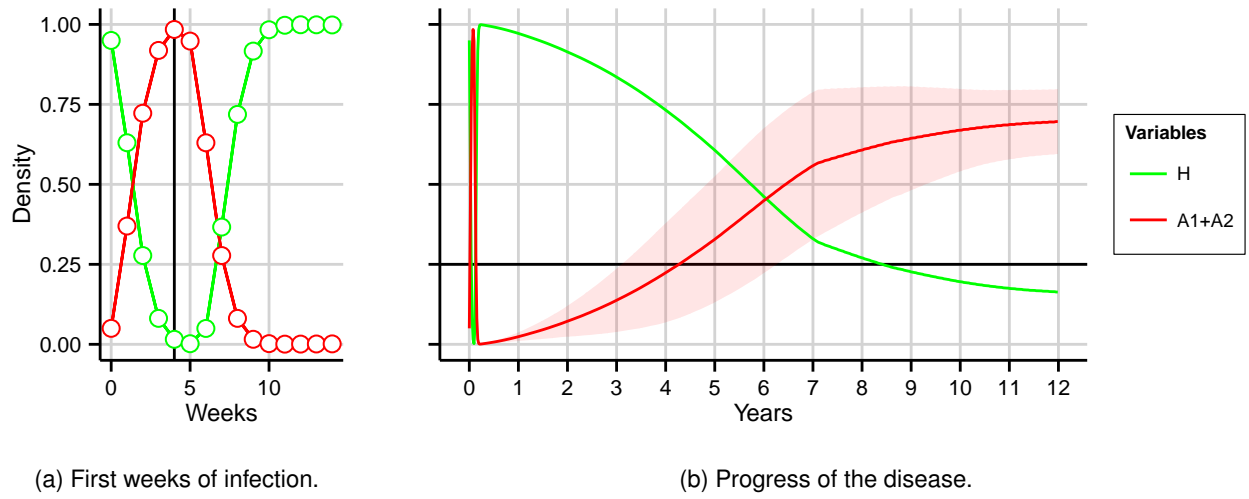


Figure 3.3: Our results based on Santos and Coutinho's model. Error bars for one standard deviation are being represented by a ribbon [CFV07]. Only error bars for A1+A2 are drawn (not H) to avoid visual clutter, because dispersion values for H are similar. The vertical black bar represents the primary infection peak, while the horizontal line would represent a very debile individual, whose T count is lower than 250 cells/ μ L. These bars are suggestive of pathogenesis milestones, and will be used later for the sensitivity analysis.

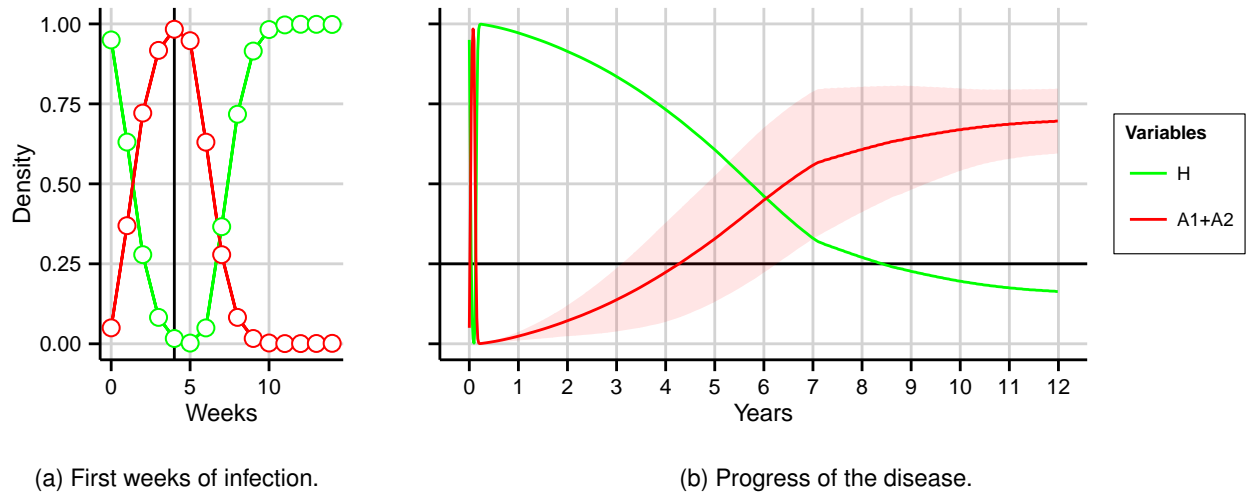


Figure 3.4: Unbounded boundary conditions reproduction of the model. In Figure 3.3, periodic boundary conditions were reproduced. This figure shows how an arguably more realistic boundary condition is similar in result.

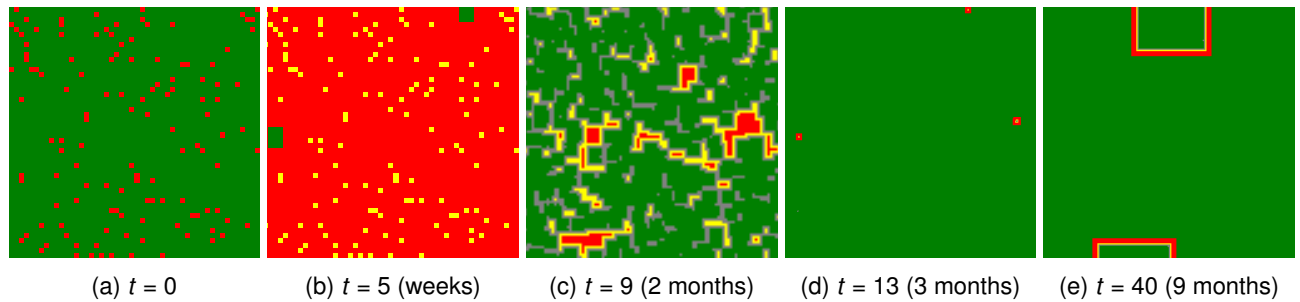


Figure 3.5: Several snapshots of the model (using 8-neighbors / Moore neighborhood). These are closeups of the pathogenesis. At the beginning of the infection, there are already a good amount of viruses; they spread quickly and die off. Because some dead cells are replaced by cells that come infected, $D \xrightarrow{p_{\text{infected}}} A1$, the infection does not die off; some of those form oscillators, as explained below, which rapidly take over.

infected, and the rest healthy. The simplicity of this model, which manages to encompass all three stages of HIV pathogenesis, is probably the main reason why it has gathered so much attention.

Results of the model are reproduced in Figure 3.3 on the previous page, as the average and deviation from 50 simulations runs of the model using default parameters as in Table 3.1 on page 26. Error bars for one standard deviation are presented for the infected cells (red line), above and below, as a light-red line. Notice that averaging simulations smooths out individual simulation runs. In a few simulations, there is a threshold whereby disease is progressing quickly and after which it suddenly stops, short of the 0.75 infection rate, at about year 7. This behavior will be understood later in the chapter in light of our study into wave patterns.

The model is first reproduced in terms of periodic boundary conditions, as in the paper (Figure 3.3 on the previous page), where the lymph node is therefore considered to be a 700×700 torus with no third dimension. It is then reproduced under unbounded boundary conditions. This condition may be more realistic, since we are assuming only part of the model can be effectively simulated (Figure 3.4 on the previous page). By taking unbounded boundary conditions, we are saying we only have computational power to simulate part of the lymph node, and those cells at the boundary act as a population of healthy cells, absorbing the diffusion wave. Interestingly, the lines show any discussion of which is more plausible to be moot: there is not much difference between the average of the simulations runs. Periodic conditions, as in most HIV CA articles, will be used throughout.

3.1.1 Sensitivity Analysis

In a follow-up article, Figueirêdo, Coutinho, and Santos [FCS08] perform sensitivity analysis for different lattice dispositions and find the model to be pretty robust. They use triangular as well as 3D and other lattice configurations.

Over Figure 3.6 on the following page, we extend it by performing sensitivity analysis to the various parameters of the model. Each parameter was changed *ceteris paribus*. That is, only one parameter was changed at a time, while all other values are fixed as in Table 3.1 on page 26. As values are changed, the pattern of the simulation remains pretty robust. Therefore, instead of plotting the entire graphic several times, we chose to plot only two times, representative of milestones of the pathogenesis.

The first represents the primary infection peak, when the virus load (amount of infected cells) reaches its highest value before cytotoxic response. The second is the phase of the immune deficiency syndrome, AIDS. It is sometimes defined in terms of white blood cells concentration in the blood: where a T count lower than 250 cells/ μL would indicate AIDS, which here we represent as $\#H \leq 0.25$. The two time milestones represented here are annotated as a vertical black line in Figure 3.3a on the previous page and as an horizontal black line in Figure 3.3b, respectively.

Time in the graphic is still represented in the x-axis for visualization easiness, even if they it is to be read as the result of the parameter change.

Interestingly, we find the model to be pretty robust to the various parameter changes, but some points ought to be made:

- The transition $(H) \xrightarrow{\#A2 \geq R} (A1)$ is not as relevant as it seems at first — increasing $R = 4 \rightarrow 9$ (which effectively disables the transition, because cells have only 8 neighbors) only has an impact of one year in the final AIDS period. Reducing it, $R \rightarrow 1$, so that both A1 and A2 become equally nocive, $(A1) = (A2)$, affect results by more.

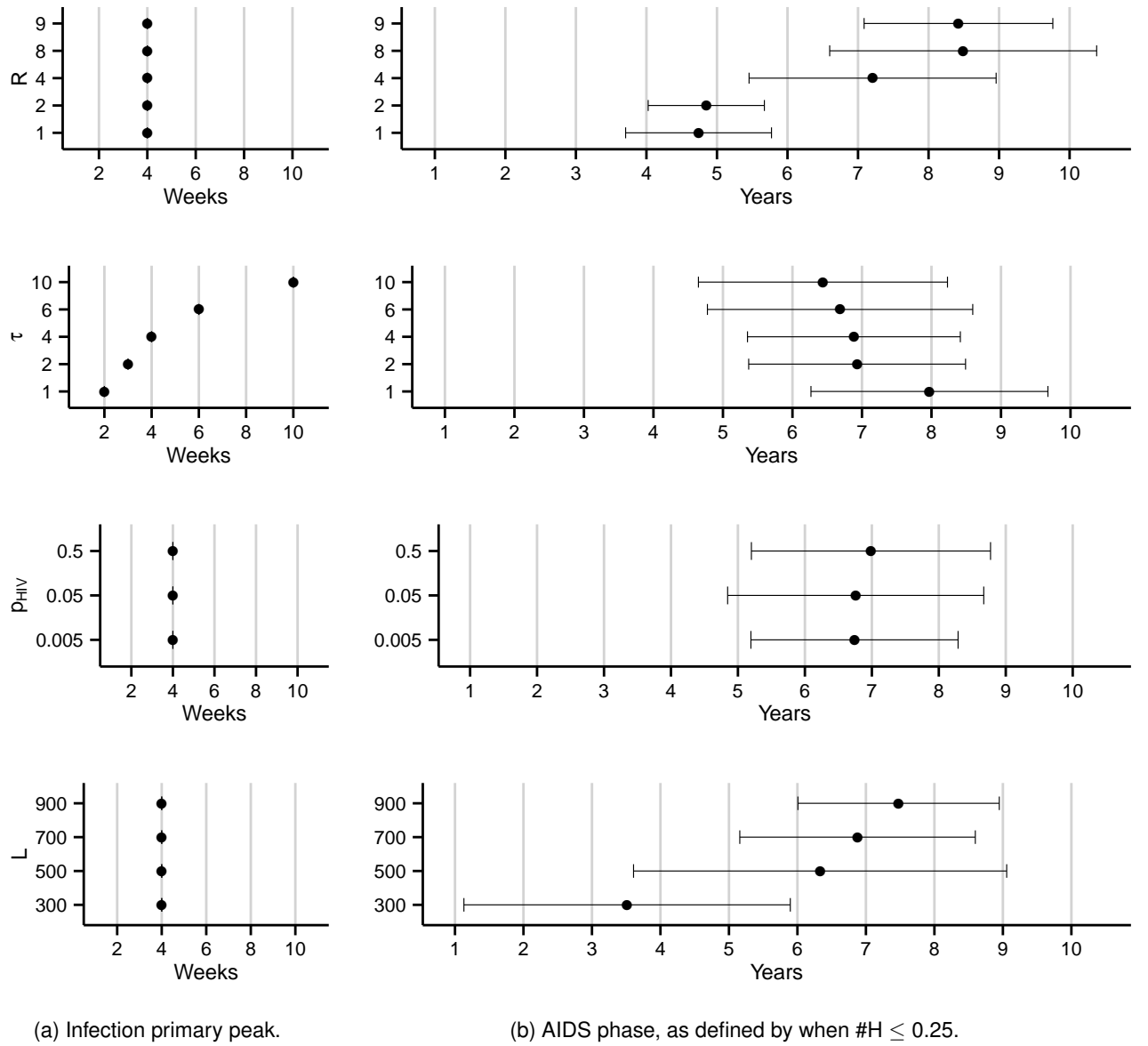


Figure 3.6: Our sensitivity analysis to various parameters, and respective results in terms of the primary peak, and AIDS phase. Error bars represent one standard deviation [CFV07] from the average of simulation runs. 50 simulation runs were performed.

- At first sight, it would seem that a reduction in R would have the same qualitative effect as increasing τ , because in the ultimate case when $R = 1$, then $(A1) = (A2)$, and so it would be effectively the same as increasing delay τ by 1, because $(A1) \xrightarrow{\tau} (A2) \rightarrow (D) = (A1) \xrightarrow{\tau} (A1) \rightarrow (D) = (A1) \xrightarrow{\tau+1} (D)$. Not surprisingly, we can see this qualitative inverse effect with changes in τ and R .
 - More interestingly, changes in τ do not affect the results as much as it would be expected — which means delays may be largely unnecessary in HIV modeling; changing $\tau = 4 \rightarrow 1$ (effectively disabling it) does not affect the general pathogenesis, except during the initial HIV peak: reducing it by two weeks, and also making that initial peak less pronounced (this latter characteristic cannot be seen in the figure).
- Initial viral concentration, $p_{HIV} \in \{0.005, 0.05, 0.5\}$, seems to affect the disease by little, but that is deceiving. Looking at the actual graphic reveals the disease is not as intense in the primary peak; this means that inversely proportional fewer transitions $(D) \rightarrow (A1)$ take place, which also explains why the AIDS phase also happens at the same time.
- The length of the lattice, L , does not significantly change results. But we can see that there is a bigger difference changing lattice's width by 200 cells when going from 500 to 300 cells width than all other lengths, even when the resulting reduction in area is much larger at larger values, $900^2 - 700^2 \gg 700^2 - 500^2 > 500^2 - 300^2$.

3.2 Wave Propagation

Few papers on CA dynamics investigate what exactly happens within the CA cellular lattice; often only graphics such as Figure 3.3 on page 27 are produced. However, these models are only useful if they can possibly elucidate us about possible unknown dynamics of the virus. Here, we shall study exactly how the virus allegedly propagates itself through the lymph node.

According to this model, viral propagation through the lymph node takes place mainly through cell-to-cell contact in the form of a wave. In the between, there are some incidents of blood diffusion, because it is assumed that when a Dead cell dies, it is replaced by a Healthy cell produced by the thymus, or, less commonly, by a cell that comes infected, $(D) \xrightarrow{p_{\text{infected}} p_{\text{replenished}}} (A1)$. In fact, based on the original parameters, this exogenous contagion (by diffusion) is critical to the pathogenesis of HIV, because the immune system manages to clear the disease at first. It is only because of infection from exogenous diffusion, from other parts of the body, that the disease manages to eventually overcome the immune system. This is no longer the case if we tweak the parameters; for instance, if we lower initial concentration, p_{HIV} , as will be seen below.

In order to investigate why exactly, according to this model, is it that the disease manages to overcome the immune system after the first infection stage, we simplify the model. For that purpose, since we are only interested in wave patterns, we simplify the model by assuming $R = 9$ and $\tau = 1$, which effectively means removing state $(A2)$. In this model, AIDS comes 2-3 years earlier, because $(A2)$ no longer acts as a soft barrier, together with harder barrier (D) . Furthermore, time delays are removed because they do not change dynamics *qualitatively*. States are simplified to those of Figure 3.7 on the following page. Waves behave identically, which are our subject of study.

In the **first stage of the disease**, the initial infectious concentration, $p_{HIV} = 0.05$, means that we are considering 5% of all the cells in the lymph node to be infected. This is why dynamics of the

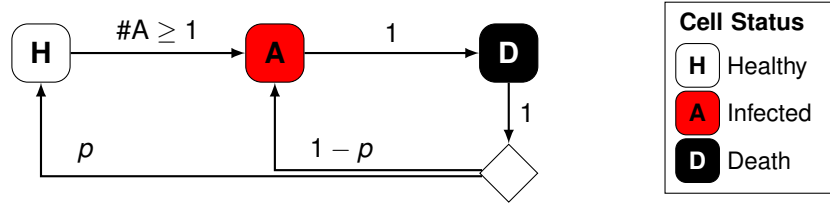


Figure 3.7: Stripped down Santos and Coutinho's model. This is a simplified version sans-delays. It is a classic stochastic cellular automaton. $p = p_{\text{infected}} = 1 \times 10^{-5}$.

first stages of the disease are so explosive. Waves form everywhere and quickly consume the entire lattice whose cells then burst or are killed by the immune system, and are then replaced by fresh Healthy cells from the thymus.

But not all cells come Healthy. With a probability of $p_{\text{infected}} = 10^{-5}$ some dead cells are replaced by infected cells diffused from elsewhere in the system, $(D) \rightarrow (A)$. These infected crumbs kick off the slow **second stage of the disease** up to the final AIDS stage. This means that, at the start of the second stage, after all cells are killed and replenished, $L^2 \times p_{\text{infected}} = 700^2 \times 10^{-5} = 4.9$ cells are replaced by (A) infected cells. These few and scattered infected cells then start growing as weak waves.

Infectious Disease doctors Strain and Levine [SL01] have criticized this parametrization of an initial infection value of 5% to start the primary stage, as being too high for the early stages of the disease. The problem is that reducing the parameter also reduces the intensity of the ensuing infection peak, as seen previously. Shi, Tridane, and Kuang [STK08] offers an ingenious solution as will be seen below (section 3.4 on page 34). Either way, the exact dynamics of the primary stage are irrelevant as to what comes next; what is important is that in the second stage, we start off with very few infected cells — 0.001%, in this case (see Figures 3.8 and 3.9).

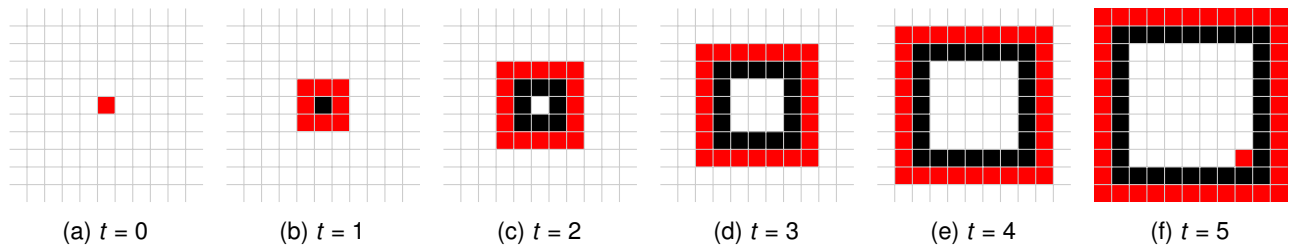


Figure 3.8: The behavior of most waves. The grow in viruses is relatively small, because their trail is rapidly cleared; and when colliding with another wave, both will dissolve. Notice how in $t = 5$, one of the Dead cells was converted into an infected A cell, because of $(D) \rightarrow (A)$ on $P = 1 - p$.

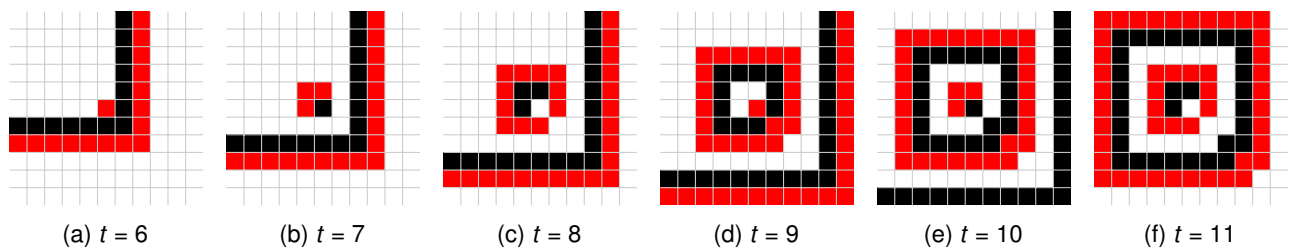


Figure 3.9: Under certain conditions, as in $t = 5$ in Figure 3.8, what is called as an “oscillator” in CA literature is formed. This is so because of the low-probability big-impact transition $(D) \rightarrow (A)$. These are powerful waves because they keep generating new waves; recreating itself after 3 periods, so $s(t) = s(t + 3)$ within the entire area of the wave.

During the second stage, since all cells are infected, on average $L^2 \times p_{\text{infected}} = 4.9$ waves are

formed. Under **normal conditions**, waves expand by growing their perimeter. Each cell within the perimeter “recruits” two new cells outwards, meaning 8 cells become 16, 16 cells become 24, and so forth. Except for the initial transition $t = 0$, when 1 cell recruits 8 cells, these well-behaved waves have a size of

$$P(t) = 8t$$

at iteration t . This means that to reach AIDS in 7 years ($t = 7 \times \frac{365}{7} = 365$), the number of waves n would have to be such that $n \times P(t) = L^2$; or, in that case, $n = \frac{700^2}{8 \times 365} \simeq 168$ waves required to conquer the entire lattice.

This linear growth rate of 8 does not categorically suffice to explain how HIV can lead to AIDS in the time frame of 6-7 years, or in any useful time, especially when considering that these waves are exclusive; that is, when they collide against another, they consume each other. To explain AIDS, we require **oscillator waves**.

Oscillator waves are waves that are formed when the inner corner of a wave is replaced by an infected cell, on the occasion of $(D) \rightarrow (A)$, with probability $p_{\text{infected}} = 10^{-5}$, as detailed in Figure 3.9 on the previous page. This is a rare event whose likelihood for each wave does not grow with t , because the number of corners in a wave is always 4, independent of perimeter. Each time this happens, new regular waves are formed, which have themselves 4 corners by which oscillator waves may form; when we have 100 waves, we can expect after $1/(100 \times 4 \times 10^{-5}) = 250$ weeks to have one of these oscillator waves.

Oscillator waves can also form in other circumstances, such as when two adjacent cells are replaced by an infected cell within the same tick.

These waves occupy the entire area given by the sum $\sum_{i=1}^t P(i)$,

$$\begin{aligned} A(t) &= 1 + \sum_{i=1}^t 8i \\ &= 1 + 8 \sum_{i=1}^t i \\ &= 1 + 4t(t+1). \end{aligned}$$

The partial sum of the natural number series was replaced by the triangular number as given by $\sum_{k=1}^n k = \frac{n(n+1)}{2}$.

Looking back to the model in Figure 3.7 on the previous page, it is clear that $(A1)$ is a transient state; it is replaced by a Dead state the next turn and so the model spends at most two-thirds of the time in $(A1)$. This can also be seen from the wave pictures from Figure 3.9 on the previous page.

Now, in order to derive a global rule for the average behavior, we have to consider the true number of infected cells is $1/3$ of the area $A(i)$. It is worth noticing that in the original model, with time delays, infected cells within the wave are given by: $P'(i) = 5P(i)$ and $A'(i) = 5/7P(i)$ because when a cell is infected it leaves a trail that takes a while to disappear. This is a minor observation, of not major impact.

In conclusion, normal waves do not explain disease dynamics because they spread slowly throughout the lattice. Oscillator patterns, on the other hand, are authentic sources of viral nests. They help explain why HIV seems dormant, and then wakes up, when the first oscillator wave is formed.

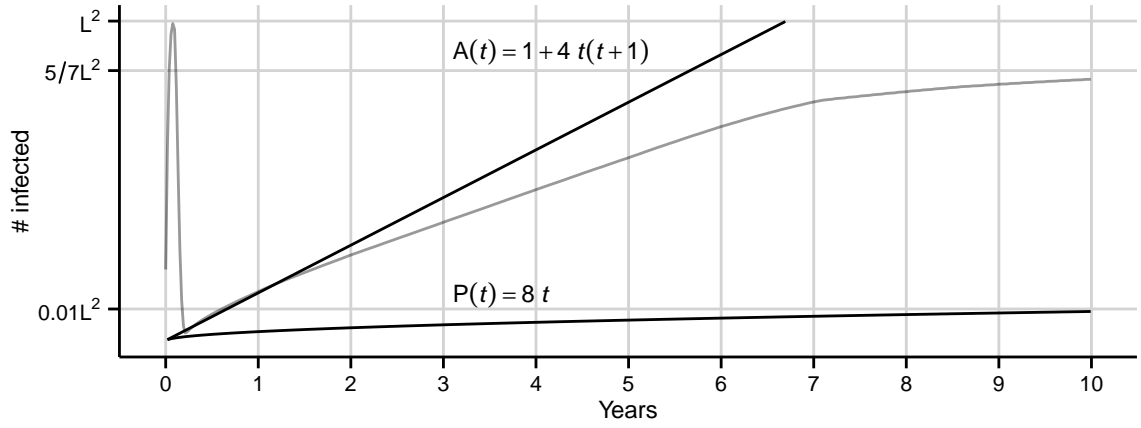


Figure 3.10: Comparing growth functions between regular and oscillator waves. The square root scale was used for y-axis, given the oscillator's wave growth function is squared, $\mathcal{O}(n^2)$. In light gray is the average of model simulations, seen in the first Figure of this chapter, Figure 3.3 on page 27. Interestingly, at $y = 5/7L^2$ point, after saturating the lattice, it seems as if it suddenly it stops growing. This growth "truncation" is particularly visible on single simulations.

3.3 Viral Incubation

One interesting twist on Santos and Coutinho's model was suggested by Shi, Tridane, and Kuang [STK08]. They proposed two big changes to the model, reproducing results similar to the original ones from Santos and Coutinho, only that the parameter dominion was made more realistic.

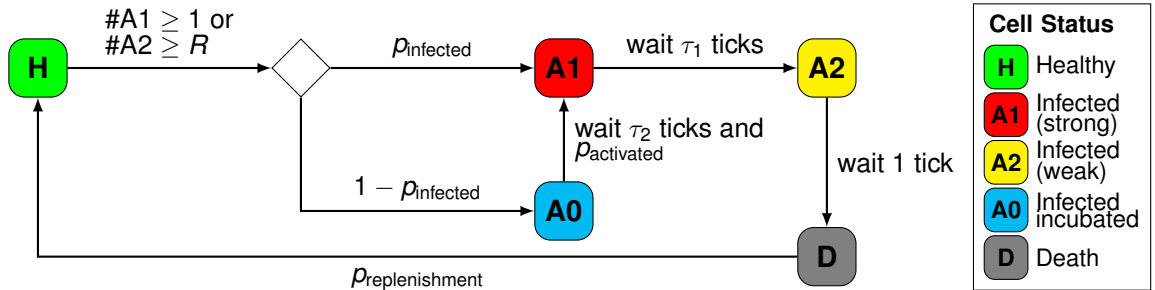


Figure 3.11: Schematic of part of the model suggested by Shi, Tridane, and Kuang [STK08] featuring viral incubation delay. Parameters: $\tau_1 = \tau = 4$, $\tau_2 = 30$, and $p_{\text{activated}} = 5 \times 10^{-4}$. They changed p_{infected} from 10^{-5} to $1 - 10^{-4}$.

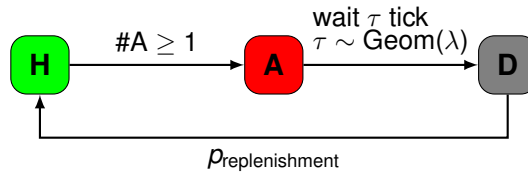


Figure 3.12: Our alternative model. It fails to produce any sensible dynamics.

Namely, they managed to scale down p_{HIV} , the initial concentration of HIV, from 0.05 to 0.005. Critiques considered 5% too high as the initial infection concentration required for the disease [SL01]. It is not clear from their model however, which changes produced this desired effect, since they presented wholesale many of the changes they proposed.

A basic rendering of their model without medication is represented in Figure 3.11. They manage to explain disease dynamics without calling for exogenous diffusion. Instead, an incubation period

was introduced. An Healthy cell may be infected into an $\boxed{A0}$; here, the viral lasts longer before bursting.

However, looking at each change individually, in a reductionist fashion, it becomes clear that:

- introducing this viral incubation period $\boxed{A0}$ is not what affects the initial concentration, p_{HIV} .
- the reason why they managed to reduce p_{HIV} without changing the results is by something else they introduce: varying neighborhood radius. Instead of always considering the 8 neighbors, they start by considering a smaller neighborhood radius of 8 at the beginning of the infection, and increase it proportionally to the debilitation of the immune system. This will be covered in the next section.

The introduction of the $\boxed{A0}$ incubation period replaces the previous explanation of exogenous diffusion. It avoids exogenous infection by introducing a low-probability big-delay infection. Both models are able to reproduce HIV dynamics, so only empirical research can resolve this dispute.

We attempted to replace both $\boxed{A0}$ and $\boxed{A1}$ by modeling τ as a Geometric distribution (Figure 3.12 on the previous page). It fails badly at reproducing the same results as before. The primary stage infection, in particular, cannot be reproduced by having stochastic delay times. The majority of cells must follow the same delays so that cells are all destroyed at the same time to pave the way to the second stage. The distribution must obligatorily be of the form, $p(\tau) = p_{\text{infected}}\delta(\tau = \tau_1) + (1 - p_{\text{infected}})\delta(\tau = \tau_2)$, where δ is the unit impulse function (delta dirac).

3.4 Neighborhood Configuration

Several CA rules exist to decide which cells qualify as neighbors. The following in 2D are two of the most important, while the third is another suggestion of ours. The neighborhood configuration we are going to try are given by the following formulas. Radius refers to how many immediate neighbors they refer to. We have been using $r = 1$. [Gra02]

- $N_{(x_0, y_0)}^M = \{(x, y) : |x - x_0| \leq r \vee |y - y_0| \leq r\}$;
- $N_{(x_0, y_0)}^V = \{(x, y) : |x - x_0| + |y - y_0| \leq r\}$;
- The 2D Hexagonal neighborhood, which can be represented in a matrix by alternating top and bottom neighbors between rows [Pat06]. For $r = 1$,

$$N_{(x_0, y_0)}^H = \begin{cases} \{(x_0 \pm 1, y_0), (x_0 - 1, y_0 \pm 1), (x_0, y_0 \pm 1)\}, & y_0 \text{ odd} \\ \{(x_0 \pm 1, y_0), (x_0, y_0 \pm 1), (x_0 + 1, y_0 \pm 1)\}, & y_0 \text{ even;} \end{cases}$$

- Cubic (3D) von Neumann and Moore neighborhood will also be evaluated, which means adding a 3rd dimension to (a) and (b).

For this kind of models, only general qualitative analysis make sense, since it is yet impossible to calibrate the model with real data. The modus operandi behind HIV cell-to-cell transmission is unknown. The idea behind these models is exactly proposing plausible hypothesis for the phenomenon. Here we contrast neighborhood configuration to see if there is another which might make more sense.

In order for the logic behind the rule “ $\#A1 \geq R$ ” to remain intact, we are going to take R as being half the number of immediate neighbors: $|N|/2$, as described in Table 3.2 on the following page.

Interestingly there are not many differences between these different rules. All 2D lattice configurations (L^2) use $L = 700$. When in an 3D lattice (L^3), Figueirêdo, Coutinho, and Santos [FCS08] have

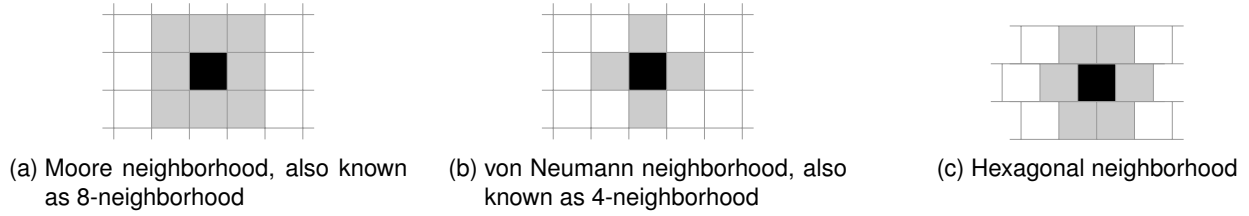


Figure 3.13: Contrasting neighborhood configurations. ($r = 1$)

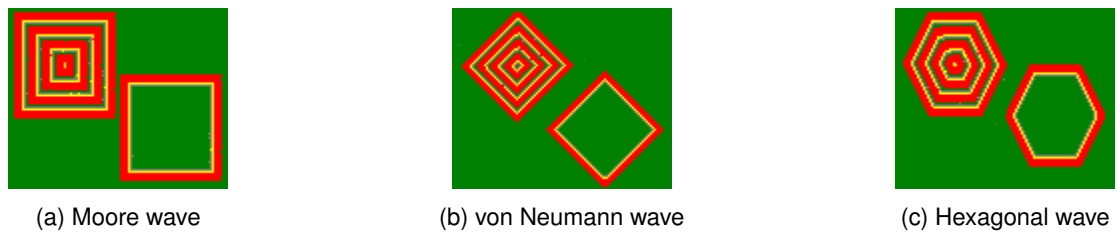


Figure 3.14: The different wave patterns, for the aforementioned 2D rules.

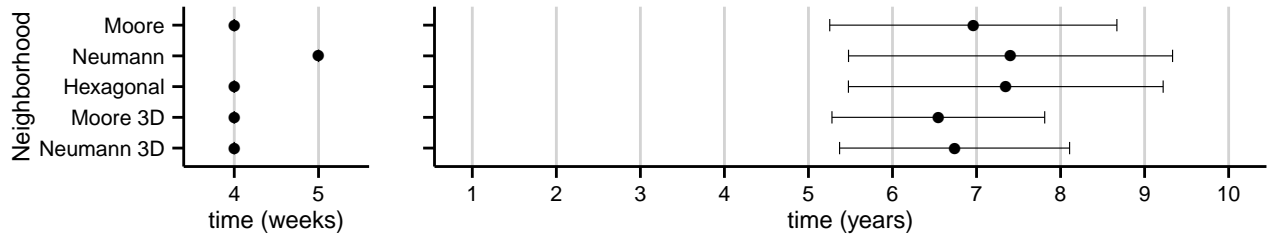


Figure 3.15: Our sensitivity analysis to various periods and respective result in terms of the primary peak, and AIDS phase. 50 simulation runs were performed, with error bars representing one standard deviation. $L = 700$ for 2D, and $L = 300$ for 3D. Furthermore, R has been defined as half of the immediate neighborhood. In the end, we can safely say lattice configuration is largely irrelevant with regard to HIV dynamics.

Neighborhood	$ N $	$R = N /2$
Moore	8	4
Neumann	4	2
Hexagonal	6	3
Moore 3D	26	13
Neumann 3D	6	3

Table 3.2: Infected A2 radius R considered for different neighborhood rules.

found $L = 300$ to be a good value, which reproduces the AIDS period within the ordinary 6-7 year time frame. We also tested with $L = 250$, but AIDS started much earlier. L is much more sensitive when in 3D. It is not yet clear what the relation between the 2D and 3D lattice is with regard to HIV modeling.

3.4.1 Variable Neighborhood

As mentioned before, Shi, Tridane, and Kuang [STK08] reduced the initial HIV concentration, p_{HIV} , by considering different neighborhood configuration as disease spreads. The idea is to have the number of neighbors being considered to grow as more viruses are released. Virus load, V , is used to represent viral spread.

Several new parameters have been calibrated by the authors. Virion decay $c = 0.3$, and the number of virions per infected cell is set at $n = 480q$, with q being a probability given by the current treatment being applied, so $q = 1$ represents no treatment. V then evolves following the difference equation:

$$\Delta V = \#A1n - cV.$$

This amount represents a virus reservoir within the infected cell, and the higher this virus concentration, the authors hypothesize, the higher the diffusion range, and the number of neighbors M is then given by:

$$\Delta M = \begin{cases} \frac{\Delta V}{30na}, & \text{if } \#A1 \geq a \\ \frac{\Delta V}{12na}, & \text{otherwise,} \end{cases}$$

where a represents the initial infection concentration and is a constant given by $a = p_{\text{HIV}}L^2$, and the constants 30 and 12 represent conversion rates for viral load into neighborhood cells. These are values that were found by the authors, and they assume there is a discrete behavior in the radius dynamics. As the initial condition, we have that initial neighbors $M(0) = 8$ (Moore neighborhood). This number very quickly rises to 12, which compensates for the lower p_{HIV} . After the initial peak, M comes back down to 4, and stays under 8 for many years, until it very slowly grows back again to 12 in the AIDS period.

Finally, given that there are M number of neighbors to choose from, it is not obvious what strategy to employ to choose from which of them to diffuse virus. The authors of the paper kindly provided me with the source code which answers this important question. The authors have chosen a constant list of neighbors, e.g. $\{(-1, 0), (0, -1), (+1, 0), \dots\}$ which encompasses several radii, and the first M neighbors are then chosen from that list. This list needs to be constant, and never changed, otherwise there would be no point in this method, since, at iteration t , let us say the cell at the left $(-1, 0)$ is chosen while, at iteration $t + 1$, the cell at the right $(+1, 0)$ is chosen, thus negating the entire point of the infection spreading through M neighbors, since the effects would end up being similar to those of the previous model (except in making oscillators more likely).

The initial condition for the viral load is set to $V(0) = an + \delta$, where δ is an unexplained residue and the authors have used $\delta = 3528000$. The authors probably wanted to nudge viral load graphical units to resemble those of real patients. Either way, this number is irrelevant. V is never used directly. M depends on ΔV , never on V .

The dynamics are simulated over Figure 3.16 on page 38. Interesting to note that in this model, treatment that reduces q does not lead to a less severe AIDS phase. The disease stabilizes into the

same ratio of healthy to infected cells. However, it is beneficial because it delays that final apocalypse, though even when using $q = 0.10$, the gain is of only of a couple of months, which means the medicine may not be worth the cost in life quality and possible secondary effects (Figure 3.17). It also implies that this kind of medicine, which restricts the infectious neighborhood, is completely irrelevant after the AIDS stage. More will be said about HIV treatment in the next section.

It should be noted that Shi, Tridane, and Kuang [STK08] managed to reduce p_{HIV} from 0.05 to 0.005. But Strain and Levine [SL01] suggest initial viral concentration may be as low as 10^{-10} . Furthermore, while Shi, Tridane, and Kuang's model offers some interesting extensions to Santos and Coutinho's original model, the variability in simulations is too low (Figures 3.11, 3.17 and 3.18 on the next page). Given the very high variability in HIV actual patients, it is hard to take serious a stochastic model which features so highly deterministic trajectories.

3.5 Treatment

In a latter article, González et al. [Gon+13], authors of the original model from 2001, incorporate both reverse transcriptase inhibitor and protease inhibitor treatments into the model (Figure 3.19 on page 39). Shi, Tridane, and Kuang [STK08] also makes an interesting suggestion which is also depicted here (Figure 3.18 on the next page).

In [Gon+13], a leviathan model is presented which seems unnecessarily convoluted. Here we present an approximation (Figure 3.20 on page 39), whereby transitions have no memory. This is not 100% faithful to their model, but it does approximate the model very well, only getting a transition wrong 1 every 34 times by our simulations, using $p_P = p_{RT} = 0.20$. If we embrace this transition-amnesic approximation, then we can further simplify it by replacing all states by the union of them all: $\boxed{H_T} \leftarrow \boxed{H_P} \cup \boxed{H_{RT}} \cup \boxed{H_{RTP}}$, since knowing which exact medication is in effect, at any point in time, can be easily analytically calculated, and is uninteresting in any case. This means we can then calculate the probability of being in this new state as $p = P(H_T) = p_P + p_{RT} - p_P p_{RT}$, using the probability rule of the union of non-mutually exclusive events.

In [STK08], medication affects viruses molecules, not T_H cells. The approach in both cases is a distinction without a difference in practice; the effect is the same. Both cases mean there is a protection against an infection working. This is very interesting because it suggests there might be situations when two very different classes of medication are symptomatically equivalent.

Interestingly, both these models suggest treatment vectors which can actually make diffusion easier, thereby increasing the pace of the disease as can be seen in Figure 3.11 on page 33. This happens because this kind of treatment makes delays asynchronous by depleting the barrier created by dead cells around the diffusion, making oscillator patterns more likely. In Figure 3.22 and 3.23 on page 39, treatment was started at around 4 and a half months into the initial contagion. In both cases, roughly the same Δt is illustrated, thus suggesting early treatment may be prejudicial. Treatment accelerates disease diffusion, thereby making disease reach stable equilibrium faster, more or less so depending on the intensity of the treatment. Obviously, however, in the extreme, when $p = 1$, the disease is rapidly disabled.

But, remarkably, virus severity at the final stable equilibrium point is lower, so treatment is *always* beneficial if started once equilibrium is reached or shortly before. These models are at most qualitatively correct, so no quantification of p will be attempted here.

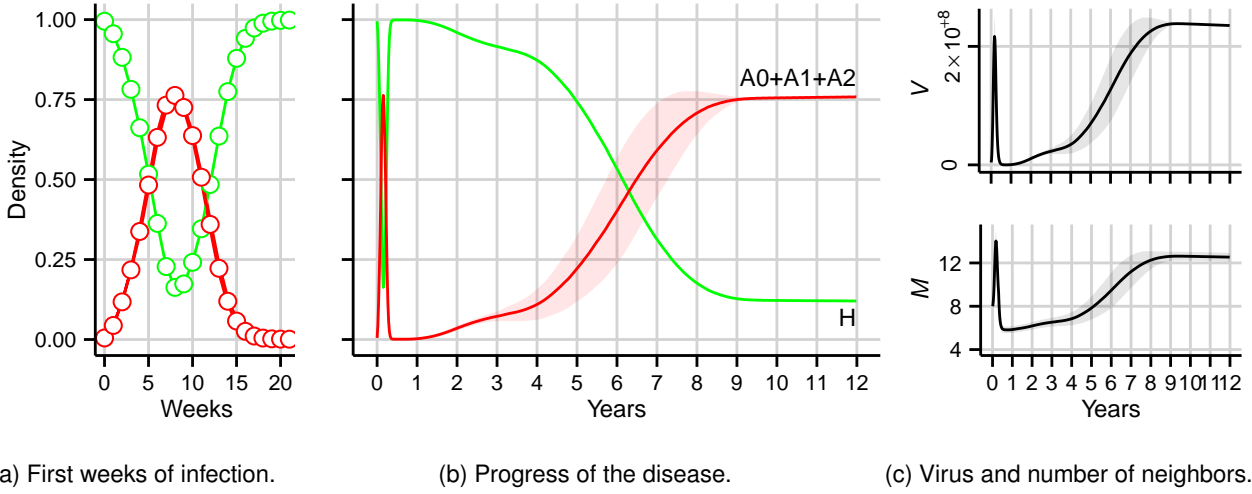


Figure 3.16: [STK08]'s model. Our simulation of natural HIV dynamics (without human treatment: $p = q = 1$). One standard deviation error bars for infected cells are drawn in light color (healthy cells deviation follow a similar pattern).

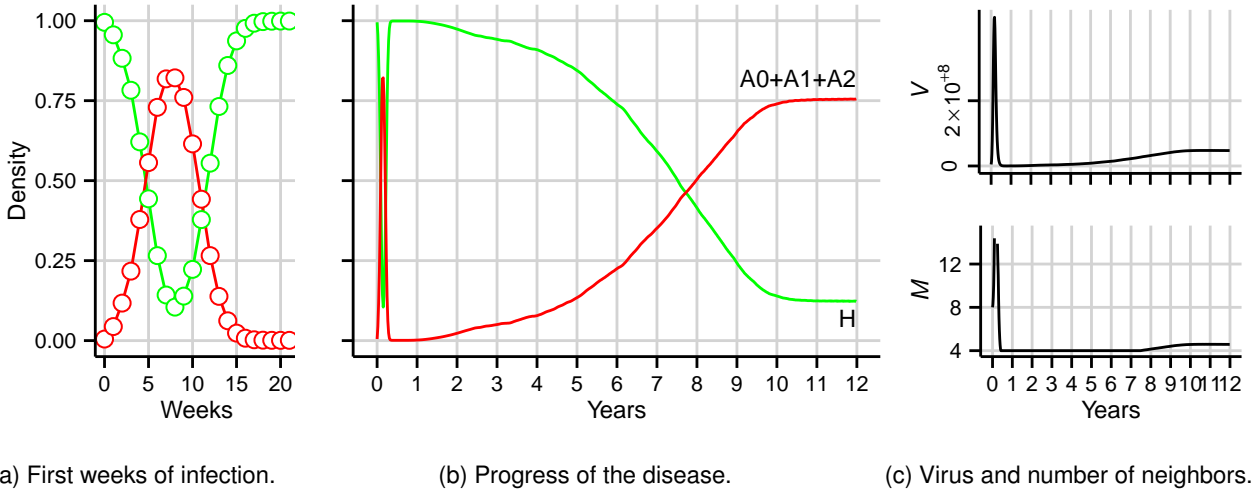


Figure 3.17: [STK08]'s model. Our simulation with treatment by tweaking M neighborhood difference equations ($q = 0.10$ after 1 year).

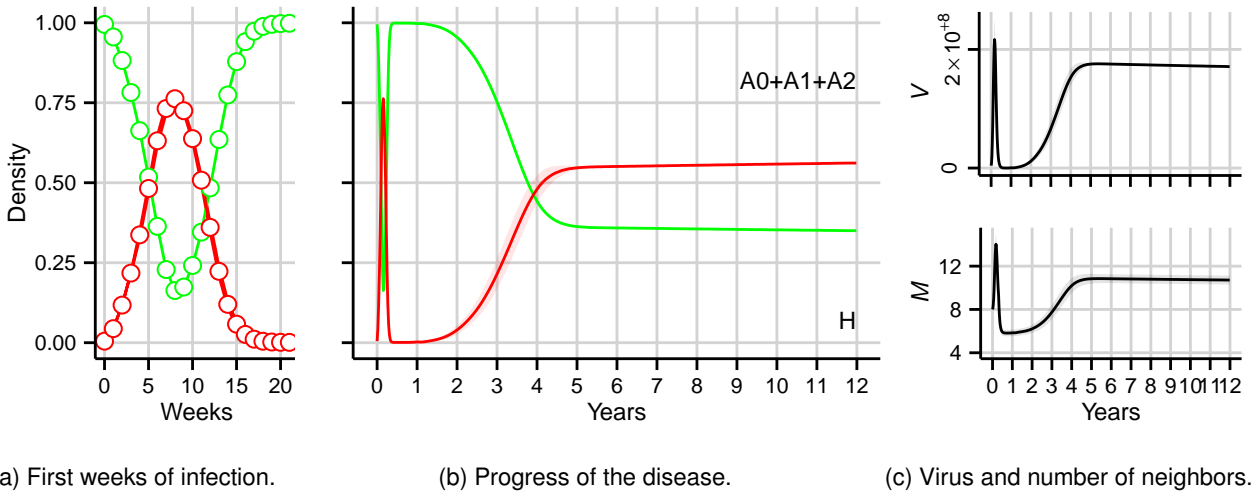


Figure 3.18: [STK08]'s model. Our simulation with treatment by tweaking the transcription inhibition level, as elaborated in section 3.5 ($p = 0.50$ after 1 year).

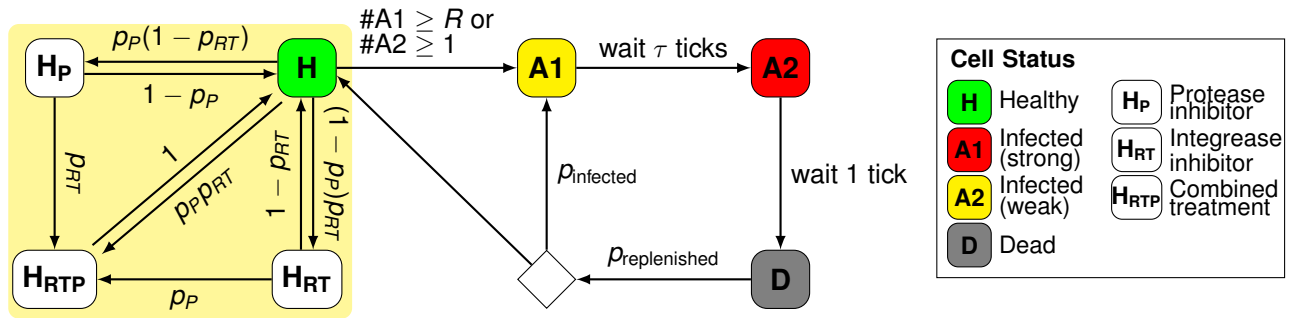


Figure 3.19: Adding treatment as in González et al. [Gon+13]. In this model, medication affects healthy cells, making them stronger to contagion.

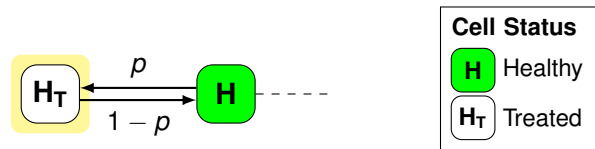


Figure 3.20: Our approximation to [Gon+13]. It is not effectively the same, but it comes very close. Here: $p = p_P + p_{RT} - p_P p_{RT}$.

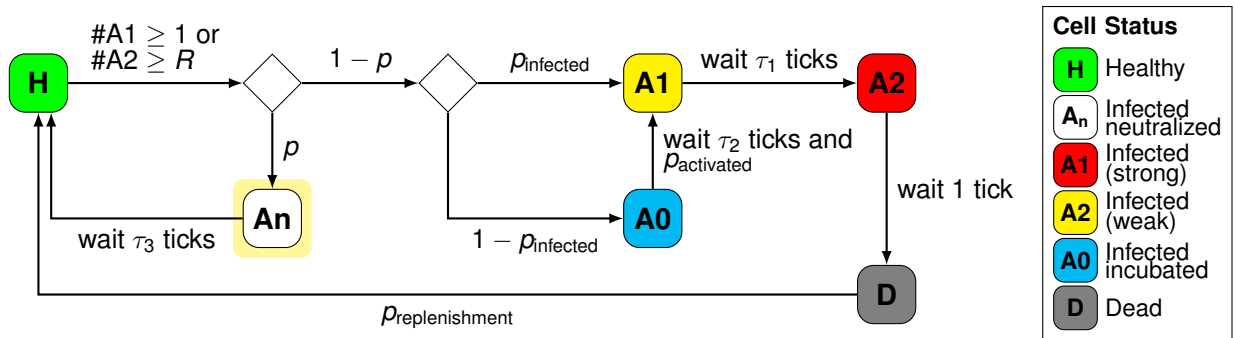


Figure 3.21: Adding treatment to the model as suggested by Shi, Tridane, and Kuang [STK08]. Highlighted is the new infected by innocuous virus state. In this view, medication affects the virus.

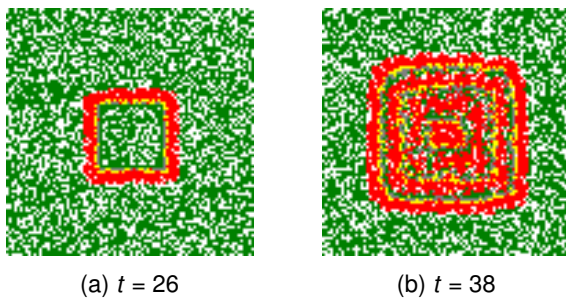


Figure 3.22: Counter-intuitively, disease resistance actually makes diffusion more aggressive by making oscillator patterns more likely. ($p = 0.20$)

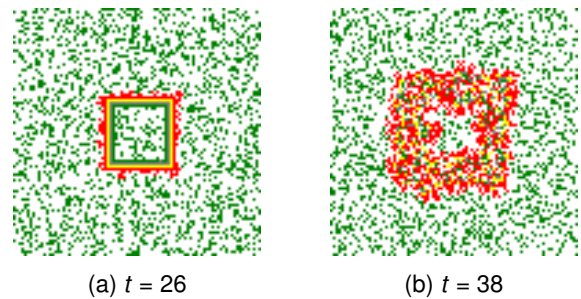


Figure 3.23: However, under a more aggressive treatment, oscillator patterns become again less likely. ($p = 0.50$)

This study of treatment dynamics also explain why HIV delays in HIV dynamics must be deterministic, or at least look deterministic within the 1 week range being modeled, as seen before.

In a follow up article, González, Figueirêdo, and Coutinho [GFC13] further complicate their model by adding a second CA layer, which represents free virions. Both layers interact by having the cellular layer produce viruses into the viral layer, and the viral layer infecting cells of the cellular layer. Viruses in the viral layer are extremely fast lived (lasting 1 tick/week). It was not clear from the paper nor from our results what did this second layer do. It did not change the results significantly.

Treatment Inferences. Most work in CA modeling has been derivative work from Santos and Coutinho [SC01]'s original model. That model has been extended and tweaked to a great degree. These changes usually come bundled with grand statements about what the results mean to physicians. These recommendations, such as avoiding treatment until the AIDS phase, because making T_H cell more resilient results in oscillators, making virus spread even faster, seem implausible in its face. Furthermore, there is evidence from the massive study START program, whose results have been just released, showing that early treatment is always beneficial [NN15]. This suggests one should be extremely cautious when taking these models seriously. And, in fact, while many CA models list treatment implications, no medical paper was found within the papers citing [SC01].

Data validation not being possible, the scientific method should consist in dissecting and simplifying the model to study how its several parts contribute to the phenomenon. No author has investigated wave dynamics, nor how model changes reflect on them.

Furthermore, many models add too much at the same time, in an attempt to be holistic. In effect, this gallant addition of new whistles and bells to the original model means no cross-testing of their effects is performed. In some papers, it is impossible to say the effect of each one of the individual change in the results.

Given that these models are not validated by observation, it is not clear that they inform us more than they disinform us. It seems at this stage, it is unwarranted to make any inference from these models, especially for treatment. In systems biology, the Cellular Potts Model, an Ising-based model, is a spatial simulation under which models are constructed in concert with a laboratory and *in-vivo* observation [GG92]. It might prove a sound venue of research. Alas, no work in HIV was found to have been performed with this model. It somewhat resembles CA, so it is possible both methods might be used to cross-check the simpler CA models.

Chapter 4

Differential Equations Models

A model is a story about an imaginary world that's both simple enough to understand completely and complicated enough to teach us something about the world we live in — like a fable, only more compelling.

Steven E. Landsburg, *The Big Questions*

Systems of **ordinary differential equations (ODEs)** relate variables through their derivatives. As one of the most common modeling methods, ODEs were naturally the first HIV mathematical models to be used. Within this method, the derivatives of the populations of such cells as the T cells are written as a function of HIV molecules, and vice-versa. The chapters are organized not by chronological order but in a more easily understood sequence.

The first models started cumbersome and terribly sophisticated, featuring variables representing many kinds of cells in several states of excitement. Perelson and Nowak [Per+96; NB96], in time, simplified the models into the aggregate model presented in the following section, whose final form is stripped of many of the dynamics and requires the measurement of only three variables. Their basic model has been used with actual data as a descriptive and perspective model. While measurable, these models lack any sense of causation, failing to provide a complete picture of the pathogenesis.

We start by presenting what we labeled the fundamental aggregate model, and some of the attempts at focusing on some of the aspects of the disease.

4.1 Aggregate Models

Like Santos and Coutinho [SC01]'s model within the cellular automaton (CA) realm, the following “fundamental model” of ODE HIV dynamics has been the ancestor, and instigator, of most other ODE models.

This “fundamental” model was first worked out by Perelson, Kirschner, and De Boer [PKD93], in 1993. The model tracked 4 variables, and also included such dynamics as carrying capacity dynamics. Several simplifications were proposed in a later article [Per+96]. Carrying capacity dynamics were eliminated, though some authors add them back in, and two variables were merged: latently infected T_H cells, and productively infected T_H cells.

It was then fully rendered in its full form by Nowak and Bangham [NB96], as presented below. This simple system of ODEs can provide for a statistically significant fit of a patient's disease history; hence fitting its coefficients to the patient's data can possibly illustrate some interesting properties about their disease history. Most models have since been derived from it.

$$\begin{cases} \dot{x} = \lambda - dx - \beta xv \\ \dot{y} = \beta xv - ay \\ \dot{v} = ky - cv \end{cases} \quad (4.1)$$

where

x, y, v are variables: healthy T_H cells, infected T_H cells and HIV copies, respectively,

$\dot{x}, \dot{y}, \dot{v}$ denotes their time derivatives,

λ is the constant rate of helper x cell production by the thymus,

d is the natural rate of death,

β is the rate at which helper x cells become infected as they interact with free virions,

a is the rate at which incubators/infected helper y cells burst,

k is the rate at which free virions v are created by infected cells,

c is the clearance rate of free virions.

Hereon we will use Nowak's notation of x, y, v to represent what Perelson and many others write as T, T^*, V . The dimension of the variables is cells per μL . The coefficient notation was sometimes standardized when we refer to the coefficient often, but we mostly keep the notation from the model's author being cited, so it may vary from model to model.

Considering the model, we can tell infected cells y are produced from interaction between healthy cells x and free virus v at a rate βxv and decline at a rate ay . Free viruses are produced from infected cells at rate ky , and declines at rate cv , also known as the clearance rate. It is not here being tacitly assumed the cause for the infected y declining rate of a , whether this decline is the result of natural death, or it is linked to the burst of the cell and the ensuing production of k free virions. Whether y death is dependent or independent of v production is a matter that we have to deal with if we are to describe this model in terms of stochastic simulations. We can also say from the model that the average lifetime of the infected y is $1/a$, and that of the free virus is $1/c$, so the total number of virus particles produced from one cell is k/a .

This model does not reproduce the three infection stages of HIV; it is to be taken as modeling the ongoing of the disease. Still we could say that the equilibrium point for a healthy individual, or prior to infection at $x(0)$, is given by $v^* = 0 \Rightarrow x^* = \lambda/d$, while after infection the system will converge, in damped oscillations, to the equilibrium

$$x^* = \frac{ac}{\beta k}, \quad y^* = \frac{\lambda}{a} - \frac{dc}{\beta k}, \quad v^* = \frac{\lambda k}{ac} - \frac{d}{\beta}.$$

The equilibrium is limited by the reduced number of cells to infect x , and the more cytopathic the virus (larger a), the smaller the steady-state abundance of free virus *ceteris paribus*. Although virus is contained at a stable equilibrium, this could still result in large virus load, severe tissue damage, and death.

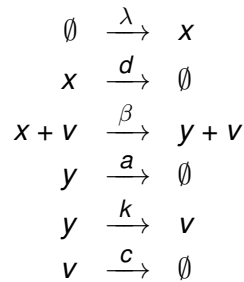
In order to study the initial behavior after infection, we can perturb the initial state, when $x = \lambda/d$, by introducing a small amount of virus. Since there are few infection virus at this point, we assume

the target cell population x remains approximately constant to its pre-infection level, and the model is then reduced to a set of linear equations [Llo01]. The basic reproductive ratio R_0 , the number of new infections due to a single infected cell, is then given by the product of the number of free virions released over the infected cell's life span, $k \frac{1}{a}$, times the number of cells infected by each free virion over its lifespan, $\beta \frac{\lambda}{d}$, and is thus:

$$R_0 = \frac{\beta \lambda k}{adc}.$$

If smaller than 1, then in the beginning of the infection each virus-infected cell produces on average less than one newly infected cell, and the infection cannot therefore spread. [NB96] If, on the other hand, $R_0 > 1$, then initially each virus-infected cell produces on average more than one cell, exactly R_0 cells, and is traditionally classified as “epidemic”.

Kinetic networks representations of ODEs will be detailed in Chapter 6. These networks encode important features of a model, and allow for both deterministic and stochastic analysis. The fundamental model of HIV dynamics could be rendered as the following kinetic network:



This model is explored as the second example in section 6.1.1 on page 72 in Chapter 6.

In 1993, the first ODE model was proposed where incubation delays are introduced. The idea being incorporated is the supposed latency period of HIV [PKD93]. The following is a model rendered by Culshaw and Ruan [CR00]:

$$\begin{cases} \dot{x} = s - \mu_x x(t) + rx(t) \left(1 - \frac{x(t)+y(t)}{x_{\max}}\right) - k_y x(t)v(t) \\ \dot{y} = k'_y x(t - \tau)v(t - \tau) - \mu_y y(t) \\ \dot{v} = N\mu_b y(t) - \mu_v v(t) \end{cases} \quad (4.2)$$

where τ is the latency period of HIV introduced as a time delay. All other coefficients are akin to the previous model. The variables notation is consistent throughout the chapter, but it was decided to keep the coefficients as in each respective paper.

Furthermore, there are aggregate models which generalize time delay τ so that, instead of a constant, it follows distribution $g(\tau)$, where \dot{y} is now computed using $\int_0^\infty g(\tau)x(t - \tau)v(t - \tau)d\tau$, which would usually be modeled by an Exponential or Gamma distribution, meaning most infected cells are expected to burst within a short time, but a few take longer to burst [NP02]. Delay techniques will be further discussed in Chapter 6, when introducing definitions and techniques of how to interpret delays within stochastic models.

A longer synthesis of ODE modeling of HIV was summarized in thesis by our colleague Carvalho [Car13]. We are not going to repeat the aggregate models summarized in her work.

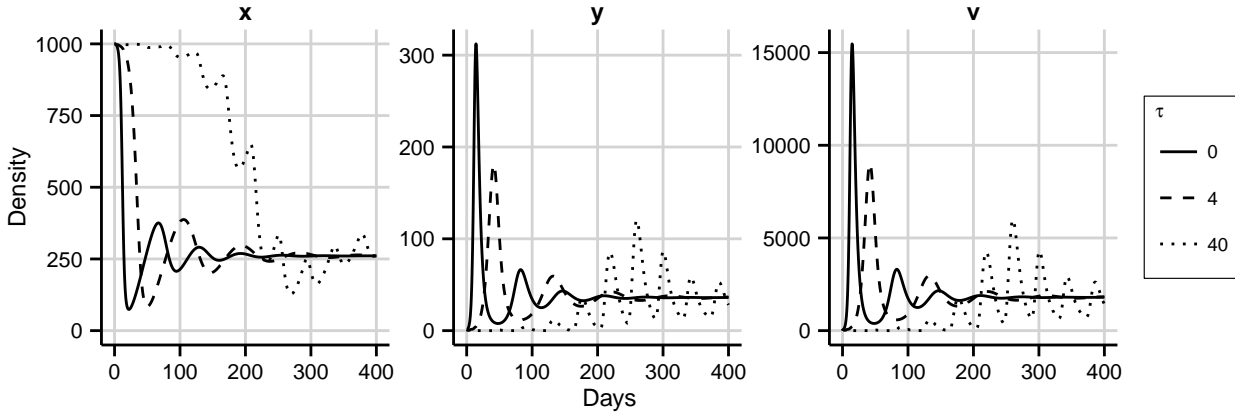


Figure 4.1: Our numerical simulations of the “fundamental model of HIV” as solid line. Delay extension (as dotted line) and parameters based on Culshaw and Ruan [CR00], with $\tau = \{0, 4, 40\}$ days (solid, dotted, and dashed, respectively, as annotated), $s = 10 \text{ day}^{-1} \text{ mm}^3$, $\mu_x = 0.02 \text{ day}^{-1}$, $r = 0.03 \text{ day}^{-1}$, $k_y = 2.4 \times 10^{-5} \text{ mm}^3 \text{ day}^{-1}$, $k'_y = 2 \times 10^{-5} \text{ mm}^3 \text{ day}^{-1}$, $\mu_y = 0.26 \text{ day}^{-1}$, $N = 500$, $\mu_b = 0.24 \text{ day}^{-1}$, $\mu_v = 2.4 \text{ day}^{-1}$, and initial conditions $x(\theta) = 1000 \text{ cells/mm}^3$, $y(0) = 0$, and $v(\theta) = 1 \times 10^{-3} \text{ copies/mm}^3$ for $\theta \in [-\tau, 0]$.

These aggregate models are modeling the virus and T cells in the blood stream, as they escape from lymph nodes where the actual action takes place. Most mathematical work is analytical, but these models can be used with actual data. We can measure patients’ T cells x , and viral RNA copies v . We cannot distinguish between healthy and infected T cell x and y , however. But Wu et al. [Wu+08] show we do not need y if we work with the derivatives of the 3rd order.

In the upcoming disaggregate models, although authors seldom explicit it, what is being modeling is the lymph node. Quantities within the lymph node are of course related to blood counts, since lymph nodes are connected to the rest of the blood, but that relationship is not linear since transitions between vessels and those organs are not arbitrary.

This distinction between aggregate and disaggregate is our own and, of course, somewhat arbitrary. It is inspired by other fields which rely heavily on ODE modeling, such as economics. The first hydraulic computer was in fact invented by an economist as an ODE model of the economy [Bis07]. With a long history of ODE, usage economists had to distinguish between older, complex models which they called micro models, and more recent post-Keynes models which capture the economy in very few variables such as GDP, and are known as macro models. These models helped conduct the economy by telling us things such as more money results in less unemployment. Still by not incorporating individual incentives, they failed to predict stagflation, which was a common phenomenon in the 70s when governments increased money but unemployment kept rising.

By this comparative study between what we coined aggregate and disaggregate models, we hope to shed some light into how they can work in harmony: economists for instance have learned to not discard micro models while studying macro models of the economy.

4.2 Disaggregate Models

4.2.1 Humoral Response

In 1983, two independent research groups isolated a new retrovirus that may have been infecting AIDS patients. The two retroviruses, called LAV and HTLV-III, were found to be the same, and in

1986 were then renamed HIV. That very same year, a mathematical paper was published by Cooper [Coo86], sketching out in a system of ODEs what was known of the virus.

Cooper presented two models — one for a “normal” virus and another for HIV, for contrasting as well as juxtaposition purposes, because co-infections were very common in AIDS patients. He hoped to understand by this two disease-model, whether that co-infection came earlier or later — and concluded that it was likely that it came earlier, and explained in those terms how HIV managed to take hold. To emphasize, it was not clear whether the other diseases were opportunistically taking advantage of weakness from HIV, or HIV was only able to take root and breed when the immune system was active in attacking a disease, and so there were many T cells for HIV to infect.

His answer made a lot of sense at the time since most patients were drug addicts or otherwise participated in what was seen at the time as risky behavior, and were not considered healthy individuals. His answer is now known to have been wrong, but this is still an interesting model to ponder at.

The two equations sets are [Coo86]:

$$\begin{array}{cc}
 \textbf{Normal Virus Model } X & \textbf{HIV Model } Y \\
 \left\{ \begin{array}{l} (\dot{B}X) = \gamma_1 BX - \gamma_2(BX)T - \lambda_1(BX) \\ (B\dot{X}T) = \gamma_2(BX)T - \lambda_2(BXT) \\ \dot{B} = \gamma_3(BXT) + \epsilon_B - \gamma_1 BX - \lambda_3 B \\ \dot{T} = \gamma_4(BXT) + \epsilon_T - \gamma_2(BX)T - \lambda_4 T \\ \dot{J}^* = \gamma_5 JX - \lambda_5 J^* \\ \dot{X} = \gamma_6 J^* - \lambda_6 X - nbBX \end{array} \right. & \left\{ \begin{array}{l} (\dot{B}Y) = \gamma_1 BY - \gamma_2(BY)(\gamma_2 T + \gamma_2' T^*) - \lambda_1(BY) \\ (B\dot{Y}T) = \gamma_2(BY)T - \lambda_2(BYT) \\ \dot{B} = \gamma_3(BYT) + \epsilon_B - \gamma_1 BY - \lambda_3 B \\ \dot{T} = \gamma_4(BYT) + \epsilon_T - \gamma_2(BY)T - \gamma_4' TY - \lambda_4 T \\ (B\dot{Y}T^*) = \gamma_2'(BY)T^* - \lambda_2'(BYT^*) \\ \dot{T}^* = \gamma_4' TY - \gamma_2'(BY)T^* - \lambda_4' T^* \\ \dot{Y} = \gamma_6'(BYT^*) - \lambda_6 Y - nbBY \end{array} \right.
 \end{array} \quad (4.3)$$

where

X is the concentration of a *normal* virus,

Y is the concentration of *HIV* virus,

B is the concentration of antigen-specific B cells,

(BX) and (BY) are antigen-specific B cells, those that can recognize and process antigen X or Y , respectively,

T are helper T cells that can interact with the antigen-specific B cells,

(BXT) and (BYT) the complex formed by B cells after being activated by the specific helper T cells,

J are the concentration of whatever cells are infected by virus X . It is assumed to be a constant j for simplification ($J = j$), since it is assumed there are too many J cells to make a difference and/or they are replenished by the system,

J^* are the concentration of infected cells by X ,

T^* are helper T cells infected by HIV.

γ_s , λ_s and ϵ_s are to be taken as parameters. λ refers to decay parameters, and ϵ refer to exogenous creation; these will be assumed too small to make a difference.

The virus is generally found in the lymph node, which is why one of its early names was LAV, or *lymphadenopathy-associated virus*, and so this model is a model of a lymph node. If HIV mechanics are unclear today, at the time, it was even less clear what the dynamics of the virus were, and much less which dynamics were significant to model. The author here decides to model humor response (from B cells producing antibodies) rather than the cell-mediated response (from killer T cells).

Antibodies are not modeled directly; instead virus is reduced at a rate of $nbBX$ or $nbBY$, respec-

tively, where n represents the number of B cells produced in the clonal expansion, while b is the rate at which individual antibodies attach to the virus. In the model antigen-specific B cells respond to identification by producing (BX) complexes which then require the presence of a T cell for clonal expansion into (BXT) complexes. These (BXT) complexes then start producing more B cells and T cells. In turn, ever more (BXT) complexes are formed, and some of the B cells start fighting their antigen-specific — directly in the model, which in actuality would happen by the action of antibodies. The “regular” X virus targets some unknown J cell for infection, and mounting its own production, while HIV Y virus targets the helper T cells, and more virus is produced when infected T^* cells help forming (BXT^*) complexes, which produce more virus rather than strengthening the immune system by further production of B and T cells.

This system is too complex for direct analytical interpretation. At the same time, numerical simulations are not helpful since the model represents immune dynamics for which quantitative information is lacking. Here we will detail with higher granularity the path and conclusions already paved by the author, to show what kind of work is done with these methods.

For analytical interpretation to be possible, some model simplification is in order; namely, we would like to tell if there is (and when) a turning point in the infection. Neglecting the decay and exogenous growth terms and assuming that $T_0 = B_0$, $(BX)_0 = (BXB)_0$ and that $\gamma_3 = \gamma_4$, then B and T cell proliferation proceeds at the same rate, $B(t) = T(t)$, and the model can be partly simplified to:

$$\begin{cases} (\dot{BX}) = \gamma_1 BX \\ (B\dot{X}B) = \gamma_2 (BX)B \\ \dot{B} = \gamma_3 (BXB) \end{cases} \quad (4.4)$$

Then, $\dot{B}(t) = \gamma_B \int_0^t B(t') \int_0^{t'} X(t'') B(t'') dt'' dt'$, with $\gamma_B = \gamma_1 \gamma_2 \gamma_3$. Since $B(t)$ is monotonically increasing (4.4), for $t'' \leq t' \leq t$, we have $B(t'') \leq B(t') \leq B(t)$. From this, since $X(t) \geq 0$,

$$\begin{aligned} \dot{B}(t) &= \gamma_B \int_0^t B(t') \int_0^{t'} X(t'') B(t'') dt'' dt' \\ &\leq \gamma_B \int_0^t B(t) \int_0^{t'} X(t'') B(t) dt'' dt' \\ &= \gamma_B B^2(t) \int_0^t \int_0^{t'} X(t'') dt'' dt' \\ &= \gamma_B B^2(t) \int_0^t \int_0^{t''} X(t') dt' dt''. \end{aligned}$$

Let $Z(t) = \gamma_B \int_0^t \int_0^{t''} X(t') dt' dt''$, then $\dot{B}(t) \leq Z(t) B^2(t)$, for all t . We get

$$\int_0^t \frac{\dot{B}(t)}{B^2(t)} dt \leq \int_0^t Z(t) dt.$$

Hence

$$\frac{1}{B(0)} - \frac{1}{B(t)} \leq \int_0^t Z(t) dt \iff B(t) \leq \frac{B_0}{1 - B_0 \int_0^t Z(t) dt}.$$

Replacing back $Z(t)$ into the last equation gives:

$$B(t) \leq \frac{B_0}{1 - B_0 \gamma_B \int_0^t \int_0^{t'''} \int_0^{t''} X(t') dt' dt'' dt''' }.$$

If we focus on the fast viral growth region, while the immune system is still mounting, we integrate only the production part of $X(t)$; neglecting the effect of the immune system and decay, we may integrate $X(t)$ by writing it as a matrix differential equation and solving it:

$$\begin{aligned} \dot{J}^* &= \gamma_5 J X \\ \dot{X} &= \gamma_6 J^* \end{aligned} \Rightarrow \begin{pmatrix} \dot{J}^* \\ \dot{X} \end{pmatrix} = \begin{pmatrix} 0 & \gamma_5 J \\ \gamma_6 & 0 \end{pmatrix} \begin{pmatrix} J^* \\ X \end{pmatrix}.$$

Given this ODE matrix has two real and distinct eigenvalues, we find that $X(t) = \frac{1}{2} X_0 \exp(\gamma_x t)$, which the article apparently approximates to $X(t) \simeq X_0 \exp(\gamma_x t)$, where $\gamma_x^2 = \gamma_5 \gamma_6 J$. By plugging this approximation of $X(t)$ back into $\int_0^t \int_0^{t'''} \int_0^{t''} X(t') dt' dt'' dt'''$, we have that:

$$\begin{aligned} \int_0^t \int_0^{t'''} \int_0^{t''} X_0 \exp(\gamma_x t) dt' dt'' dt''' &= X_0 \int_0^t \int_0^{t'''} \frac{1}{\gamma_x} (\exp(\gamma_x t'') - 1) dt'' dt''' \\ &= \frac{X_0}{\gamma_x} \int_0^t \frac{1}{\gamma_x} (\exp(\gamma_x t''') - 1) - (t''' - 0) dt''' \\ &= \frac{X_0}{\gamma_x} \left[\frac{1}{\gamma_x} \left(\left(\frac{1}{\gamma_x} \exp(\gamma_x t) - 1 \right) - t \right) - \frac{1}{2} t^2 \right] \\ &= \frac{X_0}{2\gamma_x^3} (2 \exp(\gamma_x t) - \gamma_x^2 t^2 - 2\gamma_x t - 2) \\ &\simeq \frac{X_0}{\gamma_x^3} \exp(\gamma_x t) = \frac{X(t)}{\gamma_x^3}. \end{aligned}$$

We can therefore rewrite B as $B(t) = (B_0)(1 - \gamma_B \gamma_x^{-3} B_0 X(t))^{-1}$, and so a singularity of B cells growth will occur when $X(t) \simeq \gamma_x^3 (\gamma_B B_0)^{-1}$. We can conclude that X_{\max} is always bounded above and that

$$X_{\max} \leq \frac{\gamma_x^3}{\gamma_B B_0}.$$

The real question then is how sick the person is until that point, and indeed if it survives. The model suggests that immunization can greatly be improved by increasing B_0 , which we already know from the efficacy of vaccines.

With regard to Y , the HIV virus, if we, again, discard decay terms and assume a pure infection, or when Y and/or B_y are sufficiently large relatively to any co-infection, then looking only at the rapid viral growth region (slow B cell response), we can assume $\dot{Y} = \gamma'_6 (BYT^*)$. Since Y is then monotonically increasing, we have that the production term of \dot{Y} is bounded by $c\gamma' B^2 Y^2 \geq \gamma'_6 (BYT^*) \leq 2\gamma' \gamma_B^{-1} YB$, where $\gamma' = \gamma_1 \gamma_2' \gamma_4' \gamma_6'$ and c is determined by the rates of decay of the various complexes.

Given that viral growth is bounded by $B^2 Y^2$, while virus destruction by the immune response increases as BY , then the immune response will only be enough for low values of Y and/or B . Since HIV infection takes root from a small number of viruses, then a stimulated immune system, with the presence of many B cells (and therefore infectious T cells), may be necessary for HIV viral growth to be enough to overcome virus response by the immune system. This model thus suggests a mechanism whereby a co-infection is necessary for HIV, and is not the result of AIDS. Of course, only the prior co-infection, or a posterior one, will be able to actually kill the co-infection. HIV by itself

does not harm any bodily essential functions, HIV destroys its defenses.

4.2.2 Cell-Mediated Response

The focus of the model in the previous section was only on the humoral response, which is not what medical doctors focus on today. Most research focuses on cell mediated immunity, mounted by T_C cells by killing infected T_H cell, not the virus directly.

A year afterwards, in 1987, the first model was published where cell-mediated immune response was taken as being the main immune response to HIV. Reibnegger et al. [Rei+87] take this path given neopterin levels found in HIV patients — these cytokines are produced by macrophages upon induction by the interferon γ released from activated T cells, and induces cell-mediated immunity. The model also considered co-infection. With over 20 variables, the model was too complex for any analytical interpretation to be performed. The authors could reproduce HIV dynamics only by introducing repeated infections because of the low probability of finding cell-mediated immunity in a vulnerable phase.

It is unlikely that patients were continually exposed to the virus. This provides an explanation for the surprisingly variable incubation periods and survival observed in human HIV infection. The virus “waking” up at random times would be a possible mechanism by which this model would make sense.

4.2.3 Spatial Dynamics

Within immune modeling, some others have used **partial differential equations (PDEs)**, in order to represent continuous properties such as coordinates (x, y) within a space. For instance, Su et al. [Su+09] provides an example of an immune system featuring space dimensionality by having cells move in 2D. In her model, neutrophils first appear in the antigen area, they are then inhibited by dendritic cell which come later, and so on.

In HIV modeling, a very cited paper featuring space is one by Funk et al. [Fun+05]. In this model, space is already presented as discretized system of ODEs. It is in effect the same as in PDE model given that numerical integrators would have to discretize space anyway. This model is an extension of the “fundamental model” whereby tissue is represented along a 21x21 2D plane:

$$\begin{cases} \dot{x}_{i,j} = \lambda - dx_{i,j} - \beta v_{i,j} x_{i,j} \\ \dot{y}_{i,j} = \beta v_{i,j} x_{i,j} - ay_{i,j} \\ \dot{v}_{i,j} = ky_{i,j} - cv_{i,j} - \frac{m_N}{8} \sum_{i_0=i-1}^{i+1} \sum_{j_0=j-1}^{j+1} [v_{i,j} - v_{i_0,j_0}] \end{cases} \quad (4.5)$$

Figure 4.2 on the following page shows how spatial dynamics help smooth out traditional dynamics. Virus inoculation is at the center of the lattice, $(11,11)$, whose time series resembles very closely traditional dynamics (in black). The time evolution across the rest of the lattice is offset in time, by the fact it takes some time for the virus to diffuse, and are also offset in terms of intensity because the same virus has to spread out through the entire tissue.

No ODE spatial models has been successful in reproducing all three phases of HIV. One exception is Bacelar, Andrade, and Santos [BAS10]. The authors say they were inspired by the CA model previously analyzed by Santos and Coutinho [SC01], and in fact share one co-author. In Bacelar, Andrade, and Santos [BAS10], a closed system of ODEs was used where all variables were in the

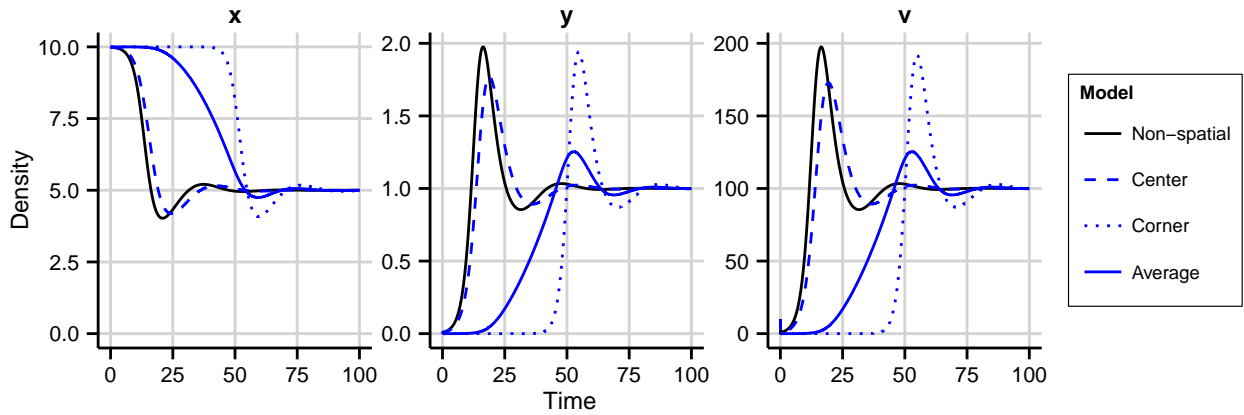


Figure 4.2: Spatial dynamics HIV ODE model.. Spatial dynamics (blue) are contrasted to traditional non-spatial dynamics (black). Average spatial dynamics, those at position (11,11) and (3,3) in the plane are represented as solid, dashed and dotted lines, respectively. Parameters used are: $\lambda = 1$, $d = 0.1$, $\beta = 0.001$, $a = 0.5$, $k = 1000$, $c = 10$, and $x_0 = 10$. The lattice is a 21×21 matrix of periodic boundary conditions with viral export m_v set to 10%. Virus is placed at the center: $v_{11,11}(0) = 10$, with all else $v_{i,j} = 0$.

[0, 1] range. In this model, after the primary stage of the infection, when virus is almost but eliminated and after T_H cell grow back in number, virions v are made to go to $v = 0$. However, by using special numerical trickery, virus count are never allowed to reach zero, but a value very close to zero, $\epsilon = 10^{-6}$. This means they never reach the (unstable) equilibrium point when $v = 0$, and follow the dynamics $\dot{v} = \dots + kv^{1.13}$. Of course, a rational number as close to zero, which on top of that is powered to a > 1 exponent, will take a very long time to grow back in number. The authors are thus able to reproduce the full cycle of the dynamics. While the model is mathematically remarkable, it is not medically useful. It was then adapted by Marinho, Bacelar, and Andrade [MBA12] to reproduce spatial dynamics. They applied spatial dynamics the same way that Funk et al. [Fun+05] applied it to the fundamental model by Perelson et al. [Per+96].

4.2.4 Shape Dynamics

Mutations were first explicitly incorporated by a model in 1990 by Nowak, May, and Anderson [NMA90]. This is also called “shape space” dynamics, because we can look at the possible mutation or shape dominion as a space, and look at virus mutation diffusion in a prism alike spatial diffusion.

$$\begin{cases} \dot{x}_i = kv_i - uvx_i \\ \dot{z} = k'v - uvz \\ \dot{v}_i = v_i(r - sz - px_i) + M(v) \end{cases} \quad (4.6)$$

where x correspond to the target T_H cell, z is the T_C cell response, and v the free virus. $M(v)$ is a stochastic factor by which a new virus is created, with $M = \epsilon$ for a new i , with a very low probability of $P = bQ' dt$. A numerical reproduction of this model can be seen in Figure 4.3 on the next page, where we have used $\epsilon = 0.0001$.

Variables are indexed to their strains/specificities. When no index is used, it should be taken as meaning the sum across all specificities (e.g. $z = \sum_i z_i$). Note that if we sum all strains, we get again the first set of ODEs, e.g. $\sum_i x_i = kv - uvx$.

The immune system is able to control the virus if, $\forall i, \dot{v}_i < 0$; in other words: $r - sz - px_i < 0$. We

can then find the maximum number of HIV strains by noting that n well-distributed strains can only be contained when:

$$\begin{aligned} n(r - sz - px_i) &< 0 \\ \Leftrightarrow n(r - sz) - px &< 0 \\ \Leftrightarrow n &< \frac{px}{r - sz} \end{aligned}$$

Calling the right-hand side n_c , we would like to find out when the system $n_c \leq n$. That is, we would like to find out the upper limit n_c of different strains that can be suppressed simultaneously by the immune system. Between the extremes $sz + px > r > sz$ lies the interesting region of dynamic behavior, when n_c diversity threshold is greater than 1 but finite, and for which it makes sense to incorporate mutations in the model.

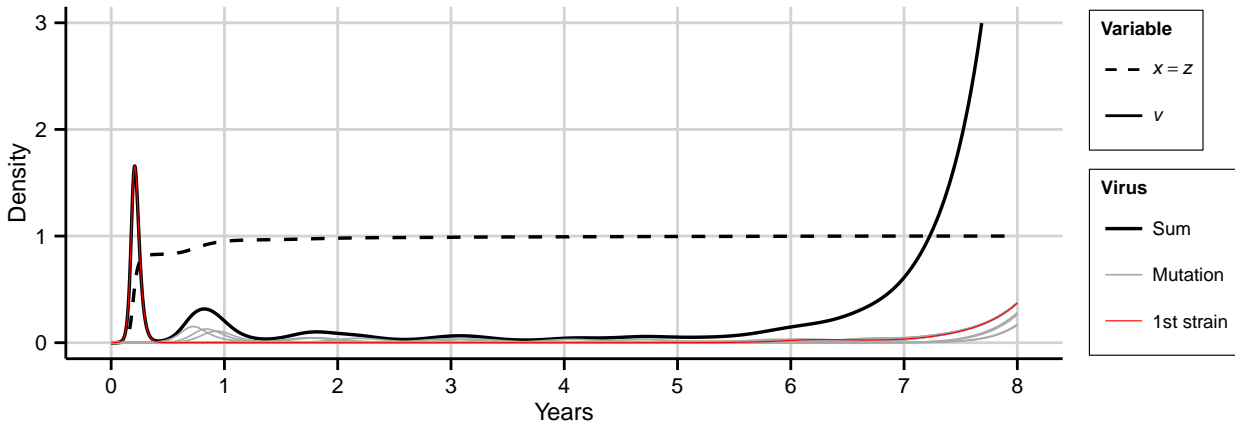


Figure 4.3: Virus mutation model by Nowak.. [NMA90] Instance of one numerical simulation using the following values from the article: $r = 5$, $s = 4.5$, $p = 5$, $k = k' = u = 1$ e $bQ' = 2$, implying a diversity threshold $n_c = 10$. The various mutations are illustrated in gray, and they sum up to the black line. In red line is the first virus (the original strain).

Over Figure 4.3, model (4.6) is reproduced numerically. As mutations build up, the immune system is eventually exhausted and is then overcome.

Another model of mutation incorporation is by Zhdanov [Zhd07]. This model requires no stochasticity, and is rendered as:

$$\begin{cases} \dot{x}_i = k_i v_i - \lambda_i x_i - \nu_i v x_i \\ \dot{k}_i = -\gamma_i v k_i \\ \dot{v}_i = r_i v_i - p_i v_i x_i + \sum_{j \neq i} (\kappa_{ji} v_j - \kappa_{ij} v_i) \end{cases} \quad (4.7)$$

The model is reproduced over Figure 4.4 on the following page.

Units of the density of population of cells and HIV copies is irrelevant here. These are not measurable amounts. These are hypothetical models. They will be the main inspiration to the main model described in the agent-based model (ABM) chapter, Chapter 5.

Also worth mentioning is the study of shape space dynamics by Hershberg et al. [Her+01]. In his

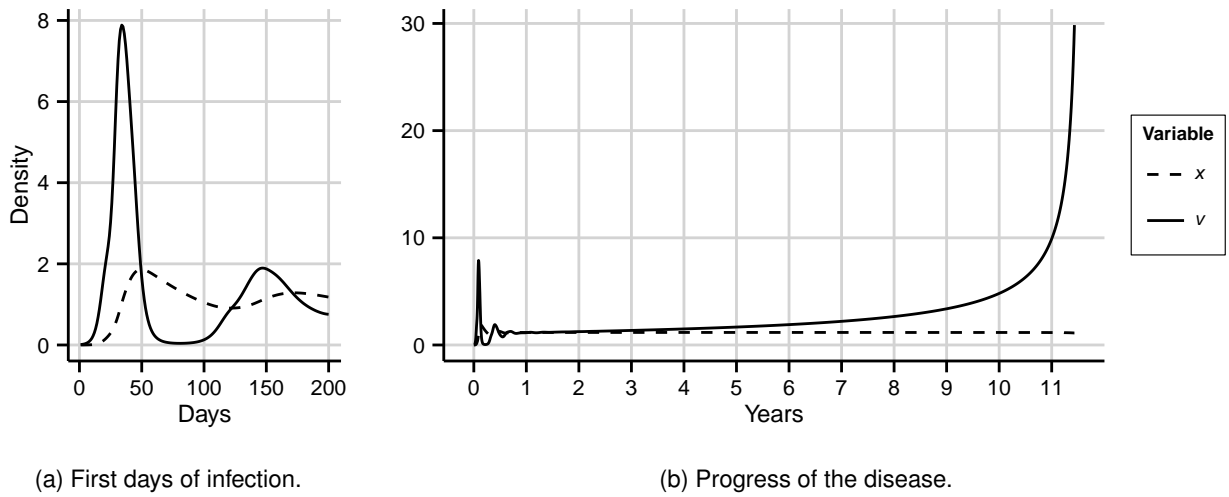


Figure 4.4: Virus mutation model by Zhdanov. [Zhd07] Numerical simulation using values from the article: $n = 10$, $r_i \in [0.2, 0.4] \text{ day}^{-1}$, $p_i \in [2, 4] \text{ day}^{-1}$, $\kappa_{ij} \in [0, 0.01] \text{ day}^{-1}$, $\lambda_i \in [0.01, 0.02] \text{ day}^{-1}$, $\nu_i \in [0.001, 0.002] \text{ day}^{-1}$, and $\gamma_i \in [1 \times 10^{-4}, 2 \times 10^{-4}] \text{ day}^{-1}$. $v_1(0) = 0.01$ and $v_i(0) = 0$ for $i > 1$, $x_i(0) = 0$.

model, he represents shape dynamics within a grid, with each cell of the grid representing a different strain. These mutations diffuse to their neighbors, in a fashion that resembles CA models. The model itself is very different than a CA model. The authors describe the model using CA language, but it is identical to any of the shape dynamics models here discussed, only that diffusion occurs in 2D coordinates, rather than 1D.

Chapter 5

Agent-Based Models

If all of science were wiped out, it would still be true and someone would find a way to figure it all out again.

Penn Jillette

One recent and very trendy method of modeling has been **agent-based models (ABMs)**. A search for HIV and ABM finds over 5 thousand papers on the topic, a good one-quarter of those found when searching for HIV and ODE, whose models are older and the most popular. Half of these papers were published in the last 6 years. Most however are either philosophical or methodological in nature, or extend closed source systems such as Simmune to which source code is not provided [MM99]; only one paper was found to describe a fully working model which reproduces the three phases of the disease [LS10].

ABMs are computer models representing and simulating the actions and interactions of autonomous agents (be they firms and government in an economy, or cells and molecules in the immune system in our case). ABMs try to reproduce the real phenomenon in the computer, and so are often used to synthesize and test the internal congruence of theories. Drawbacks of ABMs are that they scale poorly, and require firm theoretical foundations and empirical data for simulation parametrization. This is a bad premonition when it comes to HIV modeling because the numbers are of massive magnitudes and most parameters are unknown.

In these models what is modeled are individuals (or agents) and not aggregate populations. This paradigm turns things upside-down; each individual in the model stores its properties, rather than individuals being categorized into variables. Instead of having $v = 5$, we have a list v , where each virus is an object that can have a quasi-infinite number of properties. It is considered as a more natural paradigm for working with domain experts because it is logically structured closer to the phenomenon at study. It in fact sometimes hailed as a more intuitive and direct mapping from reality to the model.

More concrete **advantages** are that ABMs allow us to trace and follow the fate of a particular agent. More importantly, ABMs allow for easily association of continuous quantities to an agent; these continuous properties would have to be discretized for most other mathematical models. Continuous properties are possible using partial differential equations (PDEs), but they quickly become analytical intractable as more properties are added, and numerical integration requires them to be discretized.

anyhow. The disadvantages are that ABM are not easily to formalize or interpret analytically, since they are more of a methodology, than a specific method. Each case is a particular case. In fact, even the simulation complexity depends more heavily on the implementation than on the model.

Usually, ABM implementations in the field of *systems biology* are called **particle simulators**. These simulators have time complexity of $O(n^2)$, and space complexity of $O(n)$ [Gro15]. Interestingly, here n refers to the number of agents, not of variables as in a system of ordinary differential equations (ODEs) or reactions as in the stochastic simulation algorithm (SSA) method to be studied in the following chapter. Therefore, as we will see, it is conceivable that an ABMs is faster than a ODE model for smaller population sizes with too many properties. Such properties would have to be dubbed into variables in the ODE model, whose integrator would have to iterate. If there are many variables whose value is equal to zero, the iteration is wasteful, and ABMs may be sometimes faster in those circumstances.

If we would like to add a new agent property, whose value range is k , to an ODE model, it will require $(n - 1)k$ new variables, increasing by that same order of magnitude the complexity of the numerical integrator. Viewed in another way, in ABMs we iterate agents; in ODEs we iterate variables. ODEs do have the advantage that, being deterministic, a single run is enough to produce all statistics there are. To produce an average under an ABM, the model would have to be run several times. They do produce more statistics, namely how much the phenomenon diverges from the average. ABM computational gains may be obtained through the usage of distributed computing techniques, though this again depends very much on the implementation.

5.1 General Purpose Artificial Immune Systems

The grandfather of all agent-based lymph node simulations is ImmSim by Ceiden and Selada, developed in 1990 [Sie+90]. It is the most revered and referenced simulation. Space is discretized in a grid and diffusion happens in the fashion of Brownian motions, without a realistic concern for chemotaxis. When two agents collide, they interact according to a few rules. For instance, a free virion may be captured by a macrophage. A helper T cell then may become stimulated when interacting with the macrophage. Specificities are implemented using bit-strings — these are probabilities that two colliding agents will successful interact. Several expected behavior may be modeled in qualitative terms, such as the effect of vaccination.

Albeit revered and inspiring a generation of Artificial Immune Systems (AIS), this simulator was meant to be educational, and no simulator based on ImmSim has been cited in the medical literature. The exception is Simmune whose 2nd generation is now based on the Cellular Potts Model [GG92], and no longer on ImmSim.

ImmSim has inspired the development of a multitude of AISs, some of which are: ImmSim3, C-ImmSim, Simmune [MM99], SIS, AbAIS, Parlmm [BC01], CyCells, and CAFISS [TJ05]. Even, a Portuguese AIS was developed: Simullm [Fac05; Fac08]. An European Union funded AIS called ImmunoGrid was also under development [Hal+10], but there are no news of anything being actually delivered by the project. Unfortunately, all these systems seem to be close source. Some of them adding such things as a third space dimension. The idea behind these simulations does not seem to be producing statistically valid results, but merely to validate possible trajectories against theory.

Some of these are ports of an older AIS to a more modern language, or a complete re-implementation;

either way, all are based on the original ImmSim. In this system, cells and molecules were layed out in a grid, and move randomly. When they collide, a reaction may happen depending on if the two agents have affinity with each other. The idea behind these systems will be elaborated throughout this chapter.

5.2 Formalism

Usually, an ABM would be implemented in an **imperative language** (also known as procedural language), be it a generic language like C or Java, or a more specific language such as NetLogo [Wil99] or toolkit such as Java/Repast [Nor+13]. Such languages are structured as a recipe, or series of steps, usually called scripts, lacking (to a lesser or greater degree) higher-level constructs for how the program is structured and behaves.

Any modern high-level language allows steps to be structured into functions, a formalism expressing a self-contained way to associate transformations of input into output. Matlab, for instance, forces the programmer to structure his project into files, whereby each file may contain either a single function or be a script without any function. **Object-oriented programming** languages, such as Java, go one step further by including structures such as classes which provide formal means of expressing manipulation of data blocks through functions within said classes. This is one level of abstraction above functions. Java, in particular, forces programmers to structure their project in files, whereby each file is one class of the program. Furthermore, these languages, offer keywords such as `public` and `private` constructors, among others, allowing further expression of what level components are visible and so allow for stronger analytical introspection. [RG11]

It is a categorical error to compare object oriented programming and agent based modeling as some authors do. Object oriented programming allow for a higher layer of programming from which to manipulate code. Agent based models might benefit from that additional construct, but it need not to. In fact, NetLogo, a very popular environment for agent based modeling, uses Logo which is not an object oriented language [Wil99].

All these constructs are unnecessary for developing a computer program; any modern program could be programmed as a script, since ultimately it will be broken down to a series of steps to be run in machine code. The intended goal of every one of these constructs is to layer computer programs, allowing the navigation and introspection of the program, making programs more robust, and to make it easier to build ever more sophisticated software. The higher level the language, the more abstraction and formalism can be naturally expressed in the code. Of course, no language is programmer-proof; any optional constructs can go unused, and any enforcement mechanism can be circumvented. Ultimately, developing computer programs is an art.

As discussed before, ABMs have no formalism, and each use case is a different use case. Here comes the **Unified Modelling Language (UML)** [RJB04]; a standard for the development of computer programs using a diagrammatic language. It is an ISO standard since 2000, and while it is most often used as an inert description of an already developed computer program, this visual language can actually be used to develop software, start to finish.

A language such as UML promises to add an upper and more refined layer level to computer programs, very popular especially in embedded systems where programming errors are more costly. Its use has been explored in the field of computer biology for its rigor as a language where it is

paramount that research results are not affected by deficient programming. It also provides a visual language whose slices can be exposed for publication, while hiding more mundane lower level parts of the computer simulation. Being a diagrammatic language also eases communication between domain experts and modeling experts.

The UML standard defines how the diagrams may be converted into modern computer programming languages. The standard is divided into two parts: 4 diagram schemes for the static representation of the computer program (e.g. structure of the program into classes, functions and variables); 5 diagrams for dynamical modeling that actually specifies program behavior (for instance, how variables change to a given stimulus). Read et al. [Rea+14] discuss what and where the different diagrams can be useful in systems biology. At the static level, class diagram may be used for describing system organization. The sequence diagram, activity diagram and state machine diagram are useful at the dynamical levels, with the state diagram being the most widely adopted in general.

In the **class diagram** a relation between classes (or entities) is established using arrows. This notation is exemplified and used in 5.7 on page 63.

An example of a **state diagram** follows as Figure 5.1. This type of diagrams list the several potential states of a discrete variable, and how they transition when stimulated. Furthermore, function calls may be associated with a transition change. Most diagrams in Chapter 2 and 3 are drawn in a format very identical to that of state diagrams (with the initial state omitted).

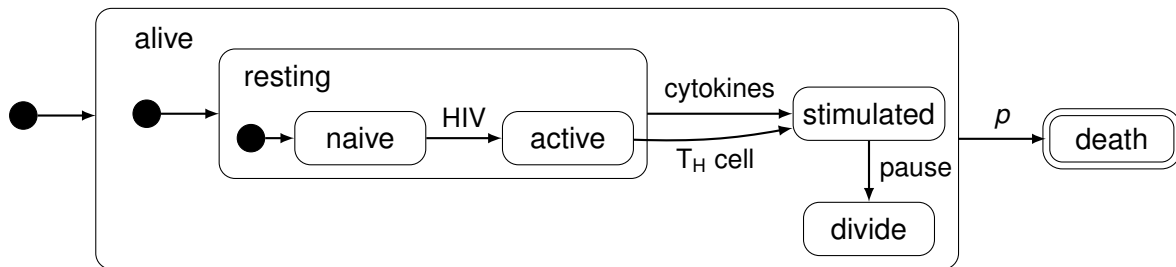


Figure 5.1: Example of a potential B cell state diagram. The diagrammatic notation is described in the text.

These diagrams models a discrete variable relatively to an exogenous stimulus, known as an event. When an event is triggered, the variable may change to another state, if it has a corresponding transition. A state is represented as a rounded square, . The initial state of the variable is indicated by the symbol . Furthermore, states may be placed within another state. These outer states are conceptual and do not actually exist. They are used to economize in transitions; meaning any transition from an outer state to another state A is the same as each of its inner states having a transition to A. Since outer states are only conceptual, a variable never has the value of the outer state, and so one of its state must be indicated as the initial state.

State diagrams are inspired by the statechart diagrams as originally designed by David Harel [Har87]. Statecharts represent variables of finite range, i.e. discrete variable, also known as state variables. These machines are then graphs or tuples describing possible transitions between values of the state variable, depending on external events (such as changing state to activated after the T cell is presented an antigen), and whose transitions may have associated actions. States may be written very succinctly by embedding them within parent states; parent states do not actually exist, and are used as virtual states meaning that any transition applied to them is automatically applied to any child state.

Harel has since applied it to the lymph node [SCH08]. In fact, one general purpose immune

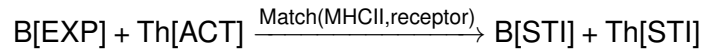
system simulator was developed by his team with the name of GemCell [Ami+08], which is unfortunately closed source. Several papers have been published by his team, but not enough diagrams are provided for other teams to work upon it.

The UML formalism is not the ideal tool for immune dynamics, as this is mostly about how two cells or molecules interact and respond to one another. UML is not made for that higher level of modeling. The modeler would need two UML diagrams: one for one cell, and one for another, with possible bugs being introduced because one has to look at two diagrams to tell what the interaction entails. Modeling at the level of the interaction is not possible with UML.

A more interesting formalism is introduced by the simulator Parlmm [BC01], an example of which is the following code:

```
INTERACTION: B, Th
SPECIFIC    : Yes
MATCH       : B-MHCIIpeptide molecule, Th-receptor
CONDITION   : IsEXP(B) AND IsACT(Th)
ACTION      : DoSTI(B) AND DoSTI(Th)
```

This format is a little verbose. A more visual formalism would be something along the line:



In one stroke, it is possible to read the entire interaction. This formalism resembles much in fact kinetic reaction networks which will be explored in Chapter 6. As we shall see, using this notation, we will be able to write the ABM later presented in this chapter and then try to improve its performance by simulating it using traditional stochastic methods.

5.3 Event-driven versus time-driven simulation

```
1: Set initial conditions for all agents and the
   environment.
2:  $t \leftarrow 0$ 
3: while  $t < t_{\max}$  do
4:   for all agents  $a_t$  do
5:      $a_{t+1} \leftarrow f(a_t)$ 
6:   end for
7:    $t \leftarrow t + 1$ 
8: end while
```

Algorithm 3: Synchronous update scheme.

```
1: Set initial conditions for all agents and the
   environment.
2:  $t \leftarrow 0$ 
3: while  $t < t_{\max}$  do
4:    $t \leftarrow$  next event in the queue  $Q$ 
5:    $a_t \leftarrow$  next agent in the queue  $Q$ 
6:    $a_{t+1} \leftarrow f(a_t, Q)$ 
7:   Queue  $Q$  may have been changed: sort
8: end while
```

Algorithm 4: Asynchronous time update scheme.

Most ABM simulations are implemented as a simple cycle, wherein time is incremented at a constant rate and there are several probabilities of events occurring (Algorithm 3). An alternative approach, especially useful when probabilities are rare, is to schedule the time to the next event, depending on these probabilities or other deterministic rules. This approach does require keeping an

extra structure for a scheduling queue of events. This approach is exhibited as Algorithm 4 on the previous page [GT08].

These two approaches are akin to the two stochastic simulations approaches where either probabilities model time increments, or probabilities model events occurring in constants intervals of time. Both approaches will be better explored in light of stochastic simulation over the following chapter.

In the specific case of HIV modeling, given the high molecular numbers and reactions going on, the synchronous time update scheme is likely to be more efficient.

5.4 From ODE to ABM

It seems, so far, this paradigm is very different than the ODE methods explored in the previous chapter. In fact, nothing could be further than the truth. Zaiyi, Kwang, and Cing [ZKC05] show that both paradigms can be used interchangeably, if only discrete properties are used. The average of several ABM runs has to be the same as ODE results because any rates described in an ODE can be transcribed into an ABM in the form of individual probabilities applied to that cell. For instance, the results from the decay

$$\dot{B} = -0.10B$$

are approximately the same as the average of several simulations running the following Java code:

```
1 for(B b: bs)
2     if(P(0.10*dt))
3         b.die()
```

Several authors which work on ABM modeling do, in fact, start their work by adapting ODE models using this approach. Population rates become individual probability rates. Bersini et al. [Ber+12] offers some examples of porting ODEs to ABM this way in the form of UML diagrams.

In the following chapter, we will explore how to perform the less common transition of ABM to Markov simulation. Interestingly, by Aristotle's law of equivalence, we can establish that these three methods are equivalent, with one caveat: parameters must be discrete, and that the population average is not always the same as the average of individual simulations when correlations are involved. Again, this will be better explored in the following chapter.

5.5 HIV Modeling

In agent-based modeling, antigens (such as HIV) are traditionally modeled as agents. The problem is that, due to the mind boggling number of HIV copies, this does not scale. One approach by Simmune [MM99] and others is to compromise on the agent modeling, and revert to ODE modeling for HIV and other molecules, such as antibodies and cytokines. These molecules are treated as values within a matrix representing the grid. This is the same approach used in Cellular Potts modeling [SH97]. We can think of this ODE layer as being an extra agent, the "environment". But agents are no longer used within this layer [GT07].

For the reason that in HIV modeling we are dealing with stupendous count scales, and by the fact that HIV molecules are "dumb" (less complex), and so no realism is lost by the lack of any kinetic logic, this compromise does not lose much in the way of agent modeling. If we would like

to incorporate mutations, we would have to revert to several layers corresponding to each strain; in effect, an indexed system of ODEs.

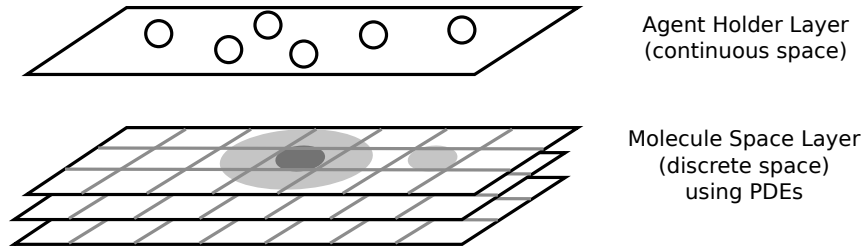


Figure 5.2: Layers in an ABM model. [GT07]

Some authors, however, do simulate each HIV molecule as a single agent. It is the case of the the foregoing modeling.

5.6 Affinities

As previously seen when considering Parlmm formalism (section 5.2), two agents may only interact with a probability relating how well their specificities combine. Each agent has a 8-bit string which provides the basis for interactions with specific cells, i.e. cells of similar affinity. This approach has started with the ImmSim simulator [Sie+90], and then Nowak et al. [Now+91].

This approach take the specificity of the receptor or paratope of each cell or virion as a 8-bit string (a byte) (see Figure 5.3). Given a Hamming complementarity distance between the strings of two agents, a binding probability is calculated based on an affinity potential function. Because molecules do bind with other molecules with whom complementarity is not perfect — an affinity function is a probability function describing the probability of success for a given molecular binding. A simple binding probability function is then given by e.g.:

$$P(i, j) = p_0 \exp(-\alpha H(i, j)),$$

where p_0 and α are constants, and $H(i, j)$ is the Hamming distance between the strings of the two interacting proteins as comparing the two binary strings bit-by-bit using a dirac delta (see also example in Table 5.1 on the next page):

$$H(i, j) = \sum_{k=1}^8 (1 - \delta_{(i_k=j_k)}).$$

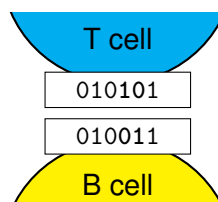


Figure 5.3: Representation of the commonest affinity interaction rules between two cells.

A binary string is used because computationally all numbers are binary strings and can be quickly compared in C (see Algorithm 5 on the next page). While seemingly unrealistic, it is not far-fetched. A point mutation, meaning when a base pair is badly transcribed, may suffice to change the specificity

```

1 int hamming_distance(unsigned x, unsigned y)
2 {
3     int      dist = 0;
4     unsigned val  = x^y;  // xor
5     while(val != 0) {
6         dist++;
7         val &= val-1;
8     }
9     return dist;
10 }

```

Algorithm 5: Hamming distance computed in C. [Weg60] (C99 version slightly simplified)

	000	001	010	011	100	101	110	111
000	0	1	1	2	1	2	2	3
001	1	0	2	1	2	1	3	2
010	1	2	0	1	2	3	1	2
011	2	1	1	0	3	2	2	1
100	1	2	2	3	0	1	1	2
101	2	1	3	2	1	0	2	1
110	2	3	1	2	1	2	0	1
111	3	2	2	1	2	1	1	0

Table 5.1: Hamming distances between two strings of 3 bits.

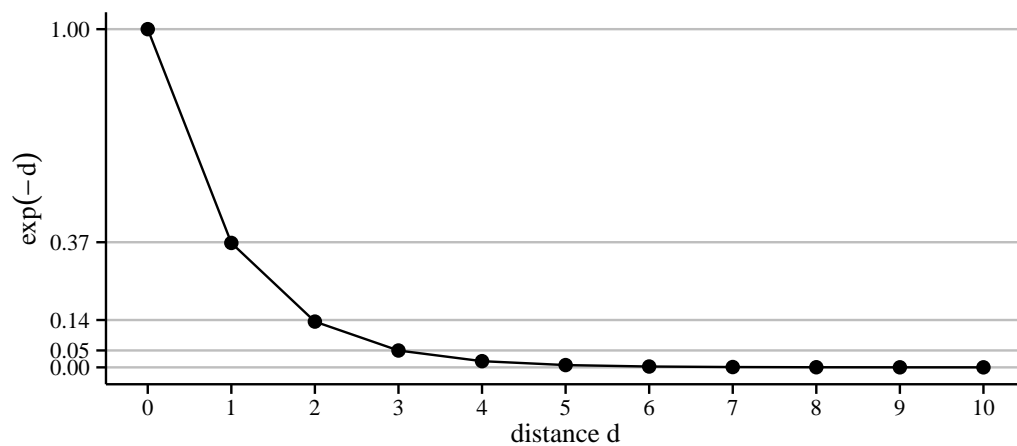


Figure 5.4: Probability of interaction as a function of the Hamming distance between two strings.

of both the transcription activation protein and its binding site [Ret+93; Smi+04]. Also, as Dasgupta and Nino [DN08] put it: «[i]n theory, any matching rule defined on a high-level representation can be expressed as a binary matching rule». There seems to be more dispute in which probability function to use, provided a Hamming distance; in general, the inverse exponential of the distance, presented before, is used.

Lin and Shuai [LS10] extends the concept by using different strains of binding molecules. They simulate a mutation by randomly flipping one bit value of the string. Notice that specificity is simulated for both: between T_C cells and the virus being presented by the infected T_H cells class I MHC, and also between T_H cells and HIV for activation. In their model, they use a 10-bit string, not a byte (8-bits) as was previously most common, having $2^{10} = 1024$ possible molecular specificities.

5.7 Lin-Shuai Model

Some authors have preferred to test specific parts of the theory in *ad-hoc* models, usually partially inspired by cellular automata models. The only self-contained ABM that managed to implement HIV three phases is the following model by Lin and Shuai [LS10]. This model will be described here, and more fully explored over the following chapter.

A matrix identifies “agents” disposed within the 2D grid which simulates a lymphatic node (see Figure 5.5). At each iteration t , agents move within a radius of 3 units, in which the next position is given by a random position taken from the possibility set: $\mathbf{p}_{t+1} = \{(x_{t+1}, y_{t+1}) : |x_{t+1} - x_t| \leq 3 \wedge |y_{t+1} - y_t| \leq 3\}$. The model considers periodic boundary conditions, meaning $\mathbf{p} = \mathbf{x} + L\mathbf{k}$ for any $\mathbf{k} \in \mathbb{Z}^2$, where L is the length of the grid.

In each entry of the grid, there can be at most one molecule of each type. It is possible for more than one molecule to be in the same entry of the grid (but not of the same type). Two molecules, i and j of the same type, will move sequentially and, in case of conflict, their positions are swapped, $\mathbf{p}_i \leftrightarrow \mathbf{p}_j$.

After the moving step, interactions are tested for. Two molecules may interact with any molecule of another type which is found in its same position. Interaction is a probability function of their affinities and constant probabilities. Molecules may be destroyed or new ones created as a result of an interaction.

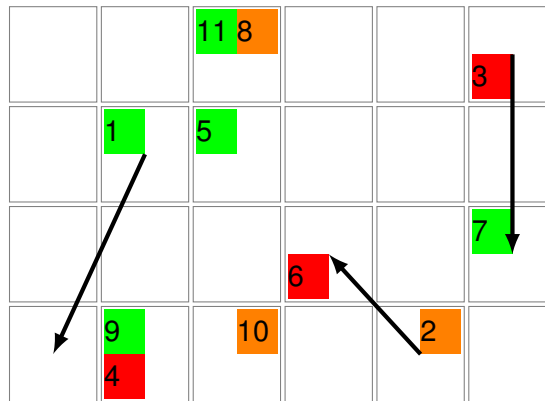


Figure 5.5: Representation of [LS10]’s model. Color: T_H cell (green), T_C cell (orange), and HIV (red). Numbers represent the identification of the “agent” and are unique; an agent may have other properties, besides type and position, which are not conveyed by the matrix. Arrows represent possible trajectories of movements from t to $t + 1$

The notation hereby used is: **x** (T_H cell), **z** (T_C cell), and **v** (HIV).

Implicitly in the grid are “agents”, meaning that each individual molecule had an unique identifier associated only with itself. This identifier maps several properties associated to that molecule. All molecules, **x**, **z** and **v** have to them associated an independent “string” which codifies the amino-acid specificity associated to the protein in its ligand regions. For example, one **x** may stimulate a **z** when its receptors are complementary, while a **z** cell destroys a **x** cell which displays a viral epitope in its MHC II that is complementary to itself.

As previously seen, these strings are represented by binary numbers, and the probability of a successful interaction is given by a distance function of their strings (see Figure 5.4 on page 60). For instance, two perfectly complementary molecules, 0000 and 1111, have interaction probabilities of 80%, while two molecules whose Hamming distance is 1, 1101 and 1111, will have an interaction probability of merely $\approx 29\%$. These probabilities are given by $P_h(a, b) = 0.80 \times \exp(-H(a, b))$, where H is the Hamming distance between the two molecules, which corresponds to a binary bit-by-bit difference.

Regardless of string, **x** cells may be infected by any **v**, which cuts into the envelope of the cell, and does not require a successful ligand. When the DNA of the retrovirus connects to cellular DNA, it reprograms the cell’s software in order to produce copies of the virus. These HIV copies stay within the cell until the cell bursts when it can no longer physiologically support more viruses (in this model, after an internal production of $n_{lys} = 5$ viruses, the cells bursts and the virus spreads around). A **x** cell has therefore the following properties:

- complementary string;
- whether it is infected (0 or 1), and, in the affirmative case, it will feature:
 - the complementary string of the virus that has infected it (viral epitope);
 - the number of virus it has produced within itself.

On the other hand, both **z** and **v** will only have a string of affinity has their properties.

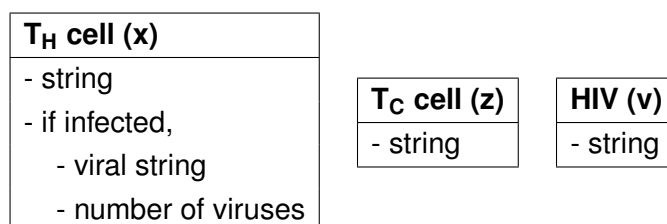


Figure 5.6: The model stores this information for each molecule.

The authors of the model have presented it without recurring to any formalism. The model is presented in the form of prose. It is possible these details are not completely correct, though our results look similar as far as one can tell comparing graphics (Figure 5.8 on page 66).

The basic structure of the model can be reproduced in succinct format through an UML class diagram (Figure 5.7 on the following page). The type of the agents, its properties, and how they inherit them are represented here, and the legend explains briefly how this type of diagrams works. The idea is that all agents have in common specificity as a property. This model does not feature many properties, which is unusual in an ABM. The algorithm is represented in pseudo-code afterwards, in Algorithm 6 on the following page. The pseudo-code, using the previously mentioned kinetic reactions network, will be presented in the following chapter, where it will be further discussed as well.

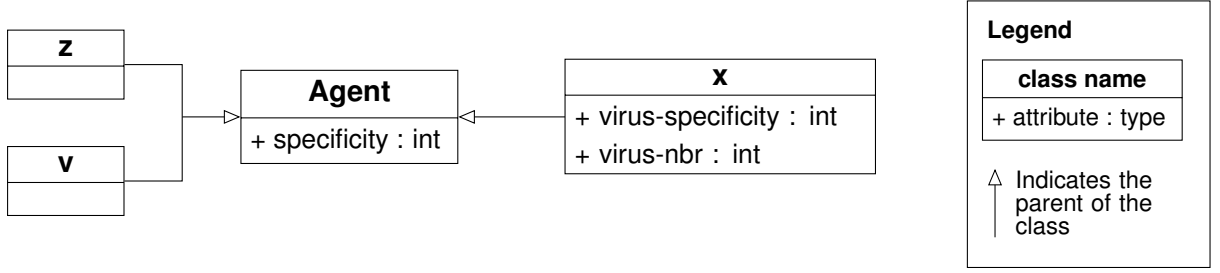


Figure 5.7: UML static class diagram of Lin Shuai's model.

```

1: for all agents do
2:   move  $[-r_m, r_m]$ 
3:   if another agent of same type there then
4:     swap them
5:   end if
6: end for
7: for all  $x + v$  do
8:   if  $x$  not infected then
9:     if  $P(p_0 P_h(x, v))$  then
10:      proliferate  $n_x$  within range  $r_x$ , if
      none there
11:    end if
12:  end if
13:  if  $P(p_v)$  then
14:    if  $P(m_v)$  then
15:      virus mutation; flips one bit
16:    end if
17:     $x.virus-specificity = v.specificty$ 
18:     $x.virus-nbr = 0$ 
19:    virus gets integrated into the cell
20:  end if
21: end for
22: for all  $x$  do
23:   if  $x$  infected then
24:     if  $P(b_v)$  then
25:        $x.virus-nbr++$ 
26:     end if
27:     if  $x.virus-nbr = n_{lys}$  then
28:        $x$  dies
29:     proliferate  $n_{lys}$  virus within range  $r_v$ ,
    if none there
30:   end if
31: end if
32: end for
33: for all  $x + z$  do
34:   if  $x$  infected and  $x.virus-nbr > 0$  then
35:     if  $P(p'_0 P_h(x, z))$  then
36:        $z$  proliferates
37:     end if
38:     if  $P(k_0 P_h(x, z))$  then
39:        $x$  killed
40:     end if
41:   end if
42: end for
43: for all  $z$  do
44:    $i \leftarrow z.specificty$ 
45:   if  $P(d_{z0} * (1 - hill(i)))$  then
46:      $z$  of strain  $i$  dies
47:   end if
48: end for
49: for all  $v$  do
50:    $i \leftarrow v.specificty$ 
51:   if  $P(d_{v0} + (1 - d_{v0}) * hill(i))$  then
52:      $v$  of strain  $i$  dies
53:   end if
54: end for
55: create  $n$   $x$  cells with  $n = x_0 * d_{x0}$  at random
    position, if none there
56: create  $n$   $z$  cells with  $n = z_0 * d_{z0}$  at random
    position, if none there
  
```

Algorithm 6: Our pseudo-code reformulation of Lin and Shuai's model. Where $Ph(i, j) = \exp(-H(i, j))$, and $H(i, j)$ is the Hamming distance between quasi-species i and j . The hill function is defined as: $hill(i) = x_i / (x_i + \theta)$ with x_i = the number of x cells of specificity= i .

UML state diagram would complicate more than it would help. Parlmm simple syntax as explored before is more helpful. The model will be rendered using that notation over the following chapter.

The original parameters of the model from the authors are presented in Table 5.2.

Parameter	Description	Value [Lin2001]
p_v	probability virion infects healthy T_H cell	0.80
b_v	probability infected T_H cell generate virion	0.80
p_0	baseline probability T_H cell is activated by a virion	0.80
p'_0	probability T_C cell is activated by an infected T_H cell	0.80
k_0	probability a virion is killed by T_C cell	0.80
m_v	probability a mutation occurs during transcription	5.5×10^{-5}
n_{lys}	lysis threshold of infected T_H cell	5
n_x	number of offspring produced on T_H cell proliferation	5
n_z	number of offspring produced on T_C cell proliferation	5
d_{v0}	natural death rate of the virus	0.01
d_{x0}	natural death rate of the T_H cell	0.01
d_{z0}	natural death rate of the T_C cell	0.1
r_m	agents movement range	0.01
v_0	initial concentration of the virus	0.03
x_0	initial concentration of T_H cells	0.8
z_0	initial concentration of T_C cells	0.1
n	strains string length (bits)	10
L	length of the lattice	100
θ	the density yielding half-maximal expression (hill function)	0.5

Table 5.2: Lin and Shuai's parametrization of the model.

At the beginning, HIV starts to dominate, since there are few specific T_C cells at that early time. But, soon after, T_C cells start destroying infected T_H cells if it recognizes the epitope shown in T_H cell's class I MHC, and puts a break on HIV (lines 33-42 on Algorithm 6). In the presence of complementary HIV, T_H cells reproduce themselves (lines 8-12), stimulating the production and also extending T_C cells's life through the hill function (lines 43-47), which go on to destroy infected T_H cells. Problem arises as HIV mutates (lines 14-16), which may require a while given the low probability of mutation, and then starts destroying T_H cells (lines 13-20, 22-32), with greater speed than the speed specific T_H cells can detect it, and proliferate. Since HIV infects any T_H cell, but every T_H cell, although fast to reproduce, can only act in the presence of its complementary HIV, they are at a disadvantage. As T_H cells reproduction halts, T_C cell reproduction also halts since the hill function depends on the number of T_H cells. In the final period of the disease, AIDS, HIV remains dominant because, even though it gets destroyed by other immune cells other than T_C cells, HIV keeps infecting T_H cells that the thymus keeps producing (line 55). These cells, which are produced at a constant rate, exogenously to the model, have low HIV affinity (unlike activated T_H cells that auto-replicate when they found HIV), so only sheer luck alone could produce another T_H cell with greater affinity to possibly produce T_C cells in quantities large enough for it to endanger HIV. HIV loses every battle, but ends up winning the war.

It is interesting to observe that given HIV reproduces asexually: its phenotype, namely its expression at the string/epitope level, is influenced by mutations alone — i.e. transcription errors (lines

14-16). This is unlike most species on Earth, which usually evolves through sexual combinations, without mutations being required. New species often arise only by sexual recombination, since copy errors (i.e. mutations) are so low [HP96]. HIV is able to evolve and “learn” even asexually, by sheer force of its high rates of infection and consequent transcription. Its RNA and DNA copy errors are also higher than those committed within human cells using the human “machinery” [San+10].

HIV drugs, in general, act with the purpose of inhibiting the various mechanisms of HIV, such as the transcription of RNA into DNA. Treatment means tweaking the probability rates to their empirical observations.

The model concludes by presenting the immune system at the beginning with a wide range of T-cell specificities, but only one HIV specificity. The immune system is however defeated. HIV molecules kill all T_H cells indiscriminately, but it also (indirectly) “binds” and stimulates T_H cells (and, by proxy, T_C cells) to proliferate. T_C cells start killing infected cells. The system has much difficulty completely eliminating every trace of HIV at any moment, but it does a good job at keeping them very close to zero. However, mutations accumulate, and, as mutations accumulate, the system starts working less well and less well, because it spreads more and more, thinner and thinner. In conclusion, there is an asymmetry in that HIV “binds” to any T_H cell, but each T_H cell and T_C cell only “bind” to a specific HIV molecule.

Results of the model are represented in Figure 5.8 on the next page. Only v strains are shown in the graphic, because thymus is always producing new x and z cells, so they always come close to the maximum of 1024 of strains, even if very few of each.

In dashed, we have reproduced the dynamics without any spatial concerns. That is, the first move step over Algorithm 6 on page 63 was replaced by a “move $[0, L]$ ”. (Actually the Fisher-Yates shuffle algorithm was used [Dur64], but it is the same thing for all purposes.) Since any agent can be at any place within the grid, this effectively makes the model position agnostic, and thus non-spatial. From the results, it is clear there is not much distinction between spatial and non-spatial dynamics, therefore the spatiality of the model have been overblown in the original article. It is completely irrelevant for the parameters used. These results are for 50 simulation runs however; with more computational power and more simulations being averaged out, it is likely both lines would converge even more.

5.7.1 Sensitivity analysis

It is of interest to analyze how sensible are model’s parameter space as we consider converting the model into kinetic reaction networks. Several notes from the sensibility analysis in Figure 5.10 on the next page:

- The larger the **string length** n (shape space domain), the easier it should be for the AIDS virus to gain traction against the immune system. Surprisingly, for $n \geq 5$, larger n , it is hard to tell if there are any gains in increasing the domain space of mutations. These are string length n values, so they represent 2^n possible strains. The strain domain is respectively: 16, 32, 64, 128, 256, 512, and 1024. There seems to be a threshold after which n does not matter any longer. It becomes difficult for the virus to take hold when $n = 4$ ($n_c = 2^4 = 16$), and impossible for $n = 3$ ($n_c = 2^3 = 8$) or for any lower values.

Model 4.6 on page 49, of the previous chapter, already showed very similar dynamics. It found a n_c strains threshold, only after which the virus was able to take hold.

- We also found that the **length of the lattice** or number of agents, L^2 , affects the simulation

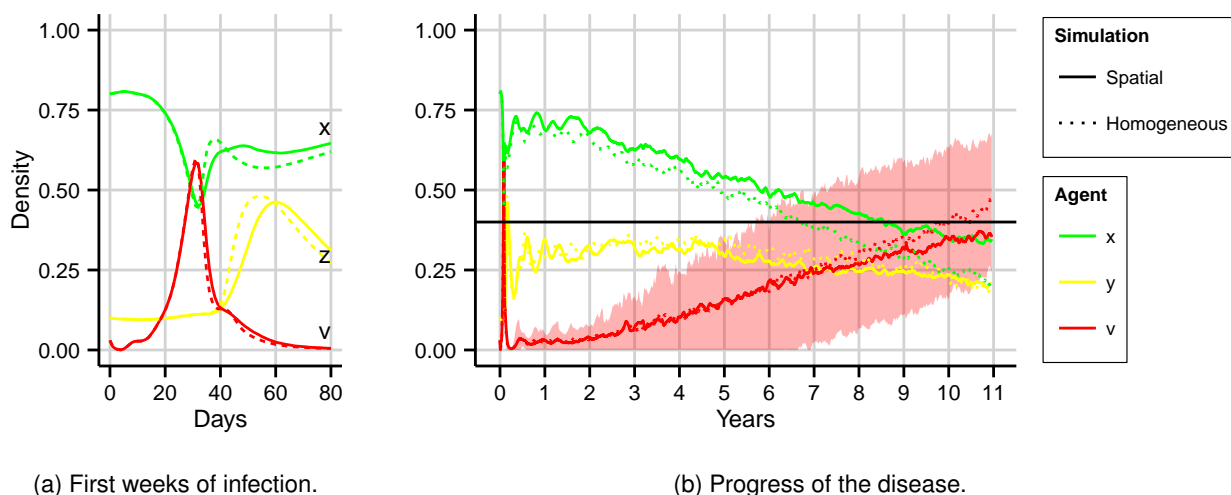


Figure 5.8: Our reproduction of the model as a timeseries of the density of agents x (T_H cell), z (T_C cell), and v (HIV). In dashed non-spatial dynamics are represented as explained in the text. In light color are error ribbons within one standard deviation [CFV07]. Only error bars for HIV/spatial are drawn to avoid visual clutter; the others follow similar patterns. Due to constraints in computational power, this is an average of 50 simulations.

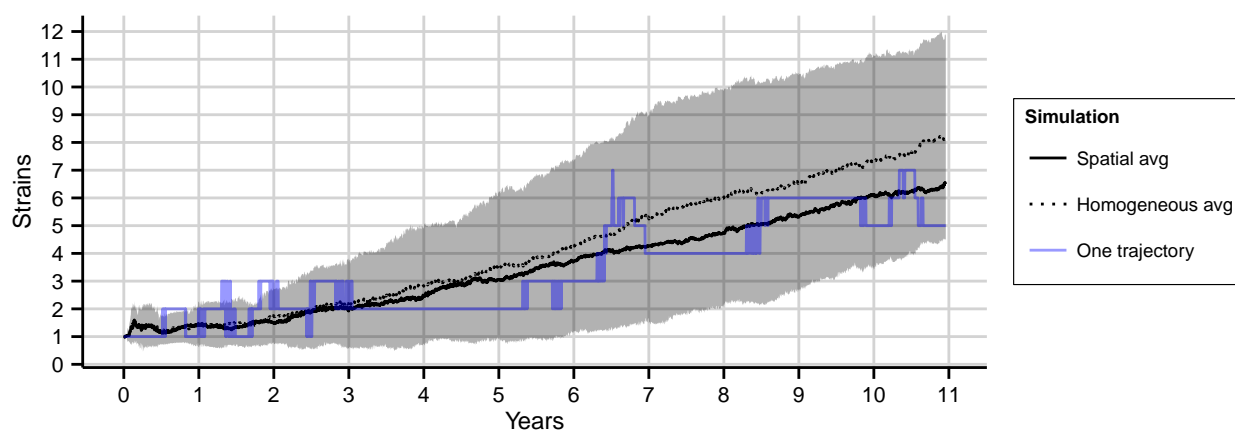


Figure 5.9: Number of HIV strains. Mutations as they appear in the simulations from the previous Figure 5.8. Strains evolve in a discrete fashion, but look continuous in the graph because it is averaged out. In blue, a single simulation is drawn to illustrate that point.

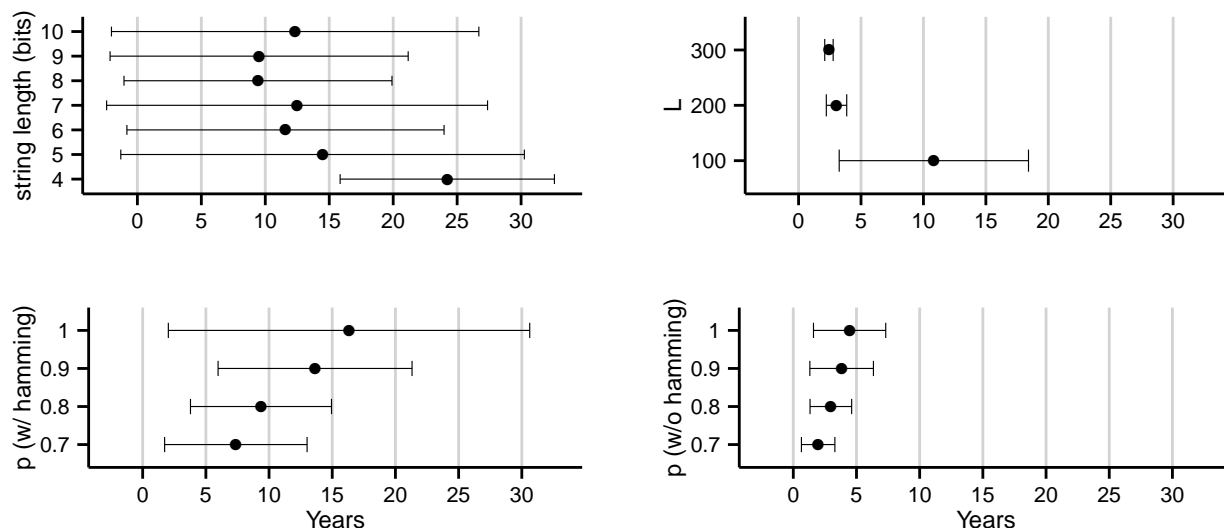


Figure 5.10: Our Lin and Shuai's model sensitivity analysis. AIDS phase as a function of several parameters. AIDS here is defined as when v reaches 40%. Error bars represent one standard deviation [CFV07] for a total of 50 simulations run.

greatly beyond the default value of $L = 100$. Lower values than $L = 100$ affect the simulation too much in the opposite direction to represent here.

- The several interaction probabilities were also analyzed, with and without the **Hamming distance**. The probability of interaction in the model is calculated as $p \times \text{Ph}(i, j)$, where p can be p_v , b_v , p_0 , p'_0 or k_0 . All these constants have a default value of 0.8, and so we call all these constants p and change them in unison. We also see the effect of disabling the Hamming distance, so that interaction only happens when two strings are equal (quasi-affinity is disabled). This, not surprisingly, benefits the virus since it only affects the immune response. The strong quantitative difference is somewhat surprising though. But the results suggest we could obtain the same results as with the original parameters, without Hamming distance, by making other parameters relating to immune response more aggressive. This casts some doubt as to the importance of immune quasi-affinity.

Chapter 6

Stochastic Simulations Models

God doesn't play dice with the world.

Albert Einstein

A stochastic formulation is sometimes more desirable and more broadly applicable than the deterministic formulation of chemical kinetics within spatially homogeneous systems. In stochastic processes, the reaction constants are viewed not as reaction “rates” but as reaction “probabilities per unit time”, and the temporal behavior of a chemically reacting system takes the form of a Markovian random walk in the N -dimensional space of the molecular populations of the N species (species in this literature is the equivalent of agents in agent-based model (ABM) or variables in ordinary differential equations (ODEs)). The system can no longer be represented by N differential equations, instead a probability is assigned to different outcomes of the system. A **master equation** is a set of linear, autonomous ODEs for each possible \mathbf{X} -state of the system, representing the probability of system being in that particular state at time t .

The master equation is rarely analytically tractable, and so we will present numerical algorithms derived from Monte Carlo techniques. Developed by Gillespie in 1976, the basic algorithm is known as the Gillespie or **stochastic simulation algorithm (SSA)** [Gil76; Gil77]. This computational method does not try to numerically solve the master equation for a given system; instead, it is a procedure in which rigorously derived Monte Carlo techniques are employed to numerically simulate the very Markov process that the master equation describes analytically. It reproduces exact single trajectories of the process; through multiple simulation runs, an approximation of the full probabilistic distribution of the system can thus be captured.

While this stochastic formulation is only valid for species homogeneously-distributed in space, we will later show how it can reproduce the heterogeneous distributions by dividing the fluid into interconnected small pools of fluid, each of which is governed by homogeneous dynamics.

From a physical point of view, the stochastic formulation of chemical kinetics is superior to the deterministic formulation. The stochastic approach is always valid whenever the deterministic approach is valid, and it is sometimes valid when the deterministic approach is not. Not only is it superior to the ODE treatment, stochastic formulation has been shown to reproduce the same results as the also stochastic ABM particle tracking simulators [And15].

Why Stochasticity? A perfectly realistic model would not require stochasticity. That being said, we may want to throw in exogenous stochasticity into our models, because we realize our models

are not perfect mirrors of reality. In order to keep our models simple, there are aspects of the system that should be modeled stochastically [Wil06, p.2]. Possibly more important, even if the model follows perfectly the real world trajectory of the phenomenon, we are many times ignorant of the initial conditions, and stochasticity can compensate for that. The introduction of stochasticity will of course matter the most when working with fewer molecules/agents represented by integer numbers, because with big numbers probabilistic effects are diluted out.

6.1 Formalism

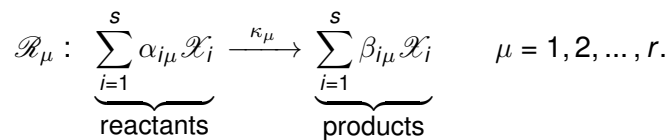
Expanding on the formalism section of the previous chapter, many processes in cellular and molecular biology can be represented by **biochemical reaction networks**. These networks may then be studied through the lens of various implementations.

In this chapter, we will focus mostly on stochastic simulation through Markov jump processes, also known in systems biology literature as **stochastic kinetic networks**. Deterministic formulations are sufficient to predict average behaviors at the population level, but they cannot address questions about noise, random switching between stable states of the system, or the behaviors of systems with very few molecules of key species. These topics are investigated with stochastic simulations. Some common applications include: [Wil06; Kli+09]

- Molecule synthesis and degradation;
- Enzymatic reactions;
- Receptor-ligand interaction;
- Gene expression and regulation;
- Ion channel dynamics and ion transport across membranes;
- Immunological processes (inter and intra cellular);
- Epidemiological models.

Biochemical reactions are probabilistic collisions between randomly moving molecules, with each event resulting in the increment or decrement of molecular species by usually integer amounts. They can be described mathematically by random processes: reactions happen unpredictably, and each sequence of random events leads to a different history of the system.

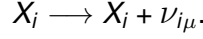
Reaction Networks. Consider a well-stirred system of “molecules” of s species, $\{\mathcal{X}_1, \dots, \mathcal{X}_s\}$, which interact through r reaction channels, $\{\mathcal{R}_1, \dots, \mathcal{R}_r\}$. We assume the system is in thermal equilibrium and confined to a finite constant volume V . A reaction network is of the form:



Stoichiometric Matrix. The stoichiometric matrix is defined as $\nu = (\nu_{i\mu})$, where

$$\nu_{i\mu} = \beta_{i\mu} - \alpha_{i\mu} \quad \text{with } i = 1, \dots, s, \text{ and } \mu = 1, \dots, r.$$

Process Definition. Let $X_i(t)$ be the number of molecules of species \mathcal{X}_i present in instant t . We want to compute the state vector's time evolution $X_i(t)$, given the initial state $\mathbf{X}(0) = \mathbf{x}_0$. Each time reaction \mathcal{R}_μ triggers, for all i , the \mathcal{X}_i state changes according to:



Let $\mathbf{K}(t)$ be the event counts of each reaction during $[0, t]$, then the system is updated by:

$$\Delta \mathbf{X}(t) = \boldsymbol{\nu} \Delta \mathbf{K}(t).$$

The stoichiometry matrix encodes important structural information about the reaction network. In particular, vectors in the left null-space of $\boldsymbol{\nu}$ correspond to conservation laws in the network; any vector \mathbf{a} of length s that satisfies $\mathbf{a}^\top \boldsymbol{\nu} = \mathbf{0}$ has the property that $\mathbf{a}^\top \mathbf{X}(t)$ remains constant for all t (from the above equation) [GW11]. Such laws can be used to reduce the dimensionality of the system under consideration by writing molecular variables as a function of the others. Reducing the dimensionality of the system is especially useful in the deterministic case, because it improves the speed/accuracy and general stability of the ODE integration algorithm [Wil06, section 7.3].

Propensity Function. The rate at which the event reaction counts \mathbf{K} evolves is a function of the **propensity function**, also known as the **hazard function**, $\lambda_\mu(\mathbf{X}, c_\mu)$.

$\lambda_\mu(\mathbf{X}, c_\mu)dt$ is the probability at which reaction \mathcal{R}_μ is triggered in interval $[t, t + dt]$ somewhere in volume V .

Table 6.1 shows examples of propensity functions for several types of reactions:

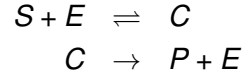
Reaction	Propensity $\lambda_\mu(\mathbf{X}, c_\mu)$	Description
$\emptyset \longrightarrow \mathcal{X}_1$	c_1	Inflow
$\mathcal{X}_1 \longrightarrow \emptyset$	$c_2 X_1$	Degradation
$\mathcal{X}_1 + \mathcal{X}_2 \longrightarrow \mathcal{X}_3$	$c_3 X_1 X_2$	Catalysation
$2\mathcal{X}_1 \longrightarrow \mathcal{X}_2$	$c_4 X_1(X_1 - 1)/2$	Dimerisation
$3\mathcal{X}_1 \longrightarrow \mathcal{X}_3$	$c_5 X_1(X_1 - 1)(X_1 - 2)/6$	Trimerisation

Table 6.1: Example of types of reactions, and respective propensity functions.

Here c_μ is the so called **stochastic rate constant**. When converting rate constants from an ODE to a reaction network caution must be taken in that deterministic models usually express amounts in terms of concentrations while we are concerned about molecules. Then, for a concentration of \mathcal{X} of $[X]$ moles per liter in a volume V liters, there are clearly $[X]V$ moles of X and hence $\mathcal{N}_A[X]V$ molecules, where $\mathcal{N}_A \simeq 6.023 \times 10^{23}$ is Avogadro's constant (the number of molecules in a mole) [Wil06, section 6.6.1]. So, for example, $\dot{X}_3 = kX_1X_2$, can be translated into the bimolecular reaction $X_1 + X_2 \xrightarrow{c} X_3 + \dots$, where $c = k/\mathcal{N}_A V$.

6.1.1 Examples

The **Michaelis-Menten enzyme kinetics** is a popular model within system biology literature [Kli+05, section 5.1.3]. The reaction network is represented by:



where S is the substance which is transformed by the reaction, E is the enzyme which facilitates the reaction, C is an intermediary species and P the final product (see Figure 6.1).

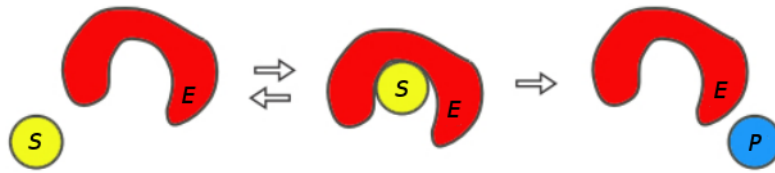
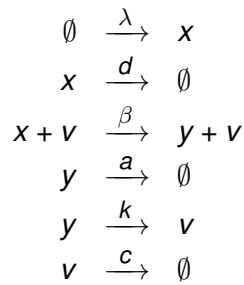


Figure 6.1: Michaelis-Menten enzyme kinetics model.

As another example, the **HIV fundamental model** (4.1) from Chapter 4 could be rendered as:



where x are healthy T_H cells, y are infected T_H cells, and v are free viral copies.

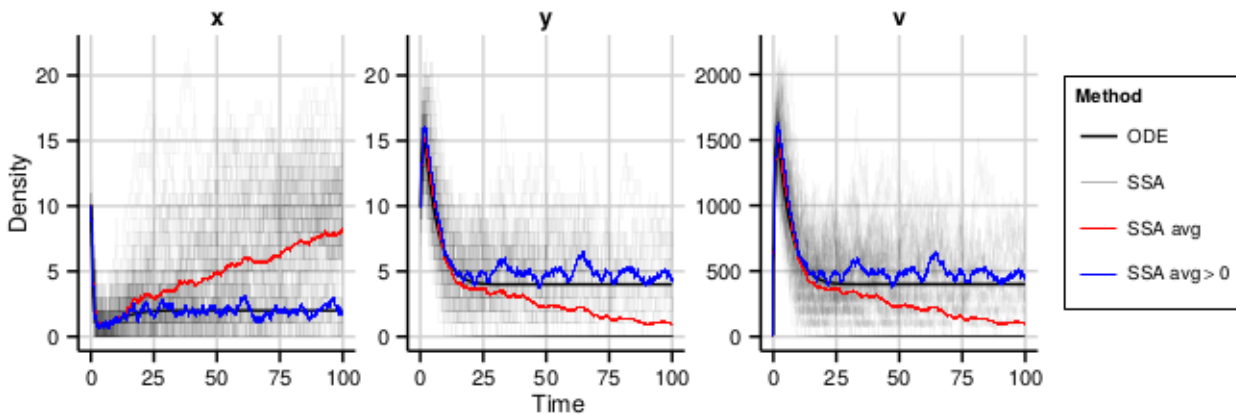


Figure 6.2: Our deterministic and stochastic reproduction of the fundamental HIV model. The average of 100 simulations (in red) is contrasted to the average of those trajectories that did not enter into an absorbed state (in blue), i.e. the quasi-stationary average. Parameters were reused from Figure 4.2 on page 49 of Chapter 4, except that the initial viral inoculation was increased from 10 to 100, otherwise most simulations would be absorbed. Behavior looks continuous; but each individual trajectories is discrete (in gray) since molecular numbers are \mathbb{Z} . The code to run such simulations is provided as Appendix B.

For illustration purposes, the stoichiometry matrix of the model (left) and the hazard function

(right) are:

$$\nu^T = \begin{array}{l} \mathcal{R}_1: \\ \mathcal{R}_2: \\ \mathcal{R}_3: \\ \mathcal{R}_4: \\ \mathcal{R}_5: \\ \mathcal{R}_6: \end{array} \begin{pmatrix} x & y & v \\ 1 & 0 & 0 \\ -1 & 0 & 0 \\ -1 & 1 & 0 \\ 0 & -1 & 0 \\ 0 & -1 & 1 \\ 0 & 0 & -1 \end{pmatrix} \quad \left| \quad \begin{array}{l} \lambda_1 = \lambda \\ \lambda_2 = dx \\ \lambda_3 = \beta xv \\ \lambda_4 = ay \\ \lambda_5 = ky \\ \lambda_6 = cv \end{array} \right.$$

The stochastic simulation is reproduced in Figure 6.2 on the previous page.

Other interesting work at converting a system of ODE to stochastic simulations is by Chao et al. [Cha+04].

6.1.2 Assumptions

To emphasize, underlying reaction networks are **two hypothesis**:

1. The chemical system is under thermal equilibrium conditions. Not only that, but the chemical system is such that, at any time t , the concentration of each species is homogeneous in the reaction vessel (i.e., does not depend on space); this assumes that the diffusion rate \gg than reaction rates.
2. In a bimolecular reaction, the time to the occurrence of the reaction is largely determined by the time to the reactive collision whereas the time necessary for the chemical transformation of the colliding species into the reaction products is negligible.

6.2 Deterministic Approximation

Using the same kinetic reaction networks formalism, on larger space and time scales, the microscopic processes translate into an effective macroscopic behavior, such as the dynamics of metabolic pathways governed by kinetic laws. These reactions may therefore be represented and resolved by differential equations.

Assuming very big numbers, we can approximate \mathbf{X} and \mathbf{K} by real numbers, and write the ODEs:

$$\dot{\mathbf{x}}(t) = \nu \dot{\mathbf{k}}(t).$$

However, these ODEs are only useful if we can establish a relationship between the derivatives $\dot{\mathbf{k}}(t)$ and the variables \mathbf{x} ,

$$\dot{\mathbf{k}}(t) = \mathbf{v}(\mathbf{x}(t)).$$

Usually we adopt the so called **mass-action law** [Kli+09, section 2.1.1]. It states that the reaction rate is proportional to the probability of a collision of the reactants. This probability is in turn proportional to the concentration of reactants to the power of the molecularity, that is the number in which they enter the specific reaction:

$$v_\mu(\mathbf{x}) = c_\mu \prod_{i=1}^s x_i^{\alpha_{i\mu}}$$

which leads to reaction rate equations according to the mass-action law:

$$\dot{\mathbf{x}}(t) = \boldsymbol{\nu} v(\mathbf{x}(t)).$$

Even though deterministic modeling is widely successful, it does not come without flaws:

1. Small particle numbers in cellular subsystems (e.g. in signaling pathways) lead to random fluctuations which can change the dynamic behavior considerably;
2. Bi- or multi-stable systems cannot be described adequately;
3. Stochasticity itself can be an important property of the system, e.g. in evolution, noise-induced amplification of signals or noise-driven divergence of cell fates;
4. For very small particle numbers (e.g. single genes) the concept of continuous concentrations is not appropriate.

Also, due to correlations, averaging out dynamics may not truly represent the average of several stochastic simulations [UW11, Example 6.2]. For instance, consider the reaction $A + B \xrightarrow{k} B$, whose deterministic/average modeling (right) may result in erroneous conclusions different from those obtained by averaging many stochastic simulations (left),

$$\frac{d\langle A \rangle}{dt} = -k\langle AB \rangle \not\Rightarrow \frac{dA}{dt} = -kAB.$$

6.3 Chemical Master Equation

To represent the model stochastically, a **master equation** can be deduced [UW11, section 5.5]. Let $P(\mathbf{x}, t) = \text{Probability}\{\mathbf{X}(t) = \mathbf{x} \mid \mathbf{X}(0) = \mathbf{x}_0\}$, $P(\mathbf{x}, t + dt)$ can then be written as the sum of the probabilities of the number of ways in which the network can arrive at state \mathbf{x} by the time $t + dt$, with a dt so small that we can assume one reaction at most takes place during $[t, t + dt[$:

$$\begin{aligned} P(\mathbf{x}, t + dt) = & o(dt) + \left(1 - \sum_{\mu=1}^r \lambda_{\mu}(\mathbf{x}, c_{\mu}) dt \right) P(\mathbf{x}, t) + \\ & + \sum_{\mu=1}^r \lambda_{\mu}(\mathbf{x} - \boldsymbol{\nu}_{\cdot\mu}, c_{\mu}) dt P(\mathbf{x} - \boldsymbol{\nu}_{\cdot\mu}, t), \end{aligned}$$

where $\boldsymbol{\nu}_{\cdot\mu}$ refers to the column vector of the stoichiometric matrix for reaction μ . The second term in the RHS sum is the probability that the system undergoes no reaction during $[t, t + dt[$. The term $\lambda_{\mu}(\mathbf{x} - \boldsymbol{\nu}_{\cdot\mu}, c_{\mu}) P(\mathbf{x} - \boldsymbol{\nu}_{\cdot\mu}, t) dt$ is the probability that the system is one \mathcal{R}_{μ} reaction removed from state \mathbf{x} at time t and then undergoes such a reaction in $[t, t + dt[$.

The **Chemical Master Equation (CME)** is then given by

$$\frac{dP(\mathbf{x}, t)}{dt} = \sum_{\mu=1}^r \left[\lambda_{\mu}(\mathbf{x} - \boldsymbol{\nu}_{\cdot\mu}, c_{\mu}) P(\mathbf{x} - \boldsymbol{\nu}_{\cdot\mu}, t) - \lambda_{\mu}(\mathbf{x}, c_{\mu}) P(\mathbf{x}, t) \right].$$

This is a set of linear, autonomous ODEs. One ODE for each possible \mathbf{x} -state of the system. Solution of the \mathbf{x} th equation at time t gives the probability of system being in that particular state at time t .

Unfortunately, the master equation is only tractable for a handful of cases. Hence, for most systems of interest, an analysis via the CME will not be possible and then stochastic simulation techniques will present the only practical approach to gaining insight into a system's dynamics. The CME is too high dimensional to deal with computationally. The SSA algorithm gets around this issue by computing single realizations of the state vector rather than an entire probability distribution.

6.4 SSA Simulation (Gillespie Algorithm)

One common complaint about differential equations is that, being deterministic, they describe only the mean behavior of the phenomenon at hand. This does not bode well with HIV because the trajectory of the disease has great variance between patients, and is very abrupt, particularly at the final stage of the disease. Differential equations may be used to describe a particular patient, or to model the mean behavior in a population of patients, but not to study the disease trajectory of a random person.

While stochastic equations are often impossible to resolve analytical, individual realizations of random processes can often be obtained by stochastic simulation. Stochastic models allow us to compute mean values, fluctuations, and temporal correlations of system states.

6.4.1 Direct Method

In the 1970s, Gillespie came up with the “exact” stochastic simulation algorithm (SSA) to solve chemical kinetics [Gil76; Gil77]. This simulation is said to be exact because it simulates one possible trajectory of the Chemical Master Equation without approximations. This is known as the **Direct Method**.

The key point to design a SSA is to compute the joint density function for the following two random variables μ and τ . We can prove that this joint density is the result of two individual random variables [Hig08].

- Next reaction index μ : discrete probability distribution function $\frac{\lambda_\mu(\mathbf{x}, c_\mu)}{\lambda_\Sigma}$, i.e. choose one of the reactions given that the chance of picking the μ th reaction must be proportional to its propensity $\lambda_\mu(\mathbf{x}, c_\mu)$. Here $\lambda_\Sigma = \sum_{\mu=1}^r \lambda_\mu(\mathbf{x}, c_\mu)$;
- Time τ until next reaction, with exponential probability distribution function: $\lambda_\Sigma e^{-\lambda_\Sigma \tau}$.

The method is fully listed as Algorithm 7 on the next page. Reminder: the propensity function λ_μ returns the transition rate for reaction μ as a function of current molecular amounts \mathbf{x} , as previously described (see Table 6.1 on page 71).

6.4.2 τ -leaping Method

In order to reduce computational time, several algorithmic approximations, which make the simulation less exact, have since been suggested. All these approximations belong to the family of approximations called **τ -leaping** (tau-leaping) approximations based on a method by the same name created by Gillespie himself, presented as Algorithm 8 on the next page. These methods hold τ constant, hence approximating the events count \mathbf{k} within the interval $[t, t + \tau[$, so that several reactions are updated in one single iteration. The main problem to be aware is to avoid negative population sizes, which could happen if too much of one molecule is consumed [CGP05].

```

Require:  $t_0, \mathbf{x}_0, t_{\max}, \mathbf{c}, \nu$ 
1:  $t \leftarrow t_0$ 
2:  $\mathbf{x} \leftarrow \mathbf{x}_0$ 
3: while  $t < t_{\max}$  do
4:   calculate propensities  $\lambda_\mu \forall \mu$ 
5:    $\lambda_\Sigma \leftarrow \sum_{\mu=1}^r \lambda_\mu(\mathbf{x}, \mathbf{c}_\mu)$ 
6:    $r_1, r_2 \sim \text{Uniform}(0, 1)$ 
7:    $\tau \leftarrow \ln(r_1^{-1}) / \lambda_\Sigma$ 
8:   let  $\mu$  such that  $\sum_{i=1}^{\mu-1} \lambda_i(\mathbf{x}, \mathbf{c}_i) < r_2 \lambda_\Sigma \leq \sum_{i=1}^{\mu} \lambda_i(\mathbf{x}, \mathbf{c}_i)$ 
9:    $\mathbf{x} \leftarrow \mathbf{x} + \nu_{\cdot \mu}$ 
10:   $t \leftarrow t + \tau$ 
11: end while

```

Algorithm 7: Gillespie's Direct Method. [Gil76]

```

Require:  $t_0, \mathbf{x}_0, t_{\max}, \mathbf{c}, \nu, \tau$ 
1:  $t \leftarrow t_0$ 
2:  $\mathbf{x} \leftarrow \mathbf{x}_0$ 
3: while  $t < t_{\max}$  do
4:   calculate propensities  $\lambda_\mu \forall \mu$ 
5:   for  $\mu \leftarrow 1$  to  $r$  do
6:      $p_\mu \sim \text{Poisson}(\lambda_\mu(\mathbf{x}, \mathbf{c}_\mu), \tau)$ 
7:   end for
8:    $\mathbf{x}(t + \tau) \leftarrow \mathbf{x}(t) + \sum_{\mu=1}^r p_\mu \nu_{\cdot \mu}$ 
9:    $t \leftarrow t + \tau$ 
10: end while
11:

```

Algorithm 8: Gillespie's τ -leaping approximation.

τ -leaping assumes that there exists $\tau > 0$ that satisfies the following *leap condition*: $\forall \mu, \lambda_\mu(\mathbf{X}, \mathbf{c}_\mu) \approx$ constant in interval $[t, t + \tau[$.

We then can show [Hig08] that each reaction count number is Poisson with mean (and variance) $\lambda_\mu(\mathbf{X}, \mathbf{c}_\mu)\tau$, so that we can leap the system by τ time units:

$$\mathbf{X}(t + \tau) = \mathbf{X}(t) + \sum_{\mu=1}^r p_\mu \nu_{\cdot \mu}, \quad (6.1)$$

with $\mathbf{X}(t) = \mathbf{x}$ and $p_\mu \sim \text{Poisson}(\lambda_\mu(\mathbf{X}, \mathbf{c}_\mu)\tau)$.

Please notice that the Poisson has infinite support, and, since we are working with finite populations, some extra arrangements may be necessary, or the usage of other distributions such as the Binomial, as detailed next.

Some further optimizations exist. Interestingly, complexity of the Direct Method grows with the number of molecules/agents, but, in general, higher number of molecules may actually lead to decreasing complexity of most algorithms because they can branch out into a faster route of approximation algorithmia. An overview follows of various τ -leaping approximations [Pin08].

- **Explicit τ -Leaping (ETL)**: this was the one just presented: τ is hold constant, and a Poisson random variable is used to quantify how many reactions to trigger at each iteration. Disadvantages: if the user chooses a too large constant for τ step, inaccuracies will pop up. Also, population size can become negative (if more reactions are triggered than individuals).
- **Binomial τ -Leaping (BTL)**: building on top of ETL, a maximum number of reaction firings is calculated at each iteration in order to avoid negative populations. τ step is no longer constant.
- **Optimized τ -Leaping (OTL)**: estimates largest possible step size; reactions are partitioned into: critical sets (if population may become negative) and non-critical sets (if population is safe).

Furthermore, it has also been proposed for τ to vary along the simulation [CGP06], as well as dividing the network into slow and fast sets whose fast nodes can be approximated using CLE (as explained next) [Gil07]. Depending on the model, computational time will vary algorithm to algorithm,

as will do the inaccuracies they introduce.

We have used the model from a infectious disease [Lin+12, section 3.1 A VRE Model] to illustrate the τ -leaping approximation; see performance results from Table 6.2 on the next page based on the model from Figure 6.3 on the next page. We have used R package GillespieSSA [Pin08].

6.4.3 Chemical Langevin Equation (CLE)

We could proceed to make a further approximation by assuming that we choose τ so that:

$$\lambda_\mu(\mathbf{X}, c_\mu)\tau \gg 1. \quad \forall \mu$$

Whereas the previous assumption asked for τ to be “small enough”, this assumption now asks for τ to be “large enough”. Then, we have that:

$$\mathcal{P}_\mu \approx \lambda_\mu(\mathbf{X}, c_\mu)\tau + \sqrt{\lambda_\mu(\mathbf{X}, c_\mu)\tau} \mathcal{N},$$

where $\mathcal{N} \sim \text{Normal}(0, 1)$.

A standard result from probability theory says that a Poisson random variable with large mean is well approximated by a normal random variable with the same mean and variance. By approximating a Poisson by a Normal distribution, these are now real numbers, so we use an \mathbf{Y} instead of \mathbf{X} [Hig08].

Applying this approximation to (6.1), we get the \mathbf{Y} update, by the so called Euler-Maruyama discrete approximation to Langevin equation:

$$\mathbf{Y}(t + \tau) = \mathbf{Y}(t) + \tau \sum_{\mu=1}^r \boldsymbol{\nu}_{\cdot\mu} \lambda_\mu(\mathbf{Y}(t), c_\mu) + \sqrt{\tau} \sum_{\mu=1}^r \boldsymbol{\nu}_{\cdot\mu} \sqrt{\lambda_\mu(\mathbf{Y}(t), c_\mu)} \mathcal{N}_\mu,$$

where $\mathcal{N}_\mu \sim \text{Normal}(0, 1)$.

6.5 Delay Reactions

As a case study of delays in stochastic simulation, it is worth considering model 4.2 on page 43 from Chapter 4 by Culshaw and Ruan [CR00], which features time delays. The translation into kinetic reaction networks follows. It is not immediately obvious how the model should be simulated in a stochastic context.

Before reproducing the model as a reaction network, we must take into account that these networks force us to be explicit with regard to all **reaction dependencies**. For instance, when converting a system of differential equations, we need to keep in mind that both reaction networks imply the ODE:

$$\begin{cases} \dot{a} = -ka \\ \dot{b} = +ka, \end{cases} \iff \begin{array}{c} a \xrightarrow{k} \emptyset \\ a \xrightarrow{k} a+b \end{array} \quad \vee \quad a \xrightarrow{k} b.$$

However, whether we assume the events are independent (first reaction network) or dependent (second) will result in different distributions when reproducing the network stochastically.

In the case of the model at hand, the authors describe μ_y as “lytic death” [CR00], i.e. burst, which is why we make these events dependent, thereby using a single transition rather than two transitions

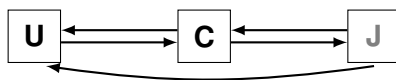


Figure 6.3: Sketch of the model being benchmarked. The fully detailed model can be found at: [Lin+12]. The meaning of the variables is immaterial; it refers to infections within an hospital: Uninfected, Colonized, and colonized in Isolation, respectively.

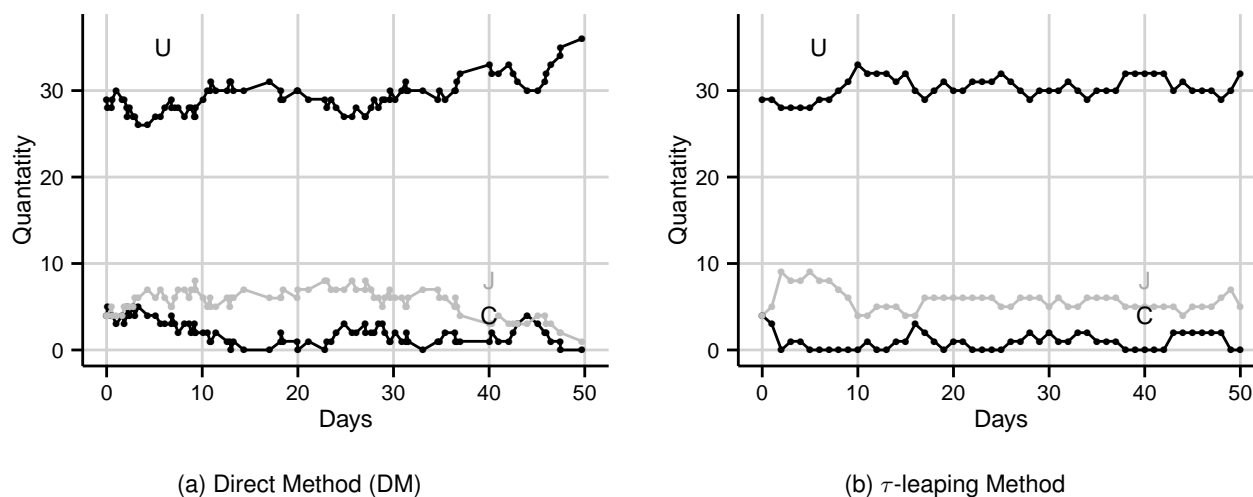


Figure 6.4: Our comparison between the DM and the τ -leaping method. Model from [Lin+12, 3.1 A VRE Model]. It is noticeable that τ -leaping approximation does either too many or too little reactions because τ is constant. Sum of initial values = 37.

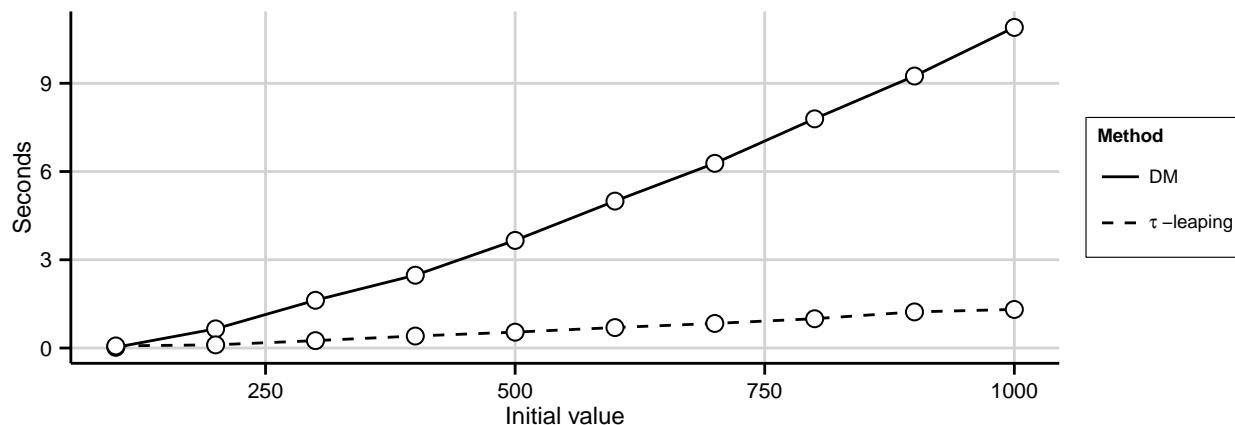


Figure 6.5: Respective performance of both methods with respect to the initial values. The Direct Method is noticeably slower than the τ -leaping approximation while keeping a good accuracy level.

Method	Time (seconds)		
	$N = 37$	$N = 370$	$N = 3700$
Direct Method	0.048	2.280	140.816
ETL	0.056	0.144	0.156
BTL	0.080	0.408	7.032
OTL	0.040	1.376	0.364

Table 6.2: Illustration of algorithm times. Model from Figure 6.3.

— except that here $\mu_y > \mu_b$ which we take it as meaning that not all viruses are released into a functional state, what we have called “superavit”.

$\mathcal{R}_1:$	x	$\xrightarrow{\mu_x}$	\emptyset	natural death
$\mathcal{R}_2:$	\emptyset	\xrightarrow{s}	x	exogenous source
$\mathcal{R}_3:$	x	\xrightarrow{r}	$2x$	endogenous growth
$\mathcal{R}_4:$	x	$\xrightarrow{r(x+y)/x_{\max}}$	\emptyset	carrying capacity
$\mathcal{R}_5:$	$x + v$	$\xrightarrow{k_y - k'_y}$	v	infection superavit
$\mathcal{R}_6:$	$x + v$	$\xrightarrow{k'_y}$	$y(t + \tau) + v$	infection
$\mathcal{R}_7:$	y	$\xrightarrow{\mu_y - \mu_b}$	\emptyset	burst superavit
$\mathcal{R}_8:$	y	$\xrightarrow{\mu_b}$	Nv	burst release
$\mathcal{R}_9:$	v	$\xrightarrow{\mu_v}$	\emptyset	viral clearance

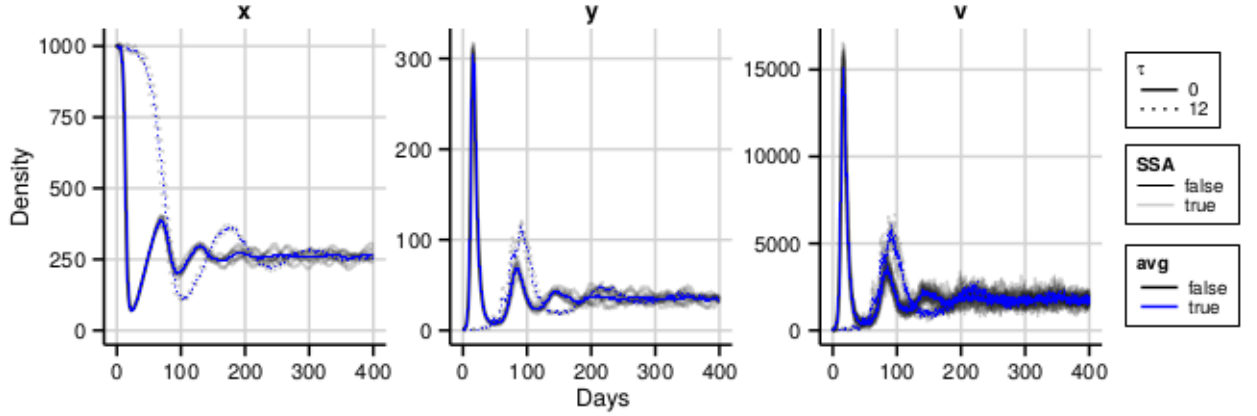


Figure 6.6: SSA reproduction of time-delay HIV model. [CR00] Non-delay $\tau = 0$ (as solid line) is contrasted with delay $\tau = 12$ (as dotted line), with parameters based on the article, as detailed in Chapter 4, Figure 4.1 on page 44. The initial conditions here have been changed so inoculation happens from one infected cell, rather than free virus, in order to kick-start the simulation under the restriction of molecular numbers being integer: $x(\theta) = 1000$ cells, $y(\theta) = 1$ cell, and $v(0) = 0$ for $\theta \in [-\tau, 0]$ within a mm^3 volume. Average of 8 simulations (individual simulation in gray); they do not exhibit much variation due to the huge molecular numbers under investigation.

In this model, there is a delay, which we would like to faithfully reproduce in the stochastic simulation. The formalization of **delays in stochastic simulation** will be different than in delay differential equations (DDEs). This is necessarily so because it is more realistic to postpone a reaction into the future as the result of a present event, rather than expressing present reactions relative to past states which would imply memory in the part of the system, as is done in DDEs. Unlike DDE integrators, most stochastic delay algorithms work by actually postponing the reaction until its respective time is reached in the loop. This is a distinction without a difference however; the deterministic solution of the reaction network ought to be identical to the DDE model we are reproducing. Code in R for this graphic is provided in Appendix B.

Some delay algorithms from the literature are explored in the following sections.

6.5.1 Delay as Duration

This is the typical delay approach used in most systems biology work, e.g. [Bra+05; Zhu+07]. The crucial idea in this algorithm is to assign a delay to a reaction so that every time the reaction starts, it is only consumed after a duration equal to the delay. In the hitherto (between the start and completion

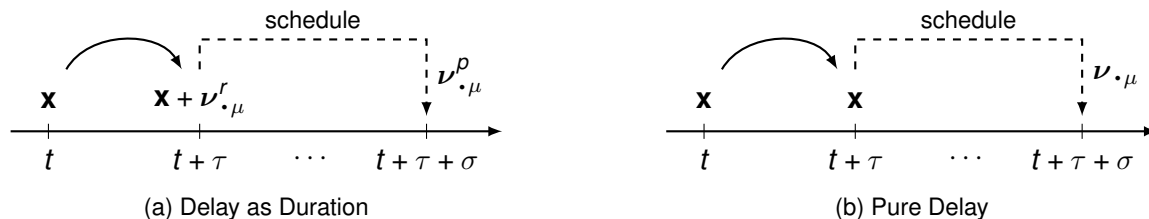


Figure 6.7: Graphical comparison of the semantic of both types of delays. [Car11, Figure 4.1, 5.1]

of the reaction), the involved reactants are “locked”, in the sense that they can not participate in other events involving the system. For each reaction μ , the stoichiometric vector $\nu_{\cdot\mu}$ is dissociated into reactants, $\nu_{\cdot\mu}^r$, and products, $\nu_{\cdot\mu}^p$, state vectors, so that:

$$\nu_{\cdot\mu} = \nu_{\cdot\mu}^r + \nu_{\cdot\mu}^p,$$

where each element of $\nu^r \leq 0$, and $\nu^p \geq 0$ (positive products, negative reagents). We have called them $-\alpha$ and β when introducing the stoichiometric matrix, over section 6.1 on page 70, but it seems more appropriate to “redefine” them relatively to the stoichiometric matrix now.

The reaction is performed in two steps:

1. As before, using Gillespie’s algorithm, two random numbers are chosen: the next τ and the respective reaction μ .
2. If a delay reaction was selected, then:
 - (a) $\mathbf{X}(t + \tau) = \mathbf{X}(t) + \nu_{\cdot\mu}^r$ (reactants are subtracted, i.e. the system is locked)
 - (b) schedule the addition of $\nu_{\cdot\mu}^p$ at time $t + \tau + \sigma$ (products are scheduled)

The fully fleshed out algorithm is given by Algorithm 9 on the following page. As mentioned, this is the typical algorithm used in delay stochastic simulation. This delay, however, is not the same delay as the delay in a DDE where no “lock” concept exists. In a DDE, reactants are consumed prior to molecules being consumed in the future, and so these reactants may participate in other reactions of the system. We will see next how it can better be approximated.

The algorithm uses two auxiliary structures: S denotes the set of all scheduled list as $S = \{(t', \nu') \mid t' \in \mathbb{R}, \nu' \in \mathbb{R}^s\}$, and R represents all reactions with R_{nd} representing those that are not delayed. The subset $S_{t,\tau}$ is defined as $S_{t,\tau} = \{(t', \nu') \in S \mid t' \leq t + \tau\}$ with $\min\{S_{t,\tau}\}$ representing the element of smallest $t + \tau$. [Car11, Chapter 4]

6.5.2 Purely Delay Approach

The algorithm we will consider now was proposed by Barbuti et al. [Bar+09], and fully formed by Caravagna [Car11] in his PhD thesis. The distinction introduced by this algorithm is in allowing reactants involved in a reaction with delay to interact with other reactants before the completion of the delayed reaction. The entire reaction is postponed, rather than only the products (Algorithm 10 on the following page).

In this approach, when a delay event is triggered, it is still true that:

$$\mathbf{X}(t) = \mathbf{X}(t + \tau).$$

Require: $t_0, \mathbf{x}_0, t_{\max}, \mathbf{c}, \nu, \sigma$

```

1:  $t \leftarrow t_0$ 
2:  $\mathbf{x} \leftarrow \mathbf{x}_0$ 
3:  $S \leftarrow \emptyset$ 
4: while  $t < t_{\max}$  do
5:   calculate propensities  $\lambda_\mu \forall \mu$ 
6:    $\lambda_\Sigma \leftarrow \sum_{j=1}^r \lambda_\mu(\mathbf{x}, c_\mu)$ 
7:   let  $r_1, r_2 \sim \text{Uniform}[0, 1]$ 
8:    $\tau \leftarrow \lambda_\Sigma^{-1} \ln(r_1^{-1})$ 
9:   let  $\mu$  such that  $\sum_{i=1}^{\mu-1} \lambda_i(\mathbf{x}, c_i) < r_2 \lambda_\Sigma \leq$ 
       $\sum_{i=1}^\mu \lambda_i(\mathbf{x}, c_i)$ 
10:  if  $S_{t,\tau} \neq \emptyset$  then
11:     $(t', \nu') \leftarrow \min\{S_{t,\tau}\}$ 
12:     $\mathbf{x} \leftarrow \mathbf{x} + \nu'_{\cdot\mu}$ 
13:     $t \leftarrow t'$ 
14:     $S \leftarrow S \setminus \{(t', \nu')\}$ 
15:  else
16:    if  $R_\mu \in R_{\text{nd}}$  then
17:       $t \leftarrow t + \tau$ 
18:       $\mathbf{x} \leftarrow \mathbf{x} + \nu_{\cdot\mu}$ 
19:    else
20:       $\mathbf{x} \leftarrow \mathbf{x} + \nu^r_{\cdot\mu}$ 
21:       $t \leftarrow t + \tau$ 
22:       $S \leftarrow S \cup \{(t + \tau + \sigma_\mu, \nu^p_{\cdot\mu})\}$ 
23:    end if
24:  end if
25: end while
    
```

Algorithm 9: Delay as duration algorithm. [Car11, Chapter 4]

Require: $t_0, \mathbf{x}_0, t_{\max}, \mathbf{c}, \nu, \sigma$

```

1:  $t \leftarrow t_0$ 
2:  $\mathbf{x} \leftarrow \mathbf{x}_0$ 
3:  $S \leftarrow \emptyset$ 
4: while  $t < t_{\max}$  do
5:   calculate propensities  $\lambda_\mu \forall \mu$ 
6:    $\lambda_\Sigma \leftarrow \sum_{\mu=1}^r \lambda_\mu(\mathbf{x}, c_\mu)$ 
7:   let  $r_1, r_2 \sim \text{Uniform}[0, 1]$ 
8:    $\tau \leftarrow \lambda_\Sigma^{-1} \ln(r_1^{-1})$ 
9:   let  $\mu$  such that  $\sum_{i=1}^{\mu-1} \lambda_i(\mathbf{x}) < r_2 \lambda_\Sigma \leq$ 
       $\sum_{i=1}^\mu \lambda_i(\mathbf{x}, c_i)$ 
10:  if  $S_{t,\tau} \neq \emptyset$  then
11:     $(t', \nu', \nu'') \leftarrow \min\{S_{t,\tau}\}$ 
12:    if  $\nu'' \prec \mathbf{x}$  then
13:       $\mathbf{x} \leftarrow \mathbf{x} + \nu_{\cdot\mu}'$ 
14:    end if
15:     $t \leftarrow t'$ 
16:     $S \leftarrow S \setminus \{(t', \nu', \nu'')\}$ 
17:  else
18:    if  $R_\mu \in R_{\text{nd}}$  then
19:       $t \leftarrow t + \tau$ 
20:       $\mathbf{x} \leftarrow \mathbf{x} + \nu_{\cdot\mu}$ 
21:    else
22:       $t \leftarrow t + \tau$ 
23:       $S \leftarrow S \cup \{(t + \tau + \sigma_\mu, \nu_{\cdot\mu}, \nu^r_{\cdot\mu})\}$ 
24:    end if
25:  end if
26: end while
    
```

Algorithm 10: Purely delay algorithm. [Car11, Chapter 5]

Only after σ time, will we have:

$$\mathbf{X}(t + \tau + \sigma_\mu) = \mathbf{X}(t + \tau) + \nu_{\cdot\mu},$$

plus any reactions that took place during the σ_μ hitherto. The symbol \prec is used in the pseudo-code to represent an element-to-element \leq -operator.

This seems to have fixed the discrepancy between the DDE model and its reproduction as a reaction network using the previous algorithm. However, this approach creates several problems, which explain why the previous algorithm is the one predominantly in use. One of these is: if we allow reactants to participate during the period $[\tau, \tau + \sigma_\mu]$, what happens if one or more reactants are fully consumed after the delay interval? The answer proposed by Caravagna is: to ignore it. In other words, at time $\tau + \sigma_\mu$, when the reaction is to take place (and reagents consumed and products produced), only perform the reaction when it is possible, i.e. if there are sufficient reactants ($\mathbf{X} + \nu_{\cdot\mu} \geq 0$).

This is not the sole problem. When a reaction takes place, any one of n reactants i may be used.

We ignore the delay when $n < x_i$. This means, from all delay triggered in the queue, we are biasing the delay in the direction of those who were first placed in the queue.

The author proposed two fixes to his algorithm in his PhD thesis, whose complexity is much higher. The semantics of these delays are identical to those of the purely delay approach, except they fix the several issues presented in that first putative algorithm. We will briefly summarize them here. We shall use the second approach over the next section.

1. **History-dependent delay** [Car11, Chapter 6]. The way by which delay DDE integrators work is by keeping an extra structure, an history list of previous system states that can be accessed by time delayed variables. The system's memory is accomplished by an ordered history list, which will be constituted by iterative states of the system, i.e. $\mathbf{H} = [\mathbf{x}_{t_0}, \mathbf{x}_{t_0+\tau}, \mathbf{x}_{t_0+2\tau}, \dots]$, where $\mathbf{x} \in \mathbb{Z}_+^s$ is, as before, the vector state of the system for the various molecular numbers, and s is the number of species in the system. The author proposed an exact method inspired by the previous description of delay DDE integrators.
2. **Delay with markings** [Car11, Chapter 7]. To track, in list form, those reagents subject to reactions that may be delayed. We can see this algorithm as effectively transforming all delay reagents into ABM simulations where parallel to the Continuous Time Markov Chain (CTMC) (where each variable x_i represents the number s of molecules of species i), we have a set of tuples containing the type i and the time of reaction, whose set is ordered by this time attribute.

Beware the overlap in notation: in DDE literature τ usually refers to the time delay, while the letter σ is the one commonly used to represent the time delay in SSA/Gillespie literature, since τ already refers to the time jump. In τ -leaping approximations, $\tau = dt$ of the ODE integrators.

6.6 From Agents to Markov Chains

One interesting SSA work on HIV was a “comparison of computational efficiencies of stochastic algorithms” by Link et al. [Lin+12], where HIV, healthy and infected T_H cell and T_C cell are all represented in a cell mediated response reaction network. This work however was meant to compare computational efficiencies and it fails to reproduce the three phases of HIV pathogenesis.

In the work that follows, the model presented in section 5.7 on page 61 of the previous chapter is ported to reaction networks. Its stochastic simulation is then compared to the ABM method. Please refer back to the previous chapter for the model's description.

Recall the constraints of the model:

1. One agent of each type per cell in the grid;
2. The agent could potentially interact with another agent within the same cell in the grid;
3. New agents are only created if the cell they are allocated to is vacant of an agent of the same type.

6.6.1 Well-Stirred Space

Lin and Shuai [LS10] already tried to incorporate physical space in its model. But we had already shown in Figure 5.8 on page 66 that movement, and therefore space configuration, is redundant. Given that the boundary condition is periodic and the diffusion ratio between the movement radius, r ,

and the length of the square matrix, L , is small, we will assume movement is independent of position. I.e. the probability distribution of agents across space, $\rho(\mathbf{p}, t)$ is not a function of $\rho(\mathbf{p}, t - 1)$.

Assuming spatial homogeneity, the previous spatial configuration in the form of a grid can be disregarded, and spatial movement is no longer a concern. This does not mean that spatial aspects can be discarded. A population threshold was implicitly imposed by the physical constraints of the grid, and so an explicit carrying capacity factor needs to be reintroduced.

For the purpose of this exercise, as we study a possible transformation of the model into a reaction network, it is still useful to see agents as being placed in a fixed-sized vector representing space that is shuffled at every tick. Each value of the vector represents the agent identifier, with the zero representing no agent. These molecules are then match for collision by using their indexes.

x	0	0	5	0	0	0	0	0	1	6	0	0
z	0	0	4	2	0	0	0	0	0	0	0	0
v	0	0	0	0	0	7	0	0	0	3	0	0

Figure 6.8: Homogeneous representation of the model wherein each molecule type is spread across vectors of length L^2 and in which interactions happen by matching indexes. The numbers are not molecular amounts, but agent identifiers.

In this simplified model, interactions happen between molecules that are positioned within the same index (same column in the figure), so the set of interactions is given by $\{(x_i, z_i, v_i) : i \in [0, L^2], H(x_i) + H(z_i) + H(v_i) \geq 2\}$, where H is the Heaviside function, and vectors **x**, **z** and **v** represent T_H cell, T_C cell and free virus, respectively.

Molecular Collision

Within the L^2 vectors representing space, cells have a p probability of interacting when found in the same place of a cell of another type, and no two cells of same type can be found in the same place. We want to know at each time, how many cells are interacting.

We can use the space-vectors we just introduced as benchmarks against which we can test candidates for possible probability distributions that can model the number of interactions happening at each tick between the three participants.

A naive implementation of the ABM model could be given in R by:

```

1 LL <- 100
2 nx <- 50
3 nv <- 25
4 x <- c(rep(1, nx), rep(0, LL - nx))
5 v <- c(rep(1, nv), rep(0, LL - nv))
6 p <- 0.8
7 nsample <- 1e5
8 ns <- rep(0, nsample)
9 for(i in 1:nsample)
10   ns[i] <- sum(sample(v) & sample(x) & runif(LL) < p)

```

where **ns** represents how many times two cells (**x** and **v**) have interacted in a sample of size **nsample** within a lattice of size $L^2 = LL = 100$, and **nx** and **nv** represent $|\mathbf{x}|$ and $|\mathbf{v}|$, respectively.

The code begins by defining vectors \mathbf{x} and \mathbf{v} of equal size LL , but n_x 1s and n_v 1s, respectively, with the rest being 0. At each loop, we shuffle the vectors using the function `sample`. We also generate another vector of random uniform numbers of size LL to check if the interaction is successful with probability $p=0.8$. We finally, perform the “and” operator ($\&$) on these vectors and sum the number of interactions. An illustration exemplifying line 10 of the algorithm follows with $LL=8$. Let us define black as 1/true, and white as 0/false, then:

$$\text{sum} \left(\& \begin{pmatrix} \mathbf{x} \\ \mathbf{v} \\ P < 0.8 \end{pmatrix} \right) = \begin{pmatrix} \text{[Black, Black, White, Black, White, White, White, White]} \end{pmatrix} = 2$$

For reasons of efficiency, we are going to consider probability distributions from which to sample interaction counts. Possible candidates are:

1. Binomial $\left(L^2, p^{\frac{|\mathbf{v}||\mathbf{x}|}{L^2}}\right)$ — where at each possible place, we find the probability that two cells are interacting based on their concentrations;
2. Binomial $\left(|\mathbf{v}|, p^{\frac{|\mathbf{x}|}{L^2}}\right)$ — so that, for the cells of lowest count (\mathbf{v} in this case), we find the probability of them interacting with the other cell based on its concentration;
3. Poisson $\left(p^{\frac{|\mathbf{v}||\mathbf{x}|}{L^2}}\right)$ — both of these cases could possibly be approximated using a Poisson.

It can easily be seen that all these distributions have same mean in common, since they share the same expect valued. Remember: $E(\text{Binomial}(n, p)) = np$ and $E(\text{Poisson}(\lambda)) = \lambda$. In the first and third case, we will also need to limit the range of the random variable, since that number cannot be higher than the lowest count of cells, $|\mathbf{v}|=n_v=25$ in this case.

As will be seen over Figure 6.9 on the following page, while the second binomial more closely resembles the benchmark, the solution is still a little off. It is treating the probability of \mathbf{v} to interact with an \mathbf{x} as independent between themselves. This is not the case, since each interaction makes the next one less likely.

The exact solution can be found in the hypergeometric distribution. This discrete probability distribution is defined by three parameters, which define respectively the number of successes and the number of failures within a finite population, without reposition, in a given number of draws: [R14, dhyper]

4. Hypergeometric $\left(|\mathbf{x}|, L^2 - |\mathbf{x}|, |\mathbf{v}|\right)$.

The Kolmogorov-Smirnov (KS) test was used as the goodness of fit test between the benchmark distribution and each of the candidates. p -value and distance numbers are reproduced in Figure 6.9 on the following page. A p -value < 0.05 rejects the null hypothesis, with H_0 : both distributions are the same. The KS distance, sometimes referred to as the KS-statistic, is the maximum distance between the cumulative frequency of each distribution and that of the benchmark. This metric is many times used when looking for an approximated distribution. The hypergeometric distribution clearly best fits the benchmark.

Still, we may want to use the Poisson as an approximation for performance reasons, and to reuse our previous algorithms.

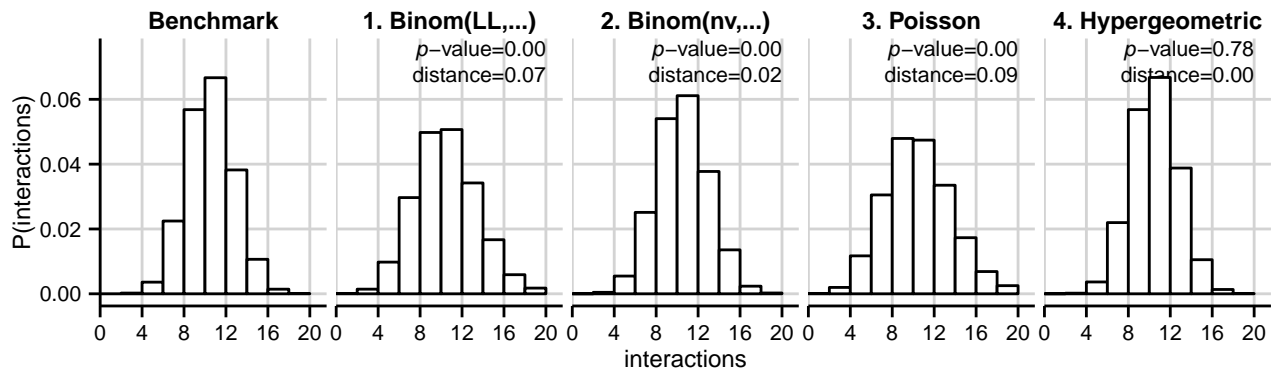


Figure 6.9: Histograms of the various candidates from which to sample interaction counts based on the ABM model by Lin and Shuai [LS10].

Carrying Capacity

In the implementation of the model as reaction networks, we must also consider carrying capacity, since in the original model new cells are only created when a vacancy is available for them (see constraint #3). The model was thus implicitly forcing a population constraint.

Again, we are going to come up with a “benchmark”. The program is in R. Please refer to the previous code snippet for details on the programming language. $\Delta x = dx$ is used to denote how many cells are being added. Please notice we only need to reshuffle either the new vector or the old one; not both.

```

1 LL <- 100
2 nx <- 80
3 dx <- 20
4 x <- sample(c(rep(1,nx),rep(0, LL-nx)))
5 nsample <- 1e5
6 ns <- rep(0, nsample)
7 for(i in 1:nsample)
8   ns[i] <- sum(!x & sample(c(rep(1,dx),rep(0, LL-dx))))

```

We would now like to find a known theoretical distribution to model this constrain. The advantage of using an already existing theoretical distribution is that random sample generators already exists and are highly optimized. Two candidates come to mind:

1. Binomial $\left(\Delta n, 1 - \frac{n}{L^2}\right)$ — the idea being that, for each one of the new molecules Δn , the probability of one being created is the concentration of vacancies as given by $1 - P(\text{occupied}) = 1 - \frac{n}{L^2}$ (probability $1 - \frac{80}{100} = 0.20$, in our code); this assumes n is so small that $P(\text{occupied})$ does not change as molecules are added;
2. Hypergeometric $\left(L^2 - n, n, \Delta n\right)$ — this is the exact distribution without the assumption that $P(\text{occupied})$ does not change as molecules are added. This distribution was studied in the previous section.

The fitting is given in Figure 6.10 on the next page. As before, we may want to use the Binomial for efficiency. This sampling will not be incorporated explicitly in the reaction network itself, and instead each reaction will be mapped through a function which may potentially limit the number of products created, to represent the carrying capacity within the model.

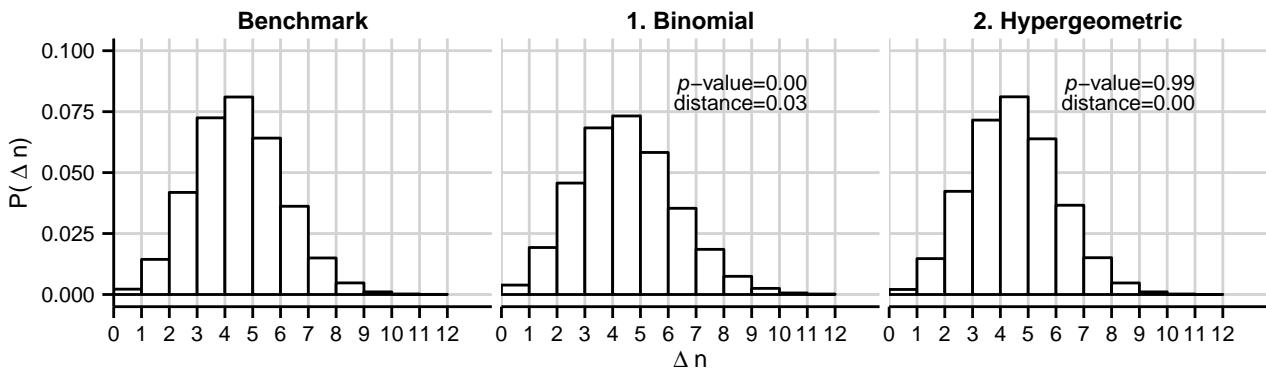


Figure 6.10: Histograms of the various candidates from which to sample how many new cells may be created based on the population constrains of the model.

6.6.2 Shape Space

The biggest changes from ABM agents to Continuous Time Markov Chains (CTMCs) is that we now have variables describing the distributions of molecules across all possible properties, instead of having a list containing all cells as in the ABM approach. So, as an example, for each HIV molecule, if we take strings as being of length 2 bits, we would have:

- In the ABM approach, $\mathbf{v} = (00, 00, 00, 01, 01, 10)$, as a list of internal states;
- The same information would be stored in a CTMC as: $\mathbf{v} = (3, 2, 1, 0)$, now as a list of molecular numbers, where the vectors represents the absolute distribution of HIV molecules with epitopes represented by strings 00, 01, 10 and 11, respectively.

Properties become variables within the CTMC. Notice this transition in principle only works when all properties are discrete or potentially discretized. The number of variables will correspond to all possible property combinations of the agents, the product of the range of each property.

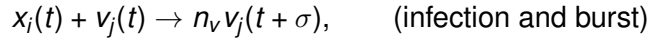
The disadvantage of the ABM approach: complexity grows with the number of agents. The disadvantage of using these methods that operate in population variables: complexity grows in consonance to the number of parameters and their range (and, possibly, number of agents, especially when simulating using exact methods). In other words, in AB modeling adding new properties has no marginal cost, which is why AB models sometimes feature a great amount of properties. Reaction networks do not cope as well with increasing variables which must be represented by new variables. Just as sparse methods exist for sparse matrices, it is possible similar methods could be uncovered for reaction networks of scarcely populated state vectors, so that only positive populations would enter the simulation.

In the case at hand, the strings representing each string are of 10 bit length. This means $2^{10} = 1024$ potential shape space variables need to be represented in the state vector, for each molecule x , z and v .

Incubation Delay

Several approaches will be considered for the viral infection and subsequent incubation time.

Virus infection could potentially be modeled by a reaction such as the following one:

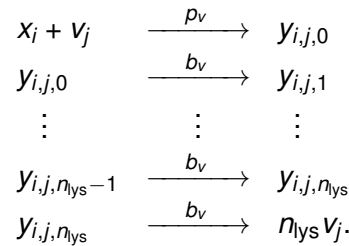


for all i and j types of strain's strings.

Since it is important for x to still serve as a reagent to other reactions in the hitherto $[t, t+\sigma]$, namely to be killed by a T_C cell, a purely delay approach or similar would have to be used (section 6.5.2 on page 80). However, we need to differentiate between healthy and infected T_H cell, so that T_C cells target only infected cells. One option would require us introducing an y variable.

A new vector for infected cells, \mathbf{y} , could be introduced, where $|\mathbf{y}| = |\mathbf{x}| \times |\mathbf{v}| \times n_{lys} = 1024 \times 1024 \times 5 = 5242880$ variables, to represent the specific x strain that has been infected by a v strain and now contains a certain number of virus inside, bursting when that number reaches n_{lys} .

Remember that, at each iteration, there is a probability $= b_v$ per unit of time of the incubated virus production and the cell bursts after n_{lys} viral units are produced. The reaction will then be represented by:



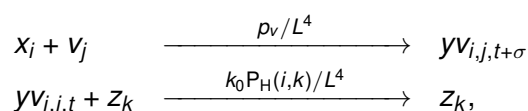
Infected cells can still be killed by T_C cells by simply adding a reaction $y_{i,j,n} + z_k \rightarrow z_k$, when a T_C cell kills its infected T_H cell counterpart of the same strain i , for any viral strain j and viral numbers n .

With over 5 million variables, the complexity involved is enormous.

One possible way to reduce this complexity is to ignore tracking the strain of virus which has infected the cell — and, when the cell bursts, go back at the period of the infection and sample from the virus distribution existing at the time of infection, one of which must have infected the cell. This does not work so well though, because the incubation period is variable. We would have to average incubation period to n_{lys}/b_v time units.

Let us propose an alternative exact solution: an auxiliary structure represented by the complex $\mathbf{y}\mathbf{v}$ will be used to track incubated viruses. This structure will work more in the veins of an ABM, as a list containing triples featuring: (the strain of the infected cell, the strain of the virus, the time of burst when n_{lys} viruses are released) $= (i, j, t)$. The model is effectively hybrid in that incubation is stored in a structure similar to the ones used by ABMs approaches, while everything else is stored in variables representing the population at the several states. To avoid unnecessary counting, we keep a proxy y_i variable that is always synchronized with $|\mathbf{y}\mathbf{v}_{i,j}|$, to use with the $y\mathbf{v}_{i,j} + z_i$ reaction.

This is in vein with the previously mentioned delay with markings approach (section 6.5.2 on page 80).



There is an implicit burst reaction $\gamma v_{i,j,t+\sigma}(t) \rightarrow v_j(t+\sigma)$ as soon as $t+\sigma$ is reached.

Incubation Period

So far we have ignored how to model the period of the incubation of the complex.

In the ABM model, we had that n incubated viruses would burst once $n = n_{lys}$, and that this n would grow at rate of b_v per tick. Again, we would like to find a theoretical distribution to model this incubation period. As we will see, two possibilities are:

1. Negative Binomial;
2. Approximate it as a Gamma.

At each tick, the virus has a given probability b_v of being incrementing by one until n_{lys} . We want to know σ so that $\sigma = \text{failed trials} + \text{successful trials}$.

We can model the number of failures as failed trials $\sim \text{NegativeBinomial}(n_{lys}, b_v)$. The negative binomial distribution is a discrete distribution of the number of failures given two parameters: the number of successes to reach at a given probability rate [R14, `dnbinom`]. We also have that successful trials = n_{lys} . Therefore, $\sigma \sim n_{lys} + \text{NegativeBinomial}(n_{lys}, b_v)$.

If we would like to now model time continuously, we could approximate it with a gamma distribution [AC94]; both the negative binomial and gamma have the same parameters in common.

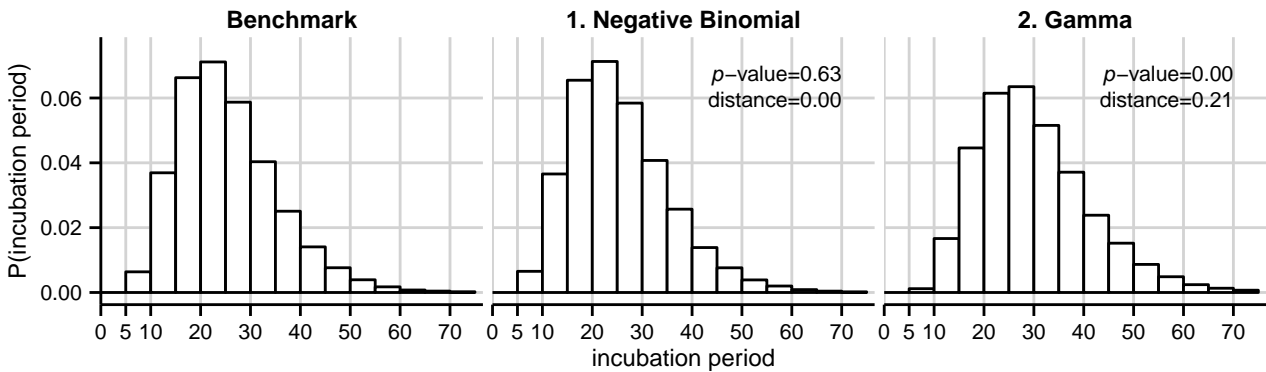


Figure 6.11: Histograms of the various candidates from which to sample the incubation period of the model.

6.6.3 Reactions Network

The model can then be translated into the following network of kinetic reactions. It should be noted that each node \mathcal{R} in the network represents multiple reactions, because they represent changes for all combinations of strains i and j :

\mathcal{R}_1 :	$x_i + v_j$	$\xrightarrow{p_0 P_H(i,j)/L^4}$	$(n_x + 1)x_i + v_j$	T_H cell activation
\mathcal{R}_2 :	$x_i + v_j$	$\xrightarrow{p_v(1-m_v)/L^4}$	$yv_{i,j,t+\sigma}$	HIV infection
\mathcal{R}_3 :	$x_i + v_j$	$\xrightarrow{p_v m_v / L^4}$	$yv_{i,j',t+\sigma}$	infection w/ mutation
\mathcal{R}_4 :	$yv_{i,j,t} + z_k$	$\xrightarrow{k_0 P_H(i,k)/L^4}$	z_k	infected T_H cell apoptosis
\mathcal{R}_5 :	$yv_{i,j,t} + z_k$	$\xrightarrow{p'_0 P_H(i,k)/L^4}$	$yv_{i,j,t} + (n_z + 1)z_k$	T_C cell activation
\mathcal{R}_6 :	v_i	$\xrightarrow{(d_{v0} + (1-d_{v0}))\text{hill}(i)}$	0	HIV depletion
\mathcal{R}_7 :	z_i	$\xrightarrow{d_{z0}(1-\text{hill}(i))}$	0	T_C cell depletion
\mathcal{R}_8 :	0	$\xrightarrow{x_0 d_{x0} L^2}$	x_i	T_H cell thymus production
\mathcal{R}_9 :	0	$\xrightarrow{z_0 d_{z0} L^2}$	z_i	T_C cell thymus production

where $P_H(i, j) = \exp(-H(i, j))$, and $H(i, j)$ is the Hamming distance between quasi-species i and j . Index j' means a shift of one random bit within the string j , and $\sigma \sim n_{lys} + \text{Gamma}(n_{lys}, b_v)$, as explained in the previous section. Recall that the hill function represents a regulating function and is defined as $\text{hill}(i) = x_i / (x_i + \theta)$.

The concept behind this network is that for each reaction type \mathcal{R} , all molecules representing the several combinations of strains $i, j \in [0, 1024[$ will interact with a given probability proportional to their specificities (as given by their Hamming distance) and a fixed probability. Notice how each one of these reaction types encompasses a wide range of reaction nodes. The division or multiplication in the propensities by L^2 represents a re-adjustment from concentration numbers, as in the previous chapter, to molecular numbers, with L^2 represent the area.

Simulating the Network

A naive approach at simulating this reaction network using τ -leaping would be to build a loop for every strain combination. \mathcal{R}_1 could be simulated as:

```

1: for  $i \leftarrow 0$  to 1024 do           #  $x$ 
2:   for  $j \leftarrow 0$  to 1024 do       #  $v$ 
3:      $\lambda \leftarrow x_i v_j p_0 / L^4$ 
4:      $\Lambda \leftarrow \text{Poisson}(\lambda \tau)$ 
5:      $x_i \leftarrow x_i + \Lambda n_x$ 
6:   end for
7: end for
    
```

But consider such cases as the first and the fifth reaction type where one of the indexes is unused within the inner loop for the purpose of creating new cells. \mathcal{R}_1 could therefore be instead simulated as:

```

1:  $\lambda \leftarrow p_0 / L^4$ 
2: for  $i \leftarrow 0$  to 1024 do           #  $x$ 
3:   for  $j \leftarrow 0$  to 1024 do       #  $v$ 
4:      $\lambda \leftarrow \lambda + x_i v_j P_H(i, j)$ 
5:   end for
6:    $\Lambda \leftarrow \text{Poisson}(\lambda \tau)$ 
7:    $x_i \leftarrow x_i + \Lambda n_x$ 
    
```

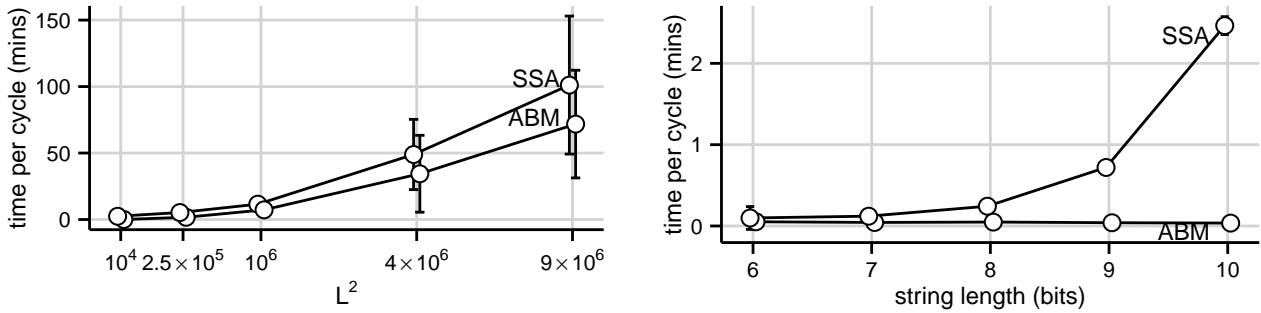

8: end for

This optimization is possible because one of the reagents is also a product, and so its stoichiometric result is zero. This reagent only concerns the computation of the propensity of the reaction, and so the number of random numbers (sampled from a Poisson) required can be diminished to 1024 for these reactions.

Not represented in this code is carrying capacity and the **yv** complex which were described earlier.

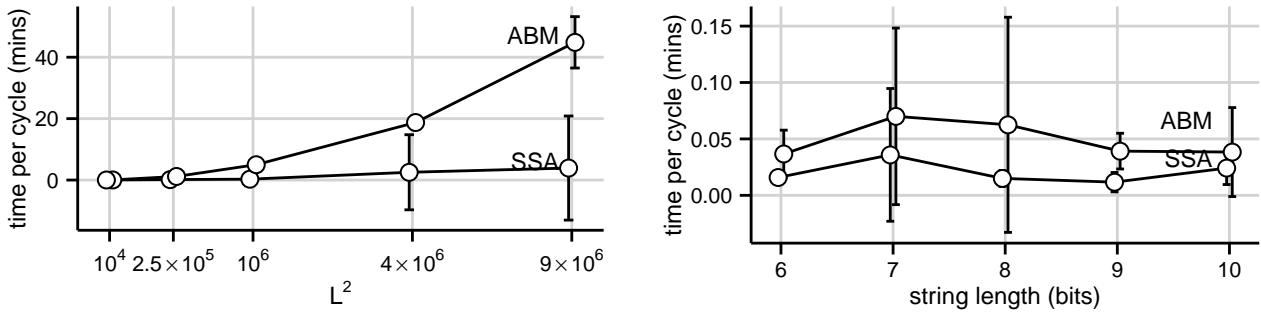
6.6.4 Results

With Hamming



(a) Time complexity as a function of the number of the maximum of agents (L^2). (b) Time complexity as a function of the string length n . Number of strains = 2^n .

Without Hamming



(c) Time complexity as a function of the number of the maximum of agents (L^2) of only perfect affinity ($i = j$). (d) Time complexity as a function of the string length n . Number of strains = 2^n of only perfect affinity ($i = j$).

Figure 6.12: Demonstration of time complexity trade-off between ABM (agents) and SSA (parameters). Time refers to the time it takes to run a single cycle/day of simulation, averaged out over 10 simulations. Error bars represent one standard deviation [CFV07] for the 10 simulations. Simulations were run in an i3@1.80GHz, developed in Java using the Apache Commons Math library for the distributions.

The simulations are identical to those presented in the previous chapter. It is interesting to compare their time complexities, as dependent on the model parameters, namely the limit on number of agents L^2 , and the strains string length n . The comparison is reproduced in Figure 6.12. As previously discussed there is a trade-off between ABM and SSA methods: number of agents versus number of parameters. The figure contrasts the case when affinity needs to be compared between each tuple (i, j) with Hamming (top), as discussed in the previous section, with the case when we are only concerned when $i = j$ (bottom).

Interestingly, the number of agents also affects SSA simulation, because random sampling al-

gorithms also grow as parameters are increased. For instance, Poisson random number sampling algorithms are usually $\mathcal{O}(\lambda)$, sometimes faster for smaller λ values [Atk79].

Our SSA recreation of the ABM model is identical. Validation was performed by building an hybrid system, in which the CTMC was converted back and forward into an ABM vector (section 6.6.2), and whereby each reaction could be executed either with the SSA code or the ABM code, alternatively. However, not many runs were performed due to lack of computer power.

6.7 Spatial Gillespie

Finally, we will end up this chapter by covering the possibility of introducing spatiality into SSA simulations.

Introducing spatiality is possible in SSA through several methods. One of these is the exact method **Next SubVolume Method** [EE04, Supplementary Methods]. But first, it makes sense to introduce the **First Reaction Method**, which is a method suggested by Gillespie back in his 1976 paper [Gil76], as a slower alternative, but an equivalent/exact alternative, to the Direct Method, which has been explored already (Algorithm 7 on page 76).

The algorithm generates a time t_μ for each reaction μ based on its propensities, and it chooses the reaction μ with the smallest t_μ . It requires r random numbers (number of reactions). Gillespie proved it to be compatible (yet slower) than DM [Gil76].

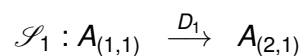
The First Reaction Method was improved by Gibson and Bruck [GB00] in what they called the Next Reaction Method (NRM).

This method consists of generating times only for reactions whose propensities have been affected by the current one. It always keeps t_μ in absolute time by adding current time: $t_\mu \leftarrow t + \tau$ and it requires the extra structures:

- a) a graph identifying reactions whose propensities may have been affected by current reaction;
- b) an event queue structure to keep t_μ sorted, avoiding performing a full sort.

It may actually be faster than the Direct Method (DM), depending on details of the model (DM always requires 2 random numbers; the model may require only 1 or more under NRM) and implementation (structures used). Iterations also have the potential to be run in parallel. [Wil06]

These two algorithms were presented to path the way for the Next Subvolume Method by Elf and Ehrenberg [EE04, Supplementary Methods] represented in Algorithm 13 on the next page. This method modifies the Next Reaction Method, so that it uses “subvolumes” instead. In each subvolume, we consider an homogeneous mixture under the Direct Method. We may in fact look at diffusion between these subvolumes as elementary reactions, where each molecule is subject to move to another subvolume, according to a diffusion rate:



Each spatial diffusion affects only 2 subvolumes, and any spatial geometry could potentially be represented (2D, 3D, graph).

In other words, the simulation occurs in parallel pools of simulations, and molecules are sometimes diffused between them. This method had already been briefly proposed in broad strokes in

```

1: while  $t < t_{\max}$  do
2:   calculate propensities  $\lambda_{\mu} \forall \mu$ 
3:    $\lambda_{\Sigma} \leftarrow \sum_{\mu=1}^r \lambda_{\mu}(\mathbf{x}, c_{\mu})$ 
4:   generate  $r$  random numbers:  $\mathbf{r}$ 
5:   simulate a time to the next reaction:  $t_{\mu} = \lambda_{\Sigma}^{-1} \ln(r_{\mu}^{-1}) \forall \mu$ .
6:   let  $\mu$  be the index of the smallest time  $\mathbf{t}$ 
7:    $t \leftarrow t + t_{\mu}$ 
8:    $\mathbf{x} \leftarrow \mathbf{x} + \nu_{\cdot \mu}$ 
9: end while

```

Algorithm 11: Gillespie's First Reaction Method. [Gil76]

```

1: For each reaction  $\mu$ , generate a putative  $t_{\mu}$ , as in the previous algorithm
2: while  $t < t_{\max}$  do
3:   let  $\mu$  be the index of the smallest  $\mathbf{t}$ 
4:    $t \leftarrow t_{\mu}$ 
5:    $\mathbf{x} \leftarrow \mathbf{x} + \nu_{\cdot \mu}$ 
6:    $\tau \leftarrow \lambda_{\Sigma}^{-1} \ln(r_{\mu}^{-1})$ 
7:   update  $\lambda_{\mu}(\mathbf{x}, c_{\mu})$  according to the new state  $\mathbf{x}$  and simulate a new time  $t_{\mu} \leftarrow t + \tau$ 
8:   for each reaction  $\eta \in [1, r]$  ( $i \neq \mu$ ) whose propensities are changed by reaction  $\mu$  do
9:     update  $\lambda'_{\eta} = \lambda_{\eta}(\mathbf{x}, c_{\eta})$  (but temporarily keep the old  $\lambda_{\eta}$ )
10:     $t_{\eta} \leftarrow t + (\lambda_{\eta} / \lambda'_{\eta})(t_{\eta} - t)$ 
11:    forget the old  $\lambda_{\eta}$ 
12:   end for
13: end while

```

Algorithm 12: Next Reaction Method. [GB00]

```

1: while  $t < t_{\max}$  do
2:   For each subvolume  $k$ , calculate rates  $r_k$  and  $s_k$  based on propensities and diffusion rates
   respectively, and generate  $t_k \leftarrow -\ln(\text{rand}) / (r_k + s_k)$ . Sort vector  $\mathbf{t}$ 
3:   For the smallest time  $\tau$  of subvolume  $\lambda$ , choose either a reaction event with  $P(r_{\lambda} / (r_{\lambda} + s_{\lambda}))$ , or
   a diffusion event otherwise
4:   if reaction event then
5:     reuse the previous random number to determine which reaction occurred, as in the DM
6:     recalculate  $r_{\lambda}$ ,  $s_{\lambda}$  and  $t_{\lambda}$  for this subvolume
7:   end if
8:   if diffusion event then
9:     reuse the previous random number to determine which molecule diffused away, given their
     respective diffusion rates
10:    another random number chooses a neighbor  $\gamma$  based on the connectivity matrix
11:    recalculate  $r$ ,  $s$  and  $t$  for both subvolumes  $\lambda$  and  $\gamma$ 
12:   end if
13: end while

```

Algorithm 13: Next SubVolume Method. [EE04, Supplementary Methods]

the original paper by Gillespie [Gil76, p 430], but was never fully implemented. An initial attempt was developed by Stundzia and Lumsden [SL96]. Several accelerations have since been proposed [RBK08].

A review of several spatial methods is presented by Andrews and Arkin [AA06]. The authors found that:

- the Gillespie simulation has larger peaks than the Langevin approximation;
- the particle tracking simulation (ABM) shows larger and fewer bursts than does the Gillespie simulation because it accurately treats diffusion at all length scales (this difference can be reduced by using smaller subvolumes).

Chapter 7

Conclusion

Th-Th-Th-Th-Th... That's all, folks!

Porky Pig, *Loony Tunes*

Several models have been treated or mentioned through the thesis:

- ordinary differential equation (ODE);
- partial differential equation (PDE);
- stochastic differential equation (SDE);
- stochastic simulation algorithm (SSA);
- cellular automaton (CA);
- agent-based model (ABM).

The first set of models concerns the mean population behavior, while the stochastic models allow the modeling of distributions of population trajectories which may also be useful in prediction. Both groups may be used to complement each other, whereby one traces tendencies, the other studies dispersion. A global qualitative comparison of the methods is given in Table 7.1 on the next page.

Further comparisons of systems biology methods are provided by Materi and Wishart [MW07] and Narang et al. [Nar+12]. In addition, Alizon and Magnus [AM12] tries to answer the question as to which method should be used for the different aspects and timescales involved in HIV modeling.

The definition of ABM was never fully clear, because no clear definition exists. At this point, we are able to put forward a putative definition, in contrast to SSA modeling. An ABM can be seen as the set S^α of tuples A . Each tuple A may be called an agent, and features several variables such as position for spatial simulations or status such as healthy or infected for cells. Complexity grows in $\mathcal{O}(n)$, where $n = |S^\alpha|$ because AB modeling consists in iterating, one form or another, synchronously or asynchronously, the set:

$$S^\alpha = \{A_1, A_2, A_3, A_4, \dots\}.$$

It can therefore, for instance, model continuous properties of the agents. This is in contrast to the SSA, which is part of the Continuous Time Markov Chain family of methods, and so information is structured in a vein more similar to ODEs, where an ordered set S^β has the size of all possible parameters and contains populations in all possible states. For instance, $S^\beta(\text{healthy}) = 50$ and $S^\beta(\text{infected}) = 20$. The sum of all variables in this list must be the same as the number of agents, $\sum_i |S^\beta| S_i^\beta = |S^\alpha|$. Therefore, the complexity of these models might be lower in some cases than ABM,

though that would depend much on the model and the exact stochastic algorithm used.

ABMs really shine when it comes to representing the agent across a wide vector of properties. If we were to add a new property, whose value range is k , to an ODE model, it would require adding $n(k - 1)$ new variables, increasing by that order of magnitude the complexity of the numerical integrator algorithm. Viewed in another way, in ABMs we iterate agents; while in ODEs, we iterate variables. ODEs do have the advantage that, being deterministic, a single run is enough to produce the desirable statistics; furthermore conclusions, and sometimes results, can be obtained analytically for the simpler models. Computation gains may be obtained through the usage of distributed computing techniques.

We put ABM in the top of the expressiveness modeling powering (Figure 7.1) because they may feature continuous variables such as PDEs, but are also stochastic.

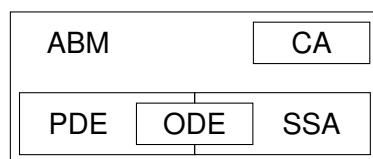


Figure 7.1: The expressive power of each modeling tool in a set diagram. This is not to say, for instance, that the SSA is a type of ABM, but that potentially any model powered by a SSA can be modeled using an ABM.

7.1 Methodology Remarks

Several conclusions have been inferred from the several methodologies. Most remarkably, the bottlenecks in their computational times comes from:

- Exact SSA: population sizes and number of parameters
- τ -leaping SSA: number of reactions
- ODE: number of variables = number of parameters
- ABM: population sizes

These conclusions are illustrated in Table 7.1.

Method	Agents \uparrow	Reactions \uparrow	Parameters \uparrow
ODE	=	=	$\uparrow\uparrow$
SSA	mostly \downarrow	\uparrow	$\uparrow\uparrow$
ABM	$\uparrow\uparrow$	=	=

(a) Time complexity from modeling complexity (the lower, the better)

Method	Variables	
	Discrete	Continuous
ODE	✓	×
SSA	✓	×
ABM	✓	✓

(b) Modeling power

Table 7.1: Qualitatively comparison of the several modeling methods.

7.2 Stochasticity

Most HIV models published have been deterministic. This makes sense: ODEs computational complexity are invariant with regard to the number of molecules, and HIV RNA copies can reach

mind boggling numbers of several billion per millimeter cubic in the ultimate AIDS stage. On the other hand, AIDS develops very differently, patient per patient, so average dynamics cannot possibly offer a faithful description of the pathogenesis.

In most work analyzed, ODE modelers seem more preoccupied with qualitative dynamics. Most mathematical work in ODE has been analytical, which is surprising since the main reason to use ODEs would be to cope with the huge numbers involved in immune dynamics. If the goal is to perform qualitative analytical work, one wonders why the scarcity in the application of stochasticity methods into modeling.

7.3 Physical Space

When does it matter to consider physical space? When constants associated with reaction are much smaller than those associated with diffusion, $k_{\text{diffusion}} \gg k_{\text{reaction}}$, the exact dynamics of the physical space can be discarded, and space treated as homogeneous. Spatial dynamics can be modeled by all stochastic methods considered, both ABM and SSA. In the later case, it can be introduced in an *ad hoc* fashion, by diffusing molecules between several simulations running in parallel, each of each representing a different subvolume along the fluid. Figure 7.2 illustrates the situation.

The only models to be able to reproduce the three stages of HIV pathogenesis were CA models (Chapter 3).

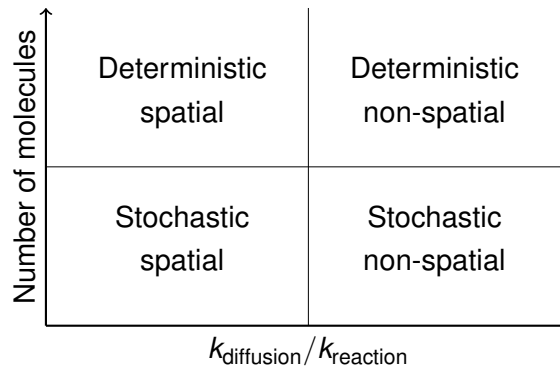


Figure 7.2: Illustrating modeling assumptions implicit in kinetic studies. [RCS12, Figure 17.1]

Santos and Coutinho [SC01]’s model is the only show in town when it comes to explain the three stages of HIV in terms of spatial dynamics. Yet the model still leaves much to be desirable. This is understandable given what we (do not) know of the disease.

Cellular Potts Model [GG92] is the go-to systems biology tool to represent space, being able to reproduce what is seen in the microscope in the laboratory. Yet we chose against covering it because no work in HIV was found.

More than a methodological stranglehold, the main obstacle in realistic modeling of physical dynamics is the biology behind it. Without a firm grasp of the biology involved, it is impossible to create a realistic computational model; biologists and mathematicians can and should cooperate in this endeavor, but it needs to be a collaborative effort with the mathematical modeling helping to test and guide the research. The most impressive research project in jumping this obstacle is ImmunoGrid, massively funded by the European Union [Hal+10].

One possible middle of the road alternative would be to discretize the human body into compartments and to introduce space at that higher level (see section 2.10.3 on page 20).

7.4 Shape Space

Mutations are the most common trope of all HIV models exhibiting the three stages of HIV pathogenesis, with the exception of CA models which manage to reproduce the three stages through physical space dynamics alone. In fact, as shown with regard to Lin and Shuai [LS10]’s model, when stripping other complexities of the model, we discover shape dynamics alone are enough for the model to explain the three stages of the pathogenesis. No other explanation was necessary. The hegemony of shape space dynamics in mathematical models makes a strong prior in favor of the importance of copy errors in HIV dynamics, which in turn makes a strong prior to invest in ways of inhibiting copy errors when doing medical research, which indeed seems to be the common pharmacy research.

Relatedly, no mathematical work has been found in immune network theory, an alternative explanation of HIV pathogenesis based on mimetic reproduction of antibody’s V-region by the virus [Hof+12].

7.5 Medical Usefulness

To better make use of the human capital being invested into mathematical modeling, it is imperative to identify the modeling vector from which to study this disease. CA seems the least promising, since it has some implausible features and already made a few factual erroneous predictions as listed:

- delays are deterministic, and there is no conceivable way to change the “fundamental” CA model;
- treatment suggestions have suggested starting treatment late, when it is known earlier is better [NN15];
- it suggests mutations are unimportant, when mutations have been judged to be the single, most terrifying barrier in combating HIV.

Interestingly, ODE models have been able to reproduce the full HIV dynamics by falling back into mutations dynamics, albeit all kinds of models have been proposed. The versatility of these models make them ideal to test new ideas, and they have been in fact at the forefront and the most used models in the understanding of HIV dynamics.

7.6 Technical Acknowledgments

The following programming languages were the most intensively used:

- **LaTeX**, the typesetting system originally developed by Donald Knuth;
- **R** for numerical integration [R14] (packages: `deSolve` [SPS10], `PBSddesolve` [Cou+14]), and stochastic simulation (package: `GillespieSSA` [Pin08]), with some algorithms implemented by hand, and also for general statistical purposes. Graphics are rendered in `ggplot2` [Wic09];

- **Java** for all cellular automaton, and the both the AB model and SSA from Chapters 5 and 6 using the Apache Commons Math library for the distributions' sampling;
- Other languages used were: **NetLogo** multi-agent modeling environment [Wil99], before all models were replaced by direct Java code for efficiency. Similarly, the modeling environments **AnyLogic** and **Nova** were also experimented with. **Maxima** for some of ODE analytical work.

Much code was develop during the thesis; some of it was not used in this writing. Please contact me if you would like access to the code, or some other information: ricardo.pdm.cruz@gmail.com. In the following Appendix, two small pieces of code are provided: an HIV CA model in NetLogo, and of an ODE/SSA delay integrator using kinetic reaction networks in R.

Bibliography

- [AA06] S. S. Andrews and A. P. Arkin. “Simulating cell biology”. In: *Current Biology* 16 (2006), pp. 523–527. DOI: 10.1016/j.cub.2006.06.048 (cited on p. 93).
- [AC94] J. A. Adell and J. D. la Cal. “Approximating Gamma Distributions by Normalized Negative Binomial Distributions”. In: *Journal of Applied Probability* 31.2 (June 1994), p. 391. DOI: 10.2307/3215032 (cited on p. 88).
- [Air+10] M. Airoldi et al. “One-pill once-a-day HAART: A simplification strategy that improves adherence and quality of life of HIV-infected subjects”. In: *Patient Preference and Adherence* 4 (2010), pp. 115–125. DOI: 10.2147/PPA.S10330 (cited on p. 19).
- [Alb+02] B. Alberts et al. *Molecular Biology of the Cell, 4th edition*. 2002 (cited on p. 6).
- [ALP15] A. K. Abbas, A. H. H. Lichtman, and S. Pillai. *Cellular and Molecular Immunology, 8th Edition*. Saunders, 2015 (cited on p. 7).
- [AM12] S. Alizon and C. Magnus. “Modelling the course of an HIV infection: Insights from ecology and evolution”. In: *Viruses* 4 (2012), pp. 1984–2013. DOI: 10.3390/v4101984 (cited on p. 95).
- [Ami+08] H. Amir-Kroll et al. “GemCell: A generic platform for modeling multi-cellular biological systems”. In: *Theoretical Computer Science* 391 (2008), pp. 276–290. DOI: 10.1016/j.tcs.2007.11.014 (cited on p. 57).
- [And15] S. Andrews. *Smoldyn about page: <http://www.smoldyn.org/about2.html>*. 2015 (cited on p. 69).
- [Atk79] A. C. Atkinson. “The Computer Generation of Poisson Random Variables”. In: *Journal of the Royal Statistical Society* 28.1 (1979), pp. 29–35 (cited on p. 91).
- [Bar+09] R. Barbuti et al. “On the Interpretation of Delays in Delay Stochastic Simulation of Biological Systems”. In: *CompMod* (2009), pp. 17–29. DOI: 10.4204/EPTCS.6.2. arXiv: 0910.1219 (cited on p. 80).
- [BAS10] F. S. Bacelar, R. F. S. Andrade, and R. M. Z. dos Santos. “The dynamics of the HIV infection: a time-delay differential equation approach”. 2010 (cited on p. 48).
- [BC01] M. Bernaschi and F. Castiglione. “Design and implementation of an immune system simulator”. In: *Computers in Biology and Medicine* 31 (2001), pp. 303–331. DOI: 10.1016/S0010-4825(01)00011-7 (cited on pp. 54, 57).
- [Ber+12] H. Bersini et al. “State-transition diagrams for biologists”. In: *PLoS ONE* 7.7 (2012), pp. 1–13. DOI: 10.1371/journal.pone.0041165 (cited on p. 58).

- [Bis07] C. Bissell. “Historical perspectives - The Moniac A Hydromechanical Analog Computer of the 1950s”. In: *IEEE Control Systems* 27.1 (Feb. 2007), pp. 69–74. DOI: 10.1109/MCS.2007.284511 (cited on p. 44).
- [BMF99] E. a. Berger, P. M. Murphy, and J. M. Farber. “Chemokine receptors as HIV-1 coreceptors: roles in viral entry, tropism, and disease.” In: *Annual review of immunology* 17 (1999), pp. 657–700. DOI: 10.1146/annurev.immunol.17.1.657 (cited on p. 10).
- [Bra+05] D. Bratsun et al. “Delay-induced stochastic oscillations in gene regulation”. In: *Proceedings of the National Academy of Sciences of the United States of America* 102.41 (2005), pp. 14593–14598. DOI: 10.1073/pnas.0503858102 (cited on p. 79).
- [Car11] G. Caravagna. “Formal Modeling and Simulation of Biological Systems with Delays”. PhD thesis. Università di Pisa, 2011 (cited on pp. 80–82).
- [Car13] A. R. Carvalho. “Modelos matemáticos para a transmissão do vírus HIV/SIDA”. PhD thesis. University of Porto, 2013 (cited on p. 43).
- [CFV07] G. Cumming, F. Fidler, and D. L. Vaux. “Error bars in experimental biology”. In: *Journal of Cell Biology* 177.1 (2007), pp. 7–11. DOI: 10.1083/jcb.200611141 (cited on pp. 27, 29, 66, 90).
- [CGP05] Y. Cao, D. T. Gillespie, and L. R. Petzold. “Avoiding negative populations in explicit Poisson tau-leaping”. In: *Journal of Chemical Physics* 123.C (2005), pp. 2418–2427. DOI: 10.1063/1.1992473 (cited on p. 75).
- [CGP06] Y. Cao, D. T. Gillespie, and L. R. Petzold. “Efficient step size selection for the tau-leaping simulation method”. In: *The Journal of chemical physics* 124 (2006), p. 044109. DOI: 10.1063/1.2159468 (cited on p. 76).
- [Cha+04] D. L. Chao et al. “A stochastic model of cytotoxic T cell responses”. In: *Journal of Theoretical Biology* 228 (2004), pp. 227–240. DOI: 10.1016/j.jtbi.2003.12.011 (cited on p. 73).
- [Coo86] L. N. Cooper. “Theory of an immune system retrovirus”. In: *Proceedings of the National Academy of Sciences of the United States of America* 83.23 (1986), pp. 9159–9163. DOI: 10.1073/pnas.83.23.9159 (cited on p. 45).
- [Cou+14] A. Couture-Beil et al. *PBSddesolve: Solver for Delay Differential Equations*. 2014 (cited on p. 98).
- [CR00] R. V. Culshaw and S. Ruan. “A delay-differential equation model of HIV infection of CD4+ T-cells”. In: *Mathematical Biosciences* 165 (2000), pp. 27–39. DOI: 10.1016/S0025-5564(00)00006-7 (cited on pp. 43, 44, 77, 79).
- [CS02] J. Chinen and W. T. Shearer. “Molecular virology and immunology of HIV infection”. In: *Journal of Allergy and Clinical Immunology* 110 (2002), pp. 189–198. DOI: 10.1067/mai.2002.126226 (cited on pp. 10, 18).
- [DN08] D. Dasgupta and F. Nino. *Immunological Computation: Theory and Applications*. Auerbach Publications, 2008 (cited on p. 61).
- [Dur64] R. Durstenfeld. “Algorithm 235: Random permutation”. In: *Communications of the ACM* 7.7 (July 1964), p. 420. DOI: 10.1145/364520.364540 (cited on p. 65).

- [EE04] J. Elf and M. Ehrenberg. “Spontaneous separation of bi-stable biochemical systems into spatial domains of opposite phases”. In: *Systems biology* 1.2 (2004), pp. 230–236. DOI: 10.1049/sb:20045021 (cited on pp. 91, 92).
- [Fac05] N. Fachada. “Simullm: An Application for the Modelling and Simulation of Complex Systems, using the Immune System as an Example”. PhD thesis. 2005 (cited on pp. v, 54).
- [Fac08] N. Fachada. “Agent-based Simulation of the Immune System”. PhD thesis. 2008 (cited on p. 54).
- [FC08] D. Floreano and Claudio Mattiussi. *Bio-Inspired Artificial Intelligence: Theories, Methods, and Technologies*. MIT Press, 2008 (cited on p. 9).
- [FCS08] P. H. Figueirêdo, S. Coutinho, and R. M. Z. dos Santos. “Robustness of a cellular automata model for the HIV infection”. In: *Physica A: Statistical Mechanics and its Applications* 387 (2008), pp. 6545–6552. DOI: 10.1016/j.physa.2008.07.011 (cited on pp. 28, 34).
- [Fun+05] G. a. Funk et al. “Spatial models of virus-immune dynamics”. In: *Journal of Theoretical Biology* 233.2 (2005), pp. 221–236. DOI: 10.1016/j.jtbi.2004.10.004 (cited on pp. 48, 49).
- [GB00] M. a. Gibson and J. Bruck. “Efficient Exact Stochastic Simulation of Chemical Systems with Many Species and Many Channels”. In: *The Journal of Physical Chemistry A* 104.9 (2000), pp. 1876–1889. DOI: 10.1021/jp993732q (cited on pp. 91, 92).
- [GFC13] R. E. R. González, P. H. de Figueirêdo, and S. Coutinho. “Cellular automata approach for the dynamics of HIV infection under antiretroviral therapies: The role of the virus diffusion”. In: *Physica A: Statistical Mechanics and its Applications* 392.19 (2013), pp. 4717–4725. DOI: 10.1016/j.physa.2012.10.036 (cited on p. 40).
- [GG92] F. Graner and J. A. Glazier. “Simulation of biological cell sorting using a two-dimensional extended Potts model”. In: *Physical Review Letters* 69.13 (1992), pp. 2013–2016. DOI: 10.1103/PhysRevLett.69.2013. arXiv: 0000135489 (cited on pp. 40, 54, 97).
- [Gil07] D. T. Gillespie. “Stochastic simulation of chemical kinetics”. In: *Annual review of physical chemistry* 58 (2007), pp. 35–55. DOI: 10.1146/annurev.physchem.58.032806.104637 (cited on p. 76).
- [Gil76] D. T. Gillespie. “A general method for numerically simulating the stochastic time evolution of coupled chemical reactions”. In: *Journal of Computational Physics* 22 (1976), pp. 403–434. DOI: 10.1016/0021-9991(76)90041-3 (cited on pp. 3, 69, 75, 76, 91–93).
- [Gil77] D. T. Gillespie. “Exact Stochastic Simulation of couple chemical reactions”. In: *The Journal of Physical Chemistry* 81.1 (1977), pp. 2340–2361. DOI: 10.1021/j100540a008 (cited on pp. 3, 69, 75).
- [Gon+13] R. E. R. González et al. “Dynamics of the HIV infection under antiretroviral therapy: A cellular automata approach”. In: *Physica A: Statistical Mechanics and its Applications* 392.19 (2013), pp. 4701–4716. DOI: 10.1016/j.physa.2013.05.056 (cited on pp. 37, 39).

- [GP13] F. Graw and A. S. Perelson. “Spatial Aspects of HIV Infection”. In: *Mathematical Methods and Models in Biomedicine*. Springer New York, 2013, pp. 3–31. DOI: 10.1007/978-1-4614-4178-6_1 (cited on pp. 2, 20).
- [Gra02] L. Gray. “A Mathematician Looks At Wolfram’s New Kind of Science”. In: *Notices of the AMS* 50.2 (2002), pp. 200–211 (cited on p. 34).
- [Gro15] B. Group. <http://www.pdn.cam.ac.uk/groups/comp-cell/StochSim.html>. 2015 (cited on pp. 2, 54).
- [GT07] Z. Guo and J. Tay. “A Hybrid Agent-Based Model of Chemotaxis”. In: *Computational Science—ICCS 2007* (2007), pp. 119–127 (cited on pp. 58, 59).
- [GT08] Z. Guo and J. C. Tay. “Multi-timescale event-scheduling in multi-agent immune simulation models”. In: *BioSystems* 91 (2008), pp. 126–145. DOI: 10.1016/j.biosystems.2007.08.007 (cited on p. 58).
- [GW11] A. Golightly and D. J. Wilkinson. “Bayesian parameter inference for stochastic biochemical network models using particle Markov chain Monte Carlo”. In: *Interface Focus* 1.6 (2011), pp. 807–820. DOI: 10.1098/rsfs.2011.0047 (cited on p. 71).
- [Haa+96] A. T. Haase et al. *Quantitative Image Analysis of HIV-1 Infection in Lymphoid Tissue*. 1996. DOI: 10.1126/science.274.5289.985 (cited on p. 17).
- [Hal+10] M. Halling-Brown et al. “ImmunoGrid: towards agent-based simulations of the human immune system at a natural scale”. In: *Philosophical transactions. Series A, Mathematical, physical, and engineering sciences* 368 (2010), pp. 2799–2815. DOI: 10.1098/rsta.2010.0067 (cited on pp. 54, 97).
- [Har87] D. Harel. “Statecharts: a visual formalism for complex systems”. In: *Science of Computer Programming* 8.3 (1987), pp. 231–274. DOI: 10.1016/0167-6423(87)90035-9 (cited on p. 56).
- [Her+01] U. Hershberg et al. “HIV time hierarchy: Winning the war while, loosing all the battles”. In: *Physica A: Statistical Mechanics and its Applications* 289 (2001), pp. 178–190. DOI: 10.1016/S0378-4371(00)00466-0. arXiv: 0006023 [nlin] (cited on pp. 23, 50).
- [Hig08] D. Higham. “Modeling and simulating chemical reactions”. In: *Psychotherapy Research* 22 (2008), pp. 1753–1759. DOI: 10.1137/060666457. arXiv: 0812.0143v2 (cited on pp. 75–77).
- [Hir+89] V. M. Hirsch et al. “An African primate lentivirus (SIVsmclosely related to HIV-2)”. In: *Nature* 339.6223 (June 1989), pp. 389–392. DOI: 10.1038/339389a0 (cited on p. 6).
- [HM07] J. Hawkins and D. Molinek. “Cellular, One-dimensional Stochastic”. In: *Topology proceedings*. Vol. 31. 2007, pp. 1–18 (cited on p. 24).
- [Ho+95] D. D. Ho et al. *Rapid turnover of plasma virions and CD4 lymphocytes in HIV-1 infection*. 1995. DOI: 10.1038/373123a0 (cited on p. 19).
- [Hof+12] G. W. Hoffmann et al. “Towards an HIV vaccine based on immune network theory”. In: 13 (2012) (cited on pp. 19, 98).
- [HP96] L. D. Hurst and J. R. Peck. “Recent advances in understanding of the evolution and maintenance of sex”. In: *Trends in Ecology & Evolution* 11.2 (Feb. 1996), pp. 46–52. DOI: 10.1016/0169-5347(96)81041-X (cited on p. 65).

- [HSP00] W. S. Hlavacek, N. I. Stilianakis, and A. S. Perelson. “Influence of follicular dendritic cells on HIV dynamics”. In: *Philosophical transactions of the Royal Society of London. Series B, Biological sciences* 355.1999 (2000), pp. 1051–1058. DOI: 10.1098/rstb.2000.0642 (cited on p. 17).
- [Jen+98] D. E. Jenkins et al. “Isolation and utilization of human dendritic cells from peripheral blood to assay an in vitro primary immune response to varicella-zoster virus peptides.” In: *The Journal of infectious diseases* 178 Suppl.Suppl 1 (1998), S39–S42 (cited on p. 7).
- [Kal+01] E. P. Kaldjian et al. “Spatial and molecular organization of lymph node T cell cortex: a labyrinthine cavity bounded by an epithelium-like monolayer of fibroblastic reticular cells anchored to basement membrane-like extracellular matrix.” In: *International immunology* 13.10 (2001), pp. 1243–1253. DOI: 10.1093/intimm/13.10.1243 (cited on p. 16).
- [Kat+04] T. Katakai et al. “A novel reticular stromal structure in lymph node cortex: An immunopatform for interactions among dendritic cells, T cells and B cells”. In: *International Immunology* 16.8 (2004), pp. 1133–1142. DOI: 10.1093/intimm/dxh113 (cited on p. 17).
- [Kaw+05] T. Kawamura et al. “The role of Langerhans cells in the sexual transmission of HIV”. In: *Journal of Dermatological Science* 40 (2005), pp. 147–155. DOI: 10.1016/j.jdermsci.2005.08.009 (cited on p. 10).
- [Kin+00] A. Kinter et al. “Chemokines, cytokines and HIV: a complex network of interactions that influence HIV pathogenesis.” In: *Immunological reviews* 177 (2000), pp. 88–98. DOI: 10.1034/j.1600-065X.2000.17708.x (cited on p. 16).
- [Kli+05] E. Klipp et al. *Systems biology in practice*. 2005, 486pp. DOI: 10.1002/3527603603 (cited on p. 72).
- [Kli+09] E. Klipp et al. *Systems Biology*. 2009, p. 592 (cited on pp. 70, 73).
- [KMV11] P. D. Katsikis, Y. M. Mueller, and F. Villinger. “The cytokine network of acute hiv infection: A promising target for vaccines and therapy to reduce viral set-point?” In: *PLoS Pathogens* 7.8 (2011). DOI: 10.1371/journal.ppat.1002055 (cited on p. 16).
- [Lin+12] K. Link et al. “A comparison of computational efficiencies of stochastic algorithms in terms of two infection models”. In: *Mathematical Biosciences and Engineering* 9 (2012), pp. 487–526. DOI: 10.3934/mbe.2012.9.487 (cited on pp. 77, 78, 82).
- [Llo01] A. L. Lloyd. “The dependence of viral parameter estimates on the assumed viral life cycle: limitations of studies of viral load data”. In: *Proceedings. Biological sciences / The Royal Society* 268.1469 (2001), pp. 847–854. DOI: 10.1098/rspb.2000.1572 (cited on p. 43).
- [LS10] H. Lin and J. W. Shuai. “A stochastic spatial model of HIV dynamics with an asymmetric battle between the virus and the immune system”. In: *New Journal of Physics* 12 (2010). DOI: 10.1088/1367-2630/12/4/043051 (cited on pp. vii, 53, 61, 63, 64, 66, 82, 85, 98).
- [MBA12] E. Marinho, F. Bacelar, and R. Andrade. “A model of partial differential equations for HIV propagation in lymph nodes”. In: *Physica A: Statistical Mechanics and its Applications* 391.1-2 (2012), pp. 132–141. DOI: 10.1016/j.physa.2011.08.023 (cited on p. 49).
- [McD+02] D. McDonald et al. “Visualization of the intracellular behavior of HIV in living cells”. In: *Journal of Cell Biology* 159.3 (2002), pp. 441–452. DOI: 10.1083/jcb.200203150 (cited on p. 22).

- [MF09] S. Moir and A. Fauci. “B cells in HIV infection and disease”. In: *Nature Reviews Immunology* 9.4 (2009), pp. 235–245. DOI: 10.1038/nri2524.B (cited on p. 13).
- [MHV04] T. R. Mempel, S. E. Henrickson, and U. H. Von Andrian. “T-cell priming by dendritic cells in lymph nodes occurs in three distinct phases.” In: *Nature* 427.January (2004), pp. 154–159. DOI: 10.1038/nature02238 (cited on p. 22).
- [Mil+02] M. J. Miller et al. “Two-photon imaging of lymphocyte motility and antigen response in intact lymph node.” In: *Science (New York, N.Y.)* 296 (2002), pp. 1869–1873. DOI: 10.1126/science.1070051 (cited on p. 21).
- [Mil+03] M. J. Miller et al. “Autonomous T cell trafficking examined in vivo with intravital two-photon microscopy”. In: *Proceedings of the National Academy of Sciences of the United States of America* 100.5 (2003), pp. 2604–2609. DOI: 10.1073/pnas.2628040100 (cited on p. 21).
- [Mil+04a] M. J. Miller et al. “Imaging the single cell dynamics of CD4+ T cell activation by dendritic cells in lymph nodes”. In: *The Journal of experimental medicine* 200.7 (2004), pp. 847–856. DOI: 10.1084/jem.20041236 (cited on p. 21).
- [Mil+04b] M. J. Miller et al. “T cell repertoire scanning is promoted by dynamic dendritic cell behavior and random T cell motility in the lymph node”. In: *Proceedings of the National Academy of Sciences of the United States of America* 101.4 (2004), pp. 998–1003. DOI: 10.1073/pnas.0306407101 (cited on p. 21).
- [Mir+11] H. P. Mirsky et al. “Systems biology approaches for understanding cellular mechanisms of immunity in lymph nodes during infection”. In: *Journal of Theoretical Biology* 287 (2011), pp. 160–170. DOI: 10.1016/j.jtbi.2011.06.037 (cited on p. 22).
- [MM99] M. Meier-Schellersheim and G. Mack. “SIMMUNE, a tool for simulating and analyzing Immune System behavior”. In: (1999), p. 23. arXiv: 9903017 [cs] (cited on pp. v, 53, 54, 58).
- [MR01] A. J. McMichael and S. L. Rowland-Jones. “Cellular immune responses to HIV”. In: *Nature* 410.April (2001), pp. 980–987. DOI: 10.1038/35073658 (cited on p. 14).
- [MW07] W. Materi and D. S. Wishart. “Computational systems biology in drug discovery and development: methods and applications”. In: *Drug Discovery Today* 12.April (2007), pp. 295–303. DOI: 10.1016/j.drudis.2007.02.013 (cited on p. 95).
- [Nar+12] V. Narang et al. “Systems immunology: A survey of modeling formalisms, applications and simulation tools”. In: *Immunologic Research* 53 (2012), pp. 251–265. DOI: 10.1007/s12026-012-8305-7 (cited on p. 95).
- [NB96] M. A. Nowak and C. R. Bangham. “Population dynamics of immune responses to persistent viruses”. In: *Science (New York, N.Y.)* 272 (1996), pp. 74–79. DOI: 10.1126/science.272.5258.74 (cited on pp. 41–43).
- [NH03] D. G. Nguyen and J. E. K. Hildreth. “Involvement of macrophage mannose receptor in the binding and transmission of HIV by macrophages”. In: *European journal of immunology* 33 (2003), pp. 483–493. DOI: 10.1002/immu.200310024 (cited on p. 10).

- [NMA90] M. A. Nowak, R. M. May, and R. M. Anderson. “The evolutionary dynamics of HIV-1 quasispecies and the development of immunodeficiency disease”. In: *AIDS* 4.11 (1990), pp. 1095–1103. DOI: 10.1097/00002030-199011000-00007 (cited on pp. 15, 49, 50).
- [NN15] U. D. o. H. NIAID and H. NIH. *START Press Release*: [http:// www.niaid. nih.gov/ news/ newsreleases/ 2015/ Pages/ START.aspx](http://www.niaid.nih.gov/news/newsreleases/2015/Pages/START.aspx). 2015 (cited on pp. 19, 40, 98).
- [Nor+13] M. J. North et al. “Complex adaptive systems modeling with Repast Symphony”. In: *Complex Adaptive Systems Modeling* 1 (2013), p. 3. DOI: 10.1186/2194-3206-1-3 (cited on p. 55).
- [Nov14] A. M. Novotny. *Fundamentals of Immunology*. EDX, 2014 (cited on p. 8).
- [Now+91] M. A. Nowak et al. “Antigenic diversity thresholds and the development of AIDS”. In: *Science* 254.5034 (1991), pp. 963–969 (cited on pp. 15, 59).
- [NP02] P. W. Nelson and A. S. Perelson. “Mathematical analysis of delay differential equation models of HIV-1 infection”. In: *Mathematical Biosciences* 179 (2002), pp. 73–94. DOI: 10.1016/S0025-5564(02)00099-8 (cited on p. 43).
- [OO10] C.-M. Ou and C. Ou. “Agent-Based Immunity for Computer Virus: Abstraction from Dendritic Cell Algorithm with Danger Theory”. In: *Advances in Grid and Pervasive Computing*. Ed. by P. Bellavista et al. 2010, pp. 670–678 (cited on p. 6).
- [Pat06] A. Patel. *Amit's Thoughts on Grids*: [http:// www-cs-students.stanford.edu/ ~amitp/ game-programming/ grids/](http://www-cs-students.stanford.edu/~amitp/game-programming/grids/). 2006 (cited on p. 34).
- [Per+96] A. S. Perelson et al. “HIV-1 dynamics in vivo: virion clearance rate, infected cell life-span, and viral generation time”. In: *Science (New York, N.Y.)* 271 (1996), pp. 1582–1586. DOI: 10.1126/science.271.5255.1582 (cited on pp. 2, 41, 49).
- [PGF93] G. Pantaleo, C. Graziosi, and A. S. Fauci. “New concepts in the immunopathogenesis of human immunodeficiency virus infection”. In: *The New England journal of medicine* 328.5 (1993), pp. 327–335. DOI: 10.1056/NEJM199302043280508 (cited on p. 20).
- [Pia+93] M. Piatak et al. “High levels of HIV-1 in plasma during all stages of infection determined by competitive PCR”. In: *Science (New York, N.Y.)* 259.March (1993), pp. 1749–1754. DOI: 10.1126/science.8096089 (cited on p. 18).
- [Pin08] M. Pineda-Krch. “GillespieSSA: Implementing the stochastic simulation algorithm in R”. In: *Journal of Statistical Software* 25.12 (2008), pp. 1–18 (cited on pp. 76, 77, 98).
- [PKD93] A. S. Perelson, D. E. Kirschner, and R. De Boer. “Dynamics of HIV infection of CD4+ T cells”. In: *Mathematical biosciences* 114.1 (1993), pp. 81–125. DOI: 8096155 (cited on pp. 2, 41, 43).
- [Plo13] H. L. Ploegh. “Logic of the immune system”. In: *Cancer immunology research* 1 (2013), pp. 5–10. DOI: 10.1158/2326-6066.CIR-13-0023 (cited on p. 15).
- [PO79] A. S. Perelson and G. F. Oster. “Theoretical studies of clonal selection: minimal antibody repertoire size and reliability of self-non-self discrimination”. In: *Journal of theoretical biology* 81 (1979), pp. 645–670. DOI: 10.1016/0022-5193(79)90275-3 (cited on pp. 15, 22).

- [PS07] V. Piguet and R. M. Steinman. “The interaction of HIV with dendritic cells: outcomes and pathways”. In: *Trends in Immunology* 28.11 (2007), pp. 503–510. DOI: 10.1016/j.it.2007.07.010 (cited on p. 10).
- [R14] R. R. *A Language and Environment for Statistical Computing*. 2014 (cited on pp. 84, 88, 98).
- [RBK08] D. Rossinelli, B. Bayati, and P. Koumoutsakos. “Accelerated stochastic and hybrid methods for spatial simulations of reaction-diffusion systems”. In: *Chemical Physics Letters* 451 (2008), pp. 136–140. DOI: 10.1016/j.cplett.2007.11.055 (cited on p. 93).
- [RCS12] H. Resat, M. N. Costa, and H. Shankaran. “Spatial Aspects in Biological System Simulation”. In: *Methods Enzymol* 487.11 (2012), pp. 485–511. DOI: 10.1016/B978-0-12-381270-4.00017-2.Spatial (cited on p. 97).
- [Rea+14] M. Read et al. “Modelling biological behaviours with the unified modelling language: an immunological case study and critique”. In: *Journal of The Royal Society Interface* 11.99 (2014). DOI: 10.1098/rsif.2014.0704 (cited on p. 56).
- [Rei+87] G. Reibnegger et al. “Theoretical implications of cellular immune reactions against helper lymphocytes infected by an immune system retrovirus”. In: *Proceedings of the National Academy of Sciences of the United States of America* 84.20 (1987), pp. 7270–7274. DOI: 10.1073/pnas.84.20.7270 (cited on p. 48).
- [Ret+93] D. M. Retallack et al. “A single-base-pair mutation changes the specificities of both a transcription activation protein and its binding site”. In: *Proceedings of the National Academy of Sciences of the United States of America* 90.October (1993), pp. 9562–9565. DOI: 10.1073/pnas.90.20.9562 (cited on p. 61).
- [RG11] S. F. Railsback and V. Grimm. *Agent-Based and Individual-Based Modeling: A Practical Introduction*. Princeton University Press, 2011 (cited on p. 55).
- [RJB04] J. Rumbaugh, I. Jacobson, and G. Booch. *The Unified Modeling Language Reference Manual (2nd Edition)*. Pearson Higher Education, 2004 (cited on p. 55).
- [San+10] R. Sanjuan et al. “Viral Mutation Rates”. In: *Journal of Virology* 84.19 (Oct. 2010), pp. 9733–9748. DOI: 10.1128/JVI.00694-10 (cited on p. 65).
- [SC01] R. M. Z. dos Santos and S. Coutinho. “Dynamics of HIV Infection: A Cellular Automata Approach”. In: *Physical Review Letters* 87 (2001). DOI: 10.1103/PhysRevLett.87.168102 (cited on pp. 25–27, 31, 33, 37, 40, 41, 48, 97, 111, 112).
- [SCH08] N. Swerdlin, I. Cohen, and D. Harel. “The Lymph Node B Cell Immune Response: Dynamic Analysis “In-Silico””. In: *Proceedings of the IEEE* 96 (2008). DOI: 10.1109/JPROC.2008.925435 (cited on p. 56).
- [SF03] G. Silvestri and M. B. Feinberg. “Turnover of lymphocytes and conceptual paradigms in HIV infection”. In: *Journal of Clinical Investigation* 112.6 (2003), pp. 821–824. DOI: 10.1172/JCI200319799 (cited on p. 17).
- [SH97] N. J. Savill and P. Hogeweg. “Modelling morphogenesis: from single cells to crawling slugs”. In: *J. Theor. Biol.* 184 (1997), pp. 229–235. DOI: 10.1006/jtbi.1996.0237 (cited on p. 58).

- [Sie+90] H. B. Sieburg et al. *Simulation of HIV infection in artificial immune systems*. 1990. DOI: 10.1016/0167-2789(90)90184-Q (cited on pp. 11, 15, 54, 59).
- [SL01] M. C. Strain and H. Levine. “Comment on “Dynamics of HIV Infection: A Cellular Automata Approach””. In: *Physical Review Letters* 87.168102 (2001) (cited on pp. 26, 31, 33, 37).
- [SL96] A. B. Stundzia and C. J. Lumsden. “Stochastic simulation of coupled reaction–diffusion processes”. In: *Journal of computational physics* 127 (1996), pp. 196–207. DOI: 10.1006/jcph.1996.0168 (cited on p. 93).
- [Smi+04] D. J. Smith et al. “Mapping the antigenic and genetic evolution of influenza virus”. In: *Science (New York, N.Y.)* 305.2004 (2004), pp. 371–376. DOI: 10.1126/science.1097211 (cited on p. 61).
- [Som12] L. M. Sompayrac. *How the Immune System Works*. Wiley-Blackwell, 2012 (cited on pp. 5, 12–16, 19).
- [SPS10] K. Soetaert, T. Petzoldt, and R. W. Setzer. “Package deSolve : Solving Initial Value Differential Equations in R”. In: *Journal Of Statistical Software* 33.9 (2010), pp. 1–25 (cited on p. 98).
- [STK08] V. Shi, A. Tridane, and Y. Kuang. “A viral load-based cellular automata approach to modeling HIV dynamics and drug treatment”. In: *Journal of Theoretical Biology* 253 (2008), pp. 24–35. DOI: 10.1016/j.jtbi.2007.11.005 (cited on pp. v, 26, 31, 33, 36–39).
- [Su+09] B. Su et al. “Mathematical Modelling of Immune Response in Tissues”. In: *Computational and Mathematical Methods in Medicine* 10.1 (2009), pp. 9–38. DOI: 10.1080/17486700801982713 (cited on p. 48).
- [Swi26] J. Swift. *Travels into Several Remote Nations of the World. In Four Parts. By Lemuel Gulliver, First a Surgeon, and then a Captain of Several Ships*. 1726 (cited on p. 2).
- [TJ05] J. C. Tay and A. Jhavar. “CAFISS: A Complex Adaptive Framework for Immune System Simulation”. In: *Proceedings of the 2005 ACM symposium on Applied computing - SAC '05* (2005), p. 158. DOI: 10.1145/1066677.1066716 (cited on p. 54).
- [Tur+03] S. Turville et al. “The role of dendritic cell C-type lectin receptors in HIV pathogenesis”. In: *Journal of leukocyte biology* 74.November (2003), pp. 710–718. DOI: 10.1189/jlb.0503208 (cited on p. 11).
- [Uni13] United Nations. *UN AIDS 2013 Fact Sheet*: [http:// www.unaids.org/ en/resources/ campaigns/ globalreport2013/ factsheet/](http://www.unaids.org/en/resources/campaigns/globalreport2013/factsheet/). 2013 (cited on pp. 1, 18).
- [UW11] M. Ullah and O. Wolkenhauer. *Stochastic Approaches for Systems Biology*. Springer, 2011 (cited on p. 74).
- [Weg60] P. Wegner. *A technique for counting ones in a binary computer*. 1960. DOI: 10.1145/367236.367286 (cited on p. 60).
- [Wic09] H. Wickham. *ggplot2: elegant graphics for data analysis*. Springer New York, 2009 (cited on p. 98).
- [Wil+05] D. Wilflingseder et al. “Mechanisms promoting dendritic cell-mediated transmission of HIV”. In: *Molecular Immunology* 42 (2005), pp. 229–237. DOI: 10.1016/j.molimm.2004.06.019 (cited on p. 11).

- [Wil06] D. J. Wilkinson. *Stochastic Modelling for Systems Biology*. Chapman & Hall/CRC, 2006 (cited on pp. 70, 71, 91).
- [Wil99] U. Wilensky. *NetLogo itself*. 1999 (cited on pp. 26, 55, 99, 111).
- [WNG08] L. de Witte, A. Nabatov, and T. B. H. Geijtenbeek. “Distinct roles for DC-SIGN+-dendritic cells and Langerhans cells in HIV-1 transmission”. In: *Trends in Molecular Medicine* 14.1 (2008), pp. 12–19. DOI: 10.1016/j.molmed.2007.11.001 (cited on p. 11).
- [Woo06] P. Wood. *Understanding Immunology*. Prentice Hall, 2006 (cited on pp. 13, 14, 19).
- [Wu+08] H. Wu et al. “Parameter identifiability and estimation of HIV/AIDS dynamic models”. In: *Bulletin of Mathematical Biology* 70 (2008), pp. 785–799. DOI: 10.1007/s11538-007-9279-9 (cited on p. 44).
- [Zar+10] N. Zarrabi et al. “Modeling HIV-1 intracellular replication: Two simulation approaches”. In: *Procedia Computer Science* 1.1 (2010), pp. 555–564. DOI: 10.1016/j.procs.2010.04.059 (cited on p. 22).
- [Zhd07] V. P. Zhdanov. “Kinetic model of HIV infection”. In: *Journal of Experimental and Theoretical Physics* 105.4 (2007), pp. 856–860. DOI: 10.1134/S1063776107100202 (cited on pp. 50, 51).
- [Zhu+03] P. Zhu et al. “Electron tomography analysis of envelope glycoprotein trimers on HIV and simian immunodeficiency virus virions”. In: *Proceedings of the National Academy of Sciences of the United States of America* 100 (2003), pp. 15812–15817. DOI: 10.1073/pnas.2634931100 (cited on p. 18).
- [Zhu+07] R. Zhu et al. “Studying genetic regulatory networks at the molecular level: Delayed reaction stochastic models”. In: *Journal of Theoretical Biology* 246 (2007), pp. 725–745. DOI: 10.1016/j.jtbi.2007.01.021 (cited on p. 79).
- [ZKC05] G. Zaiyi, H. H. Kwang, and T. J. Cing. “Sufficiency verification of HIV-1 pathogenesis based on multi-agent simulation”. In: *Proceedings of the 2005 conference on Genetic and evolutionary computation - GECCO '05* (2005), p. 305. DOI: 10.1145/1068009.1068059 (cited on p. 58).

Appendix A

Santos CA implementation (in NetLogo)

This is our implementation in NetLogo [Wil99] of the main model studied in Chapter 3 by Santos and Coutinho [SC01].

```
1 ; states
2 ; T healthy
3 ; A1 infected stage 1
4 ; A2 infected stage 2
5 ; D dead
6
7 globals [
8   T A1 A2 D ; status colors
9 ]
10
11 patches-own [ nA1 nA2 time ]
12
13 to setup
14   clear-all
15
16   set T green
17   set A1 red
18   set A2 yellow
19   set D gray
20
21   ask patches [
22     set pcolor T
23     set time 0
24   ]
25   ask n-of (Phiv * max-pxcor * max-pycor)
26     patches [
27       set pcolor A1
28     ]
29   reset-ticks
30 end
31
32 to-report rule1 ; T - initial healthy
33   state
34   if nA1 >= 1 or nA2 >= R [
35     report A1
36   ]
37   report T
38 end
39 to-report rule2 ; A1
40   if time >= tau [
41     report A2
42   ]
43   report A1
44 end
45
46 to-report rule3 ; A2
47   report D
48 end
49
50 to-report rule4 ; D
51   if random-float 1 < Prepl [
52     if random-float 1 < Pinf [
53       report A1
54     ]
55     report T
56   ]
57   report D
58 end
59
60 to update
61   ask patches [
62     let N neighbors
63     set nA1 count N with [ pcolor = A1 ]
64     set nA2 count N with [ pcolor = A2 ]
65   ]
66
67   ask patches [
68     let ncolor pcolor
69     ifelse pcolor = T [set ncolor rule1
70       ][
71       ifelse pcolor = A1 [set ncolor rule2
72         ][
73         ifelse pcolor = A2 [set ncolor rule3
74           ][
75           ifelse pcolor = D [set ncolor rule4
76             ][
77               ]]]]
78     ifelse ncolor != pcolor [
79       set pcolor ncolor
80       set time 0
81     ]
82   ]
83 end
```

78][81]
79	set time time + 1	82	tick
80]	83	end

The code does not work without an interface. We propose the following interface (Figure A.1).

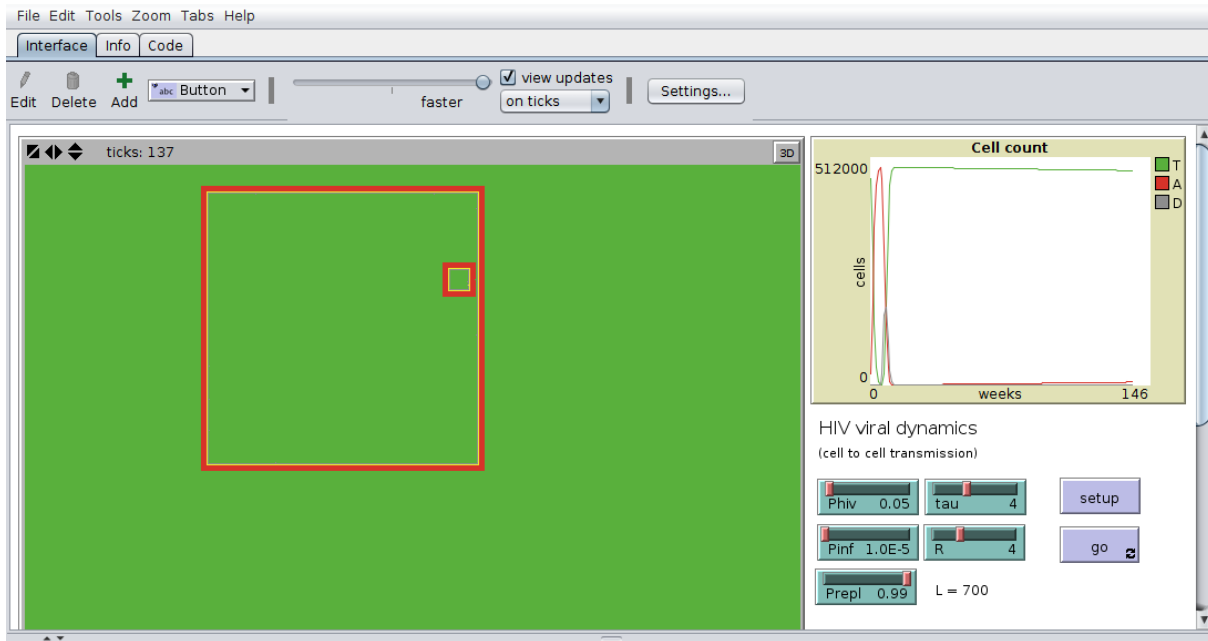


Figure A.1: Our Santos and Coutinho's model implementation in NetLogo.

Appendix B

Culshaw ODE and SSA delay implementation (in R)

This is an implementation of delays using kinetic reaction networks for deterministic and stochastic simulations, as described in the section 6.5 on page 77 of Chapter 6.

```
1 # Culshaw (2000) model
2 # T -- uT --> 0
3 # 0 -- s --> T
4 # T -- r --> 2T
5 # T -- r*(T+I)/Tmax --> 0
6 # T+V -- kI-KI' --> 0
7 # T+V -- KI' --> I
8 # I -- uI-ub --> 0
9 # I -- ub --> NV
10 # V -- uV --> 0
11
12 params <- c(
13   nuT = 0.02,
14   nuI = 0.26,
15   nub = 0.24,
16   nuV = 2.4,
17   kI = 2.4e-5,
18   kI_ = 2e-5,
19   r = 0.03,
20   N = 500, # varies
21   Tmax = 1500,
22   s = 10
23 )
24
25 # transition hazards
26 hazards <- function(X)
27   with(as.list(c(X, params)), { c(
28     s,
29     nuT*x,
30     r*x,
31     r*x*(x+y)/Tmax,
32     (kI-kI_)*x*v,
33     kI_*x*v,
34     (nuI-nub)*y,
35     nub*y,
36     nuV*v
37   )})
38
39 # stoichiometry matrix
40 V <- matrix(c(
41   +1, 0, 0, # s
42   -1, 0, 0, # nuT*T
43   +1, 0, 0, # r*T
44   -1, 0, 0, # r*T*(T+I)/Tmax
45   -1, 0, -1, # (kI-kI_)*T*V
46   -1, 0, -1, # kI_*T*V
47   0, -1, 0, # (nuI-nub)*I
48   0, -1, params['N'], # nub*I
49   0, 0, -1 # nuV*V
50 ), ncol=3, byrow=TRUE)
51
52 # delay matrix
53 D <- matrix(c(
54   0, 0, 0, # s
55   0, 0, 0, # nuT*T
56   0, 0, 0, # r*T
57   0, 0, 0, # r*T*(T+I)/Tmax
58   0, 0, 0, # (kI-kI_)*T*V
59   0, +1, 0, # kI_*T*V
60   0, 0, 0, # (nuI-nub)*I
61   0, 0, 0, # nub*I
62   0, 0, 0 # nuV*V
63 ), ncol=3, byrow=TRUE)
64
65 euler <- function(x, dt)
66   x + (hazards(x)%*%(V+D))*dt
67 gillespie <- function(x, dt)
68   sapply(x + (rpois(nrow(V), hazards(x))
69     %*%(V+D))*dt, function(x) max(x
70     , 0))
71
72 euler.tau <- function(x, dt) {
73   h <- hazards(x)
74   c(x+(h%*%V)*dt, (h%*%D)*dt)
75 }
76
77 gillespie.tau <- function(x, dt) {
```



```

75 h <- hazards(x)
76 h <- rpois(nrow(V),h)
77 h <- sapply(h, function(x) max(x,0))
78 c(x+(h%*%V)*dt, (h%*%D)*dt)
79 }
80
81 integrate <- function(method, X0, dt,
82   tmax) {
83   X <- matrix(rep(0,length(X0)*tmax/dt)
84     , ncol=length(X0))
85   colnames(X) <- c('x','y','v')
86   X[1,] <- X0
87   for(i in 1:(tmax/dt-1))
88     X[i+1,] <- method(X[i,],dt)
89   data.frame(time=seq(0,tmax-dt,dt), X)
90 }
91
92 integrate.tau <- function(method.tau, X0,
93   dt, tmax, tau) {
94   X <- matrix(rep(0,length(X0)*tmax/dt)
95     , ncol=length(X0))
96   colnames(X) <- c('x','y','v')
97   X[1,] <- X0
98   for(i in 1:((tmax-tau)/dt-1)) {
99     d <- method.tau(X[i,],dt)
100     X[i+1,] <- X[i+1,] + d[1:3]
101     X[i+1+tau/dt,] <- d[4:6]
102   }
103   for(i in ((tmax-tau)/dt):(tmax/dt-1))
104     {
105       d <- method.tau(X[i,],dt)
106       X[i+1,] <- X[i+1,] + d[1:3]
107     }
108   data.frame(time=seq(0,tmax-dt,dt),X)
109 }
110
111 dt <- 0.1
112
113 #X0 <- c(T=1000, I=0, V=1e-3) #artigo
114 X0 <- c(x=1000, y=1, v=0) #para
115 gillespie
116
117 library(reshape2)
118 Y <- NULL
119
120 for(tau in c(0,12)) {
121   # deterministic:
122   if(tau == 0)
123     X <- integrate(euler, X0, dt,
124       400)
125   else
126     X <- integrate.tau(euler.tau, X0,
127       dt, 400, tau)
128   Y <- rbind(Y, melt(data.frame(X,tau=
129     factor(tau),ssa=FALSE,i=0,avg=
130     FALSE),

```

```

121   id.vars=c('time','tau','ssa','i',
122     'avg'))))
123
124 # ssa:
125 for(i in 1:8) {
126   if(tau == 0)
127     X <- integrate(gillespie, X0,
128       dt, 400)
129   else
130     X <- integrate.tau(gillespie.
131       tau, X0, dt, 400, tau)
132   #if(i > 2)
133   # X$V <- NA
134   Y <- rbind(Y, melt(
135     data.frame(X,tau=factor(tau),
136       ssa=TRUE,avg=FALSE,i=i),
137     id.vars=c('time','tau','
138       ssa','i','avg'))))
139 }
140
141 .tau <- tau
142 X.avg <- aggregate(value ~ time+
143   variable, subset(Y,ssa==TRUE&tau
144     ==.tau), mean)
145 Y <- rbind(Y, cbind(X.avg, avg=TRUE,
146   ssa=FALSE, i=9, tau=factor(tau)))
147 }
148
149 library(ggplot2)
150 theme_set(theme_classic() +
151   theme(text=element_text('serif')) +
152   theme(strip.background=element_blank
153     ()) +
154   theme(strip.text.x=element_text(face=
155     'bold',size=12)))
156 p <- ggplot(Y, aes(time,value,group=
157   interaction(variable,tau,ssa,i,avg),
158   linetype=tau,alpha=ssa,color=avg,size
159     =ssa)) +
160   geom_line() +
161   facet_wrap(~ variable, scales='free_y
162     ') +
163   scale_alpha_manual(name='SSA',labels=
164     c('false','true'), values=c
165     (1,0.20)) +
166   scale_size_manual(name='SSA',labels=c
167     ('false','true'), values=c
168     (0.3,0.5)) +
169   scale_colour_manual(labels=c('false',
170     'true'), values=c('black','blue')
171     ) +
172   scale_linetype_manual(name=bquote(tau
173     ), values=c('solid','dotted')) +
174   expand_limits(y=0) +
175   xlab('Days') + ylab('Density')
176 print(p)

```